Journal of Photochemistry and Photobiology C: Photochemistry Reviews 23 (2015) 103–131

Contents lists available at ScienceDirect

Journal of Photochemistry and Photobiology C: Photochemistry Reviews

journal homepage: www.elsevier.com/locate/jphotochemrev

Review

Enhancing photodynamic therapy of refractory solid cancers: Combining second-generation photosensitizers with multi-targeted liposomal delivery

Ruud Weijer [a], Mans Broekgaarden [a,1], Milan Kos [a,1], Remko van Vught [b], Erik A.J. Rauws [c], Eefjan Breukink [b], Thomas M. van Gulik [a], Gert Storm [d,e], Michal Heger [a,b,d,*]

[a] Department of Experimental Surgery, Academic Medical Center, University of Amsterdam, Meibergdreef 9, 1105 AZ Amsterdam, The Netherlands
[b] Membrane Biochemistry and Biophysics, Institute of Biomembranes, University of Utrecht, Padualaan 8, 3584 CH Utrecht, The Netherlands
[c] Department of Gastroenterology, Academic Medical Center, University of Amsterdam, Meibergdreef 9, 1105 AZ Amsterdam, The Netherlands
[d] Department of Pharmaceutics, Utrecht Institute for Pharmaceutical Sciences, University of Utrecht, Universiteitsweg 99, 3584 CG Utrecht, The Netherlands
[e] Department of Controlled Drug Delivery, MIRA Institute for Biomedical Technology and Technical Medicine, University of Twente, P.O. Box 217, 7500 AE Enschede, The Netherlands

ARTICLE INFO

Article history:
Received 2 September 2014
Received in revised form 5 May 2015
Accepted 6 May 2015
Available online 11 May 2015

Keywords:
Cancer
Drug delivery
Metallated phthalocyanines
Photodynamic therapy
Photosensitizers
Reactive oxygen species
Singlet oxygen
Tumor targeting

ABSTRACT

Contemporary photodynamic therapy (PDT) for the last-line treatment of refractory cancers such as nasopharyngeal carcinomas, superficial recurrent urothelial carcinomas, and non-resectable extrahepatic cholangiocarcinomas yields poor clinical outcomes and may be associated with adverse events. This is mainly attributable to three factors: (1) the currently employed photosensitizers exhibit suboptimal spectral properties, (2) the route of administration is associated with unfavorable photosensitizer pharmacokinetics, and (3) the upregulation of survival pathways in tumor cells may impede cell death after PDT. Consequently, there is a strong medical need to improve PDT of these recalcitrant cancers. An increase in PDT efficacy and reduction in clinical side-effects may be achieved by encapsulating second-generation photosensitizers into liposomes that selectively target to pharmacologically important tumor locations, namely tumor cells, tumor endothelium, and tumor interstitial spaces. In addition to addressing the drawbacks of clinically approved photosensitizers, this review addresses the most relevant pharmacological aspects that dictate clinical outcome, including photosensitizer biodistribution and intracellular localization in relation to PDT efficacy, the mechanisms of PDT-induced cell death, and PDT-induced antitumor immune responses. Also, a rationale is provided for the use of second-generation

Abbreviations: $^1O_2$, singlet oxygen; 5-ALA, 5-aminolevulinic acid; ε, molar absorptivity; Φ_T, triplet state quantum yield; AlPC, chloroaluminum phthalocyanine; $AlPCS_4$, tetrasulfonated chloroaluminum phthalocyanine; APCs, antigen-presenting cells; ATG7, autophagy-related protein 7; BCL2, B-cell CLL/lymphoma 2; BECN1, beclin 1; BID, BH3-interacting domain death agonist; CD91, cluster of differentiation 91; CPO, 9-capronyloxytetrakis (methoxyethyl) porphycene; CTL, $CD8^+$ cytotoxic T-lymphocyte; DAMP, damage-associated molecular pattern; DC, dendritic cell; DC-chol, 3β-[*N*-(*N*′,*N*′-dimethylaminoethane)-carbamoyl] cholesterol; DOTAP, 1,2-dioleoyl-3-trimethylammonium-propane; DPPC, 1,2-dipalmitoyl-*sn*-glycero-3-phosphocholine; DPPG, 1,2-dipalmitoyl-*sn*-glycero-3-phosphoglycerol; DSPE-PEG, 1,2-distearoyl-*sn*-glycero-3-phosphoethanolamine-*N*-[methoxy(PEG)-2000]; ecto-CRT, surface-exposed calreticulin; EGFR, epidermal growth factor receptor; EPR effect, enhanced permeability and retention effect; ER, endoplasmic reticulum; ETLs, endothelial cell-targeting liposomes; Fab' fragment, antigen-binding fragment; HDL, high-density lipoprotein; HER2, human epidermal growth factor receptor 2; HMGB-1, high mobility group box-1; HpD, hematoporphyrin derivative; HPPH, 2-(1-hexyloxyethyl)-2-devinylpyropheophorbide-a; HSP, heat shock protein; HUVEC, human umbilical vein endothelial cell; ICD, immunogenic cell death; ITLs, interstitially-targeted liposomes; LD_{50}, lethal 50% dose; LDL, low-density lipoprotein; LDLR, LDL receptor; log *P*, octanol/water partition coefficient; MHC, major histocompatibility complex; MPT, mitochondrial permeability transition; MT-1-MMP, membrane type-1-matrix metalloproteinase; mTHPC, *m*-tetrahydroxyphenylchlorin; NBD, nitrobenzoxadiazole; NF-κB, kappa-light-chain-enhancer of activated B cells; NGR, asparagine–glycine–arginine; NLRP3, NLR family; NPe6, mono-L-aspartyl chlorin e6; $O_2^{\bullet-}$, superoxide anion; PAA, polyacrylamide; PAcM, poly(acryloyl morpholine); PC, phthalocyanine; PDT, photodynamic therapy; PEG, polyethylene glycol; POPC, 1-palmitoyl-2-oleoyl-*sn*-glycero-3-phosphocholine; PpIX, protoporphyrin IX; PRR, pattern recognition receptor; PS, photosensitizer; PVP, poly(vinylpyrrolidone); RAGE, receptor for advanced glycation end products; RGD, arginine–glycine–aspartic acid; RNS, reactive nitrogen species; ROS, reactive oxygen species; T4CPP, meso-tetrakis[4-(carboxymethyleneoxy)phenyl]porphyrin; TAAs, tumor-associated antigens; t-BID, truncated-BID; TLR, toll-like receptor; TTLs, tumor cell-targeting liposomes; UPR, unfolded protein response; VCAM-1, vascular cell adhesion molecule-1; VEGF, vascular endothelial growth factor; ZnPC, zinc phthalocyanine; $ZnPCS_4$, tetrasulfonated zinc phthalocyanine; ZnTPP, zinc tetraphenyl porphyrin.

* Corresponding author at: Department of Experimental Surgery, Academic Medical Center, University of Amsterdam, Meibergdreef 9, 1105 AZ Amsterdam, The Netherlands. Tel.: +31 20 566 5573; fax: +31 20 697 6621.
E-mail address: m.heger@amc.uva.nl (M. Heger).

[1] These authors contributed equally to this work.

http://dx.doi.org/10.1016/j.jphotochemrev.2015.05.002
1389-5567/

photosensitizers such as diamagnetic phthalocyanines (*e.g.*, zinc or aluminum phthalocyanine), which exhibit superior photophysical and photochemical properties, in combination with a multi-targeted liposomal photosensitizer delivery system. The rationale for this PDT platform is corroborated by preliminary experimental data and proof-of-concept studies. Finally, a summary of the different nanoparticulate photosensitizer delivery systems is provided followed by a section on phototriggered release mechanisms in the context of liposomal photosensitizer delivery systems.

Contents

1. Introduction

Photodynamic therapy (PDT) is a minimally-to-noninvasive treatment modality for numerous types of solid cancers. PDT involves the systemic administration of a photosensitizer (PS), accumulation of the PS in the tumor, and irradiation of the tumor with light of a wavelength that is well absorbed by the PS. Resonantly irradiated PSs undergo intersystem crossing from the singlet state to the triplet state, from which either an electron is transferred (type I photochemical reaction) or energy is donated (type II photochemical reaction) to molecular oxygen [1]. Type I reactions result in the formation of superoxide anion ($O_2^{\bullet -}$) and, in biological systems, derivative reactive oxygen and nitrogen species (ROS and RNS, respectively) [2], whereas type II reactions yield singlet oxygen ($^1O_2$). ROS/RNS are capable of (per) oxidizing biomolecules and ultimately induce tumor cell death by causing shutdown of intratumoral vasculature, tumor cell death, and an anti-tumor immune response (Fig. 1) [3,4].

While some solid cancer types respond very well to PDT [5–14], there are cancer types that are relatively recalcitrant to PDT, including superficial recurrent urothelial carcinoma [15], nasopharyngeal carcinoma [16], and extrahepatic cholangiocarcinoma [17,18]. In addition to the therapeutic recalcitrance, systemic administration of the PS may lead to non-selective tissue damage and phototoxic reactions due to inadvertent accumulation of the PS in the skin. With respect to the latter, patients are instructed to stay inside and avoid direct exposure to sunlight until the PS has been completely cleared to prevent unbridled photochemical damage to the skin. Although PDT is still being used in specialized treatment centers, the significant burden on patients has led several treatment centers, including ours, to abandon PDT as a treatment option for terminal cancer patients due to ethical considerations [19].

Such decisions are unfortunate in light of the relatively good treatment outcomes achieved with PDT in many other types of cancer, as a result of which researchers are striving to further improve this modality while minimizing the drawbacks. The negative side-effects associated with PDT may be circumvented in several ways. Firstly, novel and more efficacious second-generation PSs with improved photophysical and photochemical properties have emerged, including chlorins and metal-coordinated phthalocyanines. These PSs are excited at longer wavelengths at which deeper light penetration into tissue and more homogeneous treatment of the tumor can be achieved. High-power laser systems have become available to accommodate PDT with these PSs. Secondly, the new generation of PSs, which are often lipophilic, can be incorporated into nanoparticulate drug delivery systems to ensure compatibility with plasma (required for intravenous administration) and to facilitate selective targeting. The targeting is expected to improve PS accumulation in the tumor [20,21], as a result of which lower PS plasma concentrations will be required for

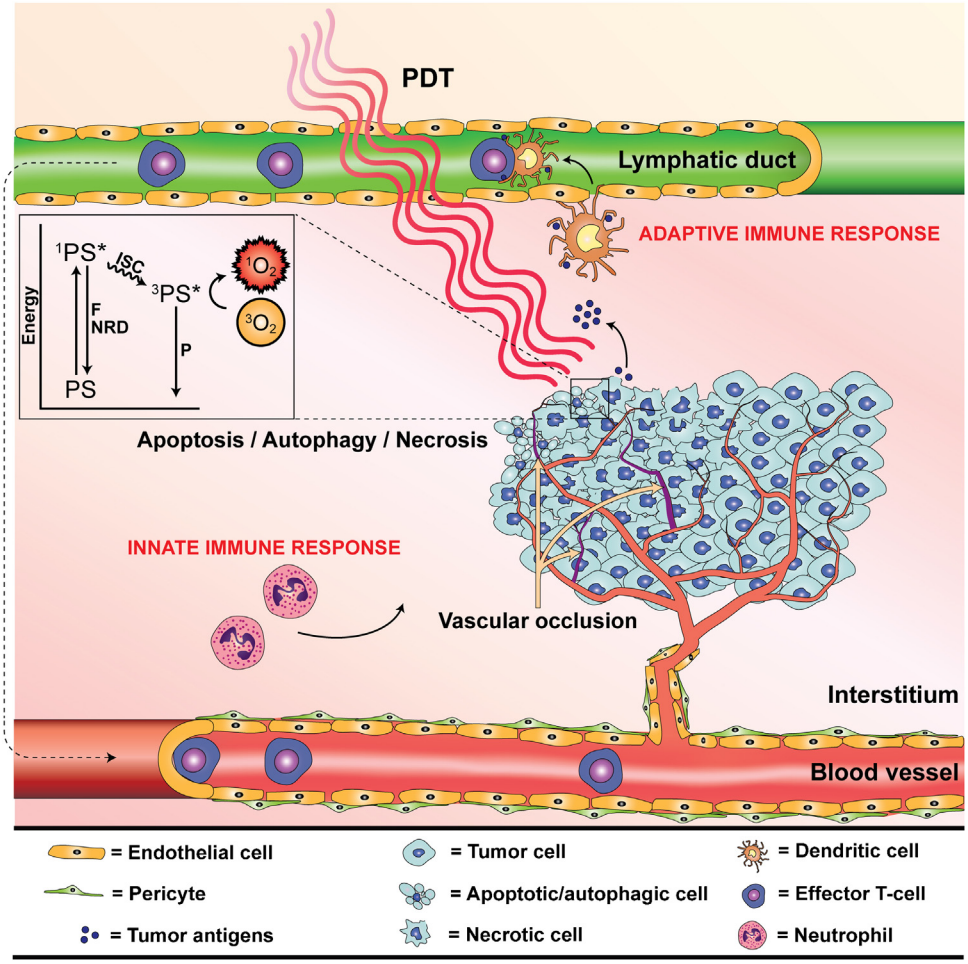

Fig. 1. Photophysical and biological mechanisms of photodynamic therapy (PDT). Tumor-replete photosensitizer (PS) molecules are activated by (laser) light to an excited singlet state photosensitizer (^{1}PS*). The ^{1}PS* can return to the ground state (PS) by emitting fluorescence (F) or by non-radiative decay (NRD), or can enter an excited triplet state *via* intersystem crossing (ISC) to yield an excited triplet state photosensitizer (^{3}PS*). ^{3}PS* can consequently transfer the triplet state electron (type I photochemical reaction) or energy (type II photochemical reaction) to molecular oxygen, yielding $O_2^{\bullet-}$ and $^1O_2$, respectively (top left), or the ^{3}PS* can return to the ground state by emitting phosphorescence (P). The generation of $O_2^{\bullet-}$ and $^1O_2$ (and its ROS/RNS derivatives) results in tumor cell death, vaso-occlusion, and an anti-tumor immune response (*via* the innate as well as the adaptive immune system) (Section 2.4).

an optimal PDT effect (compared to clinically approved PS). This should also reduce PS-associated phototoxicity. Thirdly, the use of a drug delivery system allows the co-encapsulation of adjuvant therapeutics or diagnostic/imaging agents, with which the PDT modality could be further improved.

In this review, these three aspects are addressed in light of a multi-faceted PDT modality for the treatment of recalcitrant solid cancers. Specifically, the systemic and intracellular distribution of PSs is addressed in the context of the PDT-induced mode of cell death as well as the anti-tumor immune response. Next, an overview is provided of second-generation metallated phthalocyanines (PCs) as PSs and their advantages over conventional, clinically employed PSs. Following a brief overview of the different nanoparticulate PS delivery systems currently available for PDT, an exemplary PS delivery platform is introduced that is centered on zinc phthalocyanine (ZnPC) and liposomes as an experimental PDT regimen for solid cancers.

2. Photodynamic therapy

2.1. Clinically approved photosensitizers

In the most ideal scenario, PSs should be non-toxic, should not generate toxic or mutagenic catabolites, and exhibit low-to-no dark toxicity. Moreover, ideal PSs should be chemically pure and photostable compounds that absorb maximally in the therapeutic window (650–850 nm [1]), have a high triplet state quantum yield, have a high ROS production efficiency, and accumulate selectively in the tumor tissue [22].

As detailed in Fig. 2, the four most frequently utilized clinical PSs include (1) hematoporphyrin derivative (HpD), (2) a semi-purified form of HpD known as porfimer sodium, (3) 5-aminolevulinic acid (5-ALA), which is a precursor of the mitochondrially produced PS protoporphyrin IX (PpIX), and (4) *m*-tetrahydroxyphenylchlorin (mTHPC). These PSs are associated with a considerable level of phototoxicity that is caused by long clearance times after systemic administration and extensive PS retention in the skin (Table 1). The profound skin toxicity applies to HpD [23] and porfimer sodium in particular [24], but also to a degree to PpIX [25] and mTHPC [26]. Peng et al. have determined the dermal distribution of porfimer sodium using highly light-sensitive video intensification microscopy, which revealed that porfimer sodium localizes to keratinized epithelium, hair (including follicles), and collagenous connective tissue [27]. Since PSs are slowly cleared from the skin by gradual photobleaching [28], the photosensitivity caused by HpD and porfimer sodium can persist for up to 3 months.

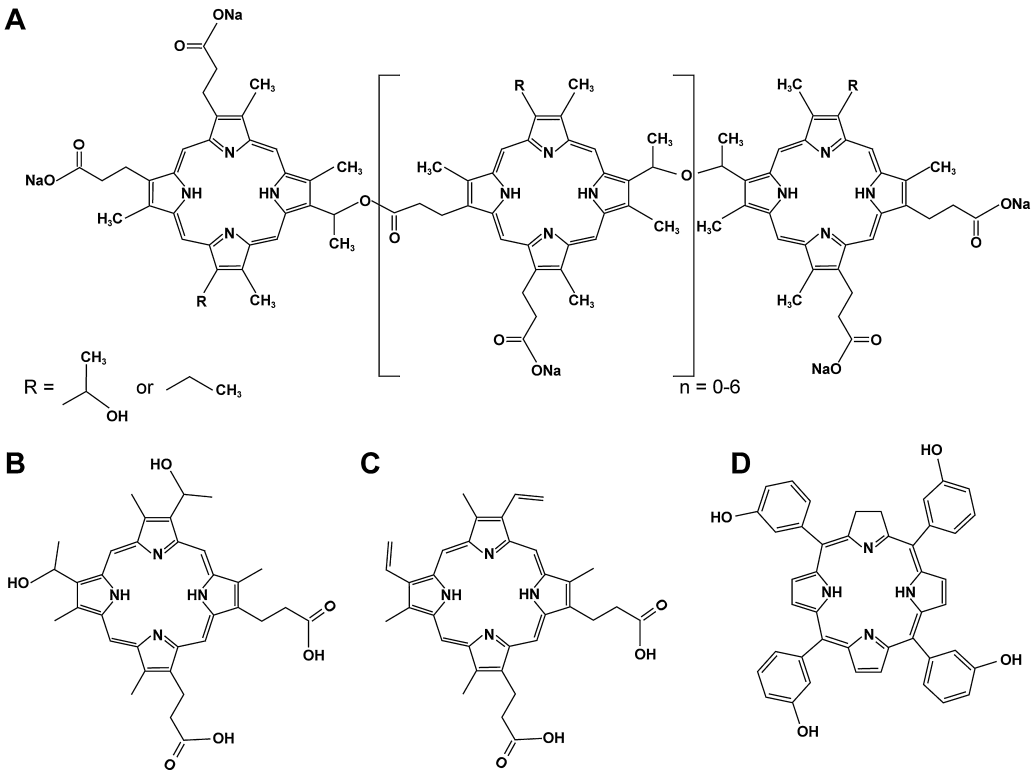

E

	Solubility	Log *P*	Q-band maximum [nm]	ε at Q-band maximum [$M^{-1} \cdot cm^{-1}$]	Triplet state quantum yield	Singlet oxygen quantum yield	[Ref]
(A) Porfimer sodium	Lipophile	8.50 (±3.34)	630	3,000	0.20	0.11	[33, 34]
(B) HpD	Lipophile	3.25 (±2.15)	630	3,000	0.83	0.56	[33-35]
(C) 5-ALA (PpIX)	Hydrophile	-1.89 (±1.08)	635	5,000	0.56	0.54	[35-37]
(D) mTHPC	Lipophile	7.40 (±2.16)	652	30,000	0.31	0.30	[35, 36, 38]

Fig. 2. Chemical structure and physicochemical properties of commonly used PSs. Chemical structure of porfimer sodium (A), hematoporphyrin (inasmuch as the exact chemical structure of HpD is unknown, the structure of hematoporphyrin is depicted) (B), PpIX (C), and mTHPC (D). The physicochemical properties are summarized in (E). Estimated octanol/water partition coefficients (log *P*) were obtained from [382].

Table 1
Pharmacokinetic, pharmacodynamic, and toxicity parameters of clinically applied and experimental photosensitizers. Abbreviations: LD_{50}, lethal 50% dose; est., estimated; IV, intravenous; NA, not assessed; d, day; wk, week; NCA, not commercially available; h, hour; ZnPC, zinc phthalocyanine; $ZnPCS_4$, tetrasulfonated zinc phthalocyanine; AlPC, chloroaluminum phthalocyanine; $AlPCS_4$, tetrasulfonated chloroaluminum phthalocyanine. *LD_{50} dark toxicity for HpD was calculated based on a molecular weight of 598.7 g/mol, as described in [307].

	Administration route	Tumor:healthy tissue ratio	Mutagenicity	Elimination (half-life)	Photosensitivity	LD_{50} dark toxicity [μM]	Est. costs per treatment ($)	[Ref]
HpD	IV	NA	Yes	17–22 d	8–12 wk	367–1136*	NCA	[181,308–310]
Porfimer sodium	IV	1.7–2:1	Yes	17 d	4–12 wk	5.3	7000	[24,176,187,192,311–313]
5-ALA	Oral/IV	2:1	Yes	5-ALA: 0.75 h PpIX: 8 h	1–2 d	9041	2000	[25,176,188,314–316]
	Topical	1.7–30:1					250	
mTHPC	IV	2–3:1	No	45 h	2–6 wk	8.46–26.4	8750	[26,176,181,182,186,189,317]
ZnPC	IV	6.3:1 [3.7–9:1]	NA	NA	NA	>5	<100	[190,191,201,301,318]
$ZnPCS_4$	IV	NA	No	NA	NA	>31.6	<100	[180,319]
AlPC	IV	NA	No	NA	NA	>10	<100	[178,179,320]
$AlPCS_4$	IV	10:1	No	NA	NA	>500	<100	[33,176,177,192]

Another limitation of the clinically approved PSs is the relatively low main absorption peak in the red spectrum (Q-band, Fig. 3A). The position of the Q-band maximum has several important clinical implications. First, short-wavelength red light has a lower optical penetration depth into tissue than longer-wavelength red light due to the competitive absorption by melanin (skin) and hemoglobin (skin and blood-containing tissue, including tumors) (Fig. 3B). The use of 630-nm light may result in insufficient PS excitation in the tumor bulk or inhomogeneous photosensitization of larger tumors due to optical shielding by blood vessels. Moving from 630-nm light to 690-nm light would significantly reduce absorption by blood, which theoretically yields a 1.67-fold increase in optical penetration depth [29]. Second, sunlight is more intense at the shorter red wavelengths (Fig. 3B) and may therefore account for more ROS generation by PSs with more blue-positioned Q-band maxima compared to PSs with more red-positioned Q-band maxima at equal dermal PS concentrations (Fig. 3B).

With respect to the abovementioned factors and on the basis of the data presented in Fig. 2, the clinically approved PSs are not ideal. This has triggered the development of PSs with better spectral and photochemical properties and technically more sophisticated PDT modalities. Readers should note that PDT may not be the treatment of choice for bulky tumors. Bulky tumors are associated with limited optical penetration depth and extensive scattering of light, particularly when a tumor has a necrotic core. In those cases, surgical resection is preferred (when possible) and/or radiotherapy/chemotherapy. Alternatively, interstitial PDT, a PDT modality where multiple light-emitting fibers are inserted into the tumor, may be employed to completely and homogenously photosensitize the malignant tissue.

2.2. Biodistribution of photosensitizers

2.2.1. Systemic distribution

Systemically infused PSs are distributed throughout the body *via* the circulation, whereby the PS typically hyperaccumulates in tumor tissue due to the enhanced permeability and retention (EPR) effect. Since the tumor endothelium is highly fenestrated and the tumor interstitium lacks lymphatic drainage, PSs are more prone to accumulate and remain in tumor tissue than in healthy tissues [30].

To study the biodistribution of a PS after systemic administration, Bellnier and co-workers injected radio-isotopically (^{14}C)-labeled porfimer sodium intravenously in mammary carcinoma (SMT-F)-bearing mice [31], and found that porfimer sodium (hydrophobic, Fig. 2) was taken up by various organs within 7.5 h after systemic administration. The highest peak concentrations were measured in the liver, adrenal gland, and bladder, whereas lower concentrations were found in the pancreas, kidney, and spleen. Even lower concentrations were measured in the stomach, bone, lung, and heart. Although the intratumoral porfimer sodium concentration was lower than in the previously mentioned organs, the porfimer sodium concentration in the tumor was higher than in skeletal muscle, skin, and brain tissue. Another study evaluated the biodistributive behavior of mono-L-aspartyl chlorin e6 (NPe6, hydrophilic) in murine mammary carcinoma (BA)-bearing mice [32]. It was shown that the highest NPe6 concentrations were reached in the liver, kidney, and spleen, whereas the lowest concentration of NPe6 was found in the brain, muscle, and esophagus. Furthermore, a substantial amount of NPe6 was localized in the skin 1 h post-injection, although this concentration rapidly declined over a period of 96 h. At 4 h, the NPe6 tumor tissue concentration was higher than in all the examined tissues, except for the liver, kidney, adrenal gland, and spleen. Additionally, Chan et al. examined the biodistribution of sulfonated chloroaluminum phthalocyanines (AlPCs) in colon carcinoma (Colo 26)-xenografted mice [33]. A positive correlation was found between the degree of intratumoral PS accumulation and the degree of sulfonation (increases hydrophilicity), where tetrasulfonated AlPC ($AlPCS_4$) was associated with the highest tumor concentration. In line with earlier studies, the sulfonated AlPCs extensively accumulated in the liver and spleen in an inversely proportional manner to the degree of sulfonation ($AlPCS_1 > AlPCS_2 > AlPCS_4 > AlPCS_3$). These studies reveal that PSs typically accumulate in all organs, where the liver, spleen, lungs, and kidneys are the most prominent sites for PS accumulation. However, the uptake of PSs by internal organs does not constitute a clinical issue on the condition that the PSs do not exhibit dark toxicity, given that the organs are usually impermeable to light from the outside. In contrast, the accumulation of PSs in the skin should be minimized to prevent severe adverse events as described in Section 2.1.

The biodistributive behavior of a PS described in the previous paragraph is dependent on its ability to: (1) refrain from aggregating, thereby avoiding preferential uptake in organs replete with cells of

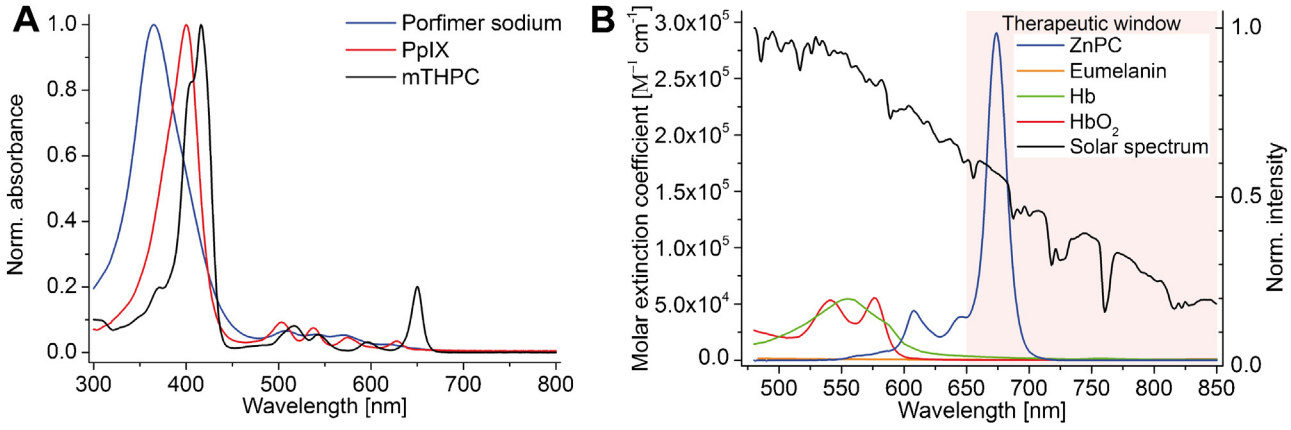

Fig. 3. (A) Normalized absorption spectra of porfimer sodium (in MilliQ), PpIX (in methanol), and mTHPC (in ethanol:MilliQ (49:51, v/v)). (B) Molar extinction coefficient of eumelanin [383], hemoglobin (Hb), oxyhemoglobin (HbO_2) [384], and zinc phthalocyanine (ZnPC, in pyridine). The solar spectrum (black trace) was recorded from direct sunlight in the 250–1,050 nm range and the spectrum was normalized to the maximum intensity (secondary *y*-axis). The pink area represents the therapeutic window for clinical PDT (650–850 nm).

the mononuclear phagocyte system (*i.e.*, liver, spleen, lung) [34], (2) bind to macromolecules, including low-density lipoprotein (LDL) [35], albumin [36], and/or lipid bodies that are abundantly expressed or metabolically exacted in the tumor environment [37,38], (3) undergo an increase in its lipophilicity (octanol/water partition coefficient or log *P*) in the more acidic tumor milieu [39], and (4) undergo pinocytosis and/or phagocytosis by tumor cells or by tumor-associated macrophages [40,41]. It should be noted that higher intratumoral PS concentrations do not necessarily correlate positively to treatment efficacy [42], as additional factors are involved in post-PDT tumoricidal mechanisms.

The binding of PSs to biomolecules (*e.g.*, LDL, transferrin, and/or albumin or their cognate receptors) and subsequent PS internalization [43] constitutes a propitious PS delivery route to tumor cells and may positively contribute to treatment outcome. The delivery mechanism is based on the tumor cell's demand for energy and building blocks required for cell sustenance and proliferation. Accordingly, tumor cells typically exhibit elevated expression of LDL- and transferrin receptors as well as enhanced albumin uptake [44–46]. Porphyrins, for instance, have a strong affinity for LDL, transferrin, and albumin [47]. Kessel found that in mice HpD associated with both LDL and HDL and that accumulation of HpD correlated with the relative number of LDL receptors present in the respective tissue [48]. This indicates that the LDL pathway serves as a delivery route of HpD and other PSs that associate with LDL to the tumor site. PCs (including ZnPC) also associate with LDL [49] and albumin [50], as a result of which these blood-borne biomolecules can be exploited as endogenous tumor-targeting PS carriers to enhance PS tumor-to-normal tissue ratios. Typically, the binding of biomolecule-conjugated PS to the corresponding cell receptor results in endocytic internalization of the PS and subsequent delivery to lysosomes [51].

2.2.2. Intracellular distribution

Cellular uptake of the PS, either by diffusion or *via* the endosomal-lysosomal pathway, is followed by translocation to distinct intracellular loci depending on the PS's chemical properties. PSs typically accumulate in various organelles, including mitochondria, lysosomes, endoplasmic reticulum (ER), and the plasma membrane. Factors that influence the subcellular localization include net ionic charge, log *P* value, and the amphiphilicity of the PS. Generally, anionic PSs (net charge of ≤ -2) end up in lysosomes, whereas cationic PSs are electrophoretically driven to the mitochondria [52] because the inner space of the mitochondrion is more negatively charged in tumor cells than in healthy cells [53]. Consequently, cationic PSs preferentially accrue and remain in the mitochondria of tumor cells [52,53]. Furthermore, hydrophilic PSs tend to localize to lysosomes [54,55], while lipophilic PSs preferentially localize to the plasma membrane and intracellular membranes, including the mitochondrial and ER membrane [56].

With respect to the intracellular localization of clinically used PSs, 5-ALA readily localizes to mitochondria, after which the mitochondrially produced PpIX translocates to the cytosol [57]. On the other hand, HpD temporarily accumulates in the plasma membrane but quite rapidly redistributes diffusely across subcellular membranes [58]. Its derivative, porfimer sodium, localizes to the plasma membrane as well, but also shows discrete association with the Golgi apparatus [59]. While mTHPC exhibits a preference for both the ER and Golgi [60], metallated PCs preferentially accumulate in the plasma-, Golgi-, and mitochondrial-membranes [61]. Studies have further shown that a PS exhibits spatiotemporal dynamics following uptake [57–60], which will ultimately affect the mode and extent of cell death upon PDT and hence therapeutic outcome (addressed in Section 2.3). For instance, mTHPC-treated human mesothelioma-bearing nude mice were susceptible to PDT-induced necrosis over a range of drug-light intervals (12 h to 4 days), although the therapeutic efficacy significantly differed among the different drug-light intervals irrespective of the tissue PS concentration [62].

2.3. Mechanisms of photodynamic therapy-mediated cell death as function of intracellular photosensitizer localization

PDT-induced mechanisms of cell death are in part dependent on the type of PS used and hence the intracellular localization of the PS. It is believed that type II photochemical reaction-derived $^1O_2$ is the most predominant type of ROS that is produced upon PDT [63,64], and, given that cytosolic $^1O_2$ diffusion is restricted to very short distances ($\sim$220 nm) [65], $^1O_2$ is only capable of oxidizing biomolecules in close proximity to its production site. The short diffusion distance of most ROS/RNS is beneficial to PDT insofar as ROS/RNS are usually not generated close to nuclear material [66] and hence do not result in sublethal oxidation of DNA and consequent malignant cell transformation (*e.g.*, by generation of 8-hydroxyguanine) in proximal non-cancerous cells, although exceptions do exist [67]. The short lifetimes of most ROS/RNS also preclude cell damage to peritumoral healthy tissue. Furthermore, PSs often target to more than one (sub) cellular location that, upon PDT, will result in concomitant activation of different cell death pathways, thereby limiting the efficacy of simultaneously activated cell survival pathways and stress responses after PDT (reviewed in [68]). In addition to intracellular PS localization, factors such as cell type, intracellular PS concentration, light dose, local oxygen tension, and residual energy status govern the eventual mode of cell death (*i.e.*, apoptosis *versus* necrosis) [69] (discussed in this section) and autophagy (addressed in Section 2.5).

As addressed in Section 2.2.2, the temporal distribution and intracellular localization of a PS is dynamic after initial cell entry. For instance, HpD, porfimer sodium, and ZnPC are initially confined to the plasma membrane, whereas at longer incubation times (>1–2 h) the PSs become more prominently localized in distinct perinuclear areas [57,58,61]. Accordingly, Hsieh et al. demonstrated that porfimer sodium accumulates in the plasma membrane directly after uptake but, at later time points, distributes to various intracellular compartments to ultimately end up mainly in the Golgi complex [59]. Irradiation of plasma membrane-localized porfimer sodium induced necrosis-like cell death, whereas irradiation of cytoplasmically localized porfimer sodium led to cell death that was characterized by cytoplasmic vacuole formulation and cell shrinkage in the presence of an intact plasma membrane.

For illustrative purposes, the effect of PS localization on PDT efficacy was evaluated in a so-called chase experiment. Human epidermoid carcinoma (A431) cells were incubated with ZnPC-encapsulating cationic liposomes (ZnPC-ETLs, Section 4.4.3) for 10 min, after which the liposome-containing medium was replaced with fresh culture medium. After specific time intervals the cells were treated with PDT and examined for cell viability, the results of which are presented in Fig. 4A. These data reveal that a higher photokilling capacity was achieved when A431 cells were irradiated at early time points after incubation ($<$4 h) compared to later time points (>4 h). In addition, confocal microscopy experiments were performed to examine the intracellular localization of ZnPC as a function of time. As shown in Fig. 4B, ZnPC is highly associated with mitochondria after 30 min and to a lesser extent after 4 h. At the 4-h time point, ZnPC exhibited a more diffuse localization, which was even more pronounced after 24 h. This is in line with the previously alluded to spatiotemporal dynamics of PSs following uptake, attesting to the importance of a well-defined PDT protocol and the fact that systematic modulation

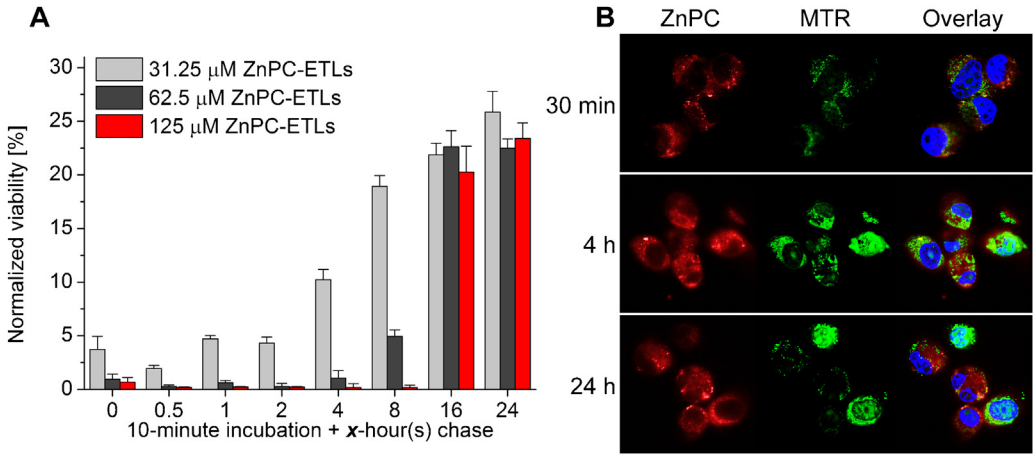

Fig. 4. (A) Effect of intracellular ZnPC dispersion time on PDT-induced cell death and spatiotemporal dynamics of intracellular ZnPC distribution. A431 cells were incubated with ZnPC-encapsulating cationic liposomes (ZnPC–ETLs) composed of DPPC:DC-chol:cholesterol:DSPE-PEG (66:25:5:4, molar ratio). ZnPC was incorporated at a ZnPC:lipid ratio of 0.003. Concentrations in the legend indicate final lipid concentrations. After 10 min, the medium was refreshed and cells were treated with PDT at the indicated time points (*x*-axis) and kept under standard culture conditions until the time of viability testing. (B) Intracellular ZnPC localization as a function of time. A431 cells were incubated with ZnPC-ETLs (ZnPC:lipid ratio of 0.030) for 10 min, after which the intracellular localization was visualized by confocal microscopy at different time points. ZnPC (red), MitoTracker Red (MTR, mitochondria, green), DAPI (nuclei, blue).

of this protocol can culminate in the activation of distinct cell death pathways.

2.3.1. Organelle-specific response

The plasma membrane is the first site that PSs encounter before entering a cell. As opposed to polar PSs, which are typically transported across the plasma membrane [70] due to the hydrophobic barrier effect imposed by the lipid bilayer, lipophilic PSs usually intercalate into the acyl chain region of the lipid bilayer. PDT-mediated ROS production in the plasma membrane can cause necrosis-like cell death that is preceded by loss of plasma membrane integrity due to peroxidation of unsaturated phospholipids [71] (usually dioxetane adduct formation when $^1O_2$ is produced and peroxide formation when oxygen radicals ($^{\bullet}OH$) are generated from type I photochemical reaction-derived O_2^- [72]). Oxidative modification of lipid constituents is associated with phospholipid packing defects and membrane permeabilization [73,74], ultimately leading to necrosis.

Lysosome-targeted PSs may induce ROS-triggered cell death in two ways: (1) *via* the discharge of cathepsins from lysosomes due to lipid (per) oxidation-mediated lysosome rupture and/or (2) PDT-induced relocalization of the PS to other organelles and subsequent induction of oxidative damage [75–77]. With respect to the first pathway, cathepsins exhibit proteolytic activity and are able to cleave BH3 interacting-domain death agonist (BID) to form truncated-BID (t-BID), which ultimately culminates in apoptosis. The second pathway comprises the redistribution of lysosomal PS molecules to other organelles such as the ER, mitochondria, and the Golgi apparatus, where site-specific damage is inflicted upon PDT.

Irradiation of PSs that localize to the ER (*e.g.*, 9-capronyloxytetrakis (methoxyethyl) porphycene (CPO) [78], hypericin [79], and mTHPC [60]) is believed to result in lipid (per) oxidation and consequent disruption of the ER membrane, accompanied by the release of Ca^{2+} as well as unfolded/misfolded proteins into the cytosol. The release of these compounds triggers Ca^{2+} signaling and the unfolded protein response (UPR), respectively. The net effect of Ca^{2+} signaling and UPR is the activation of calpain, caspase 4, and caspase 12 and ultimately caspase-mediated apoptosis [80]. Alternatively, excessive Ca^{2+} uptake by mitochondria may either lead to apoptogen release and loss of mitochondrial membrane potential followed by apoptosis [81] or mitochondrial permeability transition (MPT) ensued by ATP depletion and necrotic cell death [82]. Mitochondria-targeting PSs have been shown to rapidly induce apoptosis following photosensitization [83,84] as a result of mitochondrial lipid peroxidation. PDT-induced mitochondrial lipid peroxidation has been demonstrated with *meso*-tetrakis[4-(carboxymethyleneoxy)phenyl]porphyrin (T4CPP), a (non-exclusive) mitochondria-targeting PS [85], which resulted in $^1O_2$ generation and lipid peroxidation in isolated rat liver mitochondria and mitochondria of sarcoma 180 cells [86]. The release of pro-apoptotic factors ultimately leads to apoptosis when residual ATP levels are high enough to facilitate this energy-dependent mode of cell death [87]. Lastly, essentially three pathways have been described in which Golgi-targeting PSs induce cell death following PDT. First, ROS generation in the Golgi can cause oxidative modification and cleavage of Golgi proteins, leading to apoptosis as well as organelle fragmentation, which is an early apoptotic event [88,89]. Second, PDT-induced apoptotic signaling seems to involve the general vesicular transport factor p115. Following PDT, p115 was shown to undergo cleavage by caspase-3 and caspase-8 and to subsequently translocate to the nucleus, where it was able to stimulate apoptosis independently of Golgi fragmentation [90]. Third, a study revealed that 2,4,5,7-tetrabromorhodamine 123 bromide, a PS that selectively incorporates into the Golgi, produced both $O_2^{\bullet-}$ and $^1O_2$ after illumination and induced apoptosis *via* a calcium-dependent pathway that did not involve mitochondria [91]. These results indicate that Golgi-localized PSs induce apoptosis upon PDT *via* cell death pathways that in some respects differ from those triggered by other organelles afflicted by PDT, and may therefore amplify other PDT-induced cell death cascades.

2.4. Photodynamic therapy-mediated immune response: the role of damage-associated molecular patterns (DAMPs)

The initiation of an anti-tumor immune response is one of the main secondary mechanisms by which PDT orchestrates anti-tumor effects [92–94]. The requirement of the immune system in the PDT-induced removal of solid cancers has been clearly demonstrated in murine tumor models. Immunocompetent mammary sarcoma (EMT6)-bearing mice treated with porfimer sodium showed a complete response rate up to 90 days post-PDT [95]. In contrast, immunodeficient EMT-6 tumor-bearing mice treated under the same conditions only exhibited initial tumor

destruction. At later time points (>25 days), all immunodeficient mice had recurrent tumors [95]. These findings indicate that PDT results in direct tumor destruction, whereas prolonged tumor-free survival relies on a functional immune system. The PDT-induced anti-tumor immune response essentially comprises the initiation of a sterile inflammatory response, the maturation of dendritic cells (DCs), the presentation of tumor-associated antigens (TAAs) by DCs, the priming of a specific $CD8^+$ cytotoxic T-lymphocyte (CTL) response [96], and the removal of cancer cells, as summarized in Fig. 1 and further discussed in Section 2.4.3. Over the last years, it has become evident that damage-associated molecular patterns (DAMPs) exposed or released by PDT-treated cells play a major role in anti-tumor immunity by promoting sterile inflammation and DC maturation [97,98].

2.4.1. Damage-associated molecular patterns

DAMPs are specific molecules that emanate from stressed and dying cells and act as danger signals for the host immune system. In case of PDT, DAMPs play a crucial role in initiating and augmenting the pro-inflammatory response following therapy [99–101]. DAMPs have predominantly non-immunological functions and are normally sequestered within the cell. Once secreted, released, or surface-exposed by stressed, dying, and dead cells, the DAMPs are recognized by various receptors on immune cells, which includes the family of pattern recognition receptors (PRRs). The binding results in various pro-inflammatory effects such as maturation, activation, and antigen processing/presentation on antigen-presenting cells (APCs) such as DCs and macrophages [100]. An overview of the best characterized DAMPs that are released after PDT is provided in Fig. 5 in the context of the mode of cell death induced by PDT as well as the immunological effects.

2.4.2. Damage-associated molecular pattern release following photodynamic therapy

Heat shock proteins (HSPs) are chaperone proteins that facilitate the correct folding and transport of newly synthesized proteins. Increased expression of HSPs protects the cell under stress conditions by stabilizing unfolded proteins, promoting proteasomal degradation, and preventing apoptosis [102]. Moreover, in stressed cells the overexpressed HSPs can be surface exposed and/or released into the extracellular environment, where they exhibit immunostimulatory properties [102]. HSPs bind to numerous receptors, including Toll-like receptor 2 (TLR2), TLR4, and cluster of differentiation 91 (CD91) [103–106], resulting in the activation of various innate immune cells and anti-tumor immune responses. HSP-initiated signaling through TLR2 and TLR4 has been associated with nuclear factor kappa-light-chain-enhancer of activated B cells (NF-κB) activation (mediates a pro-inflammatory response), DC maturation, and cytokine production [107]. Signaling *via* CD91 results in phagocytosis, NF-κB activation, and antigen presentation [108–110]. HSPs are the best-characterized DAMPs associated with PDT and can be released extracellularly and/or exposed on the cell surface following PDT treatment [111–115]. It seems that PDT modalities that trigger apoptosis primarily instigate the surface exposure of HSPs such as HSP60 and HSP70 [111], whereas PDT regimes that primarily cause necrosis

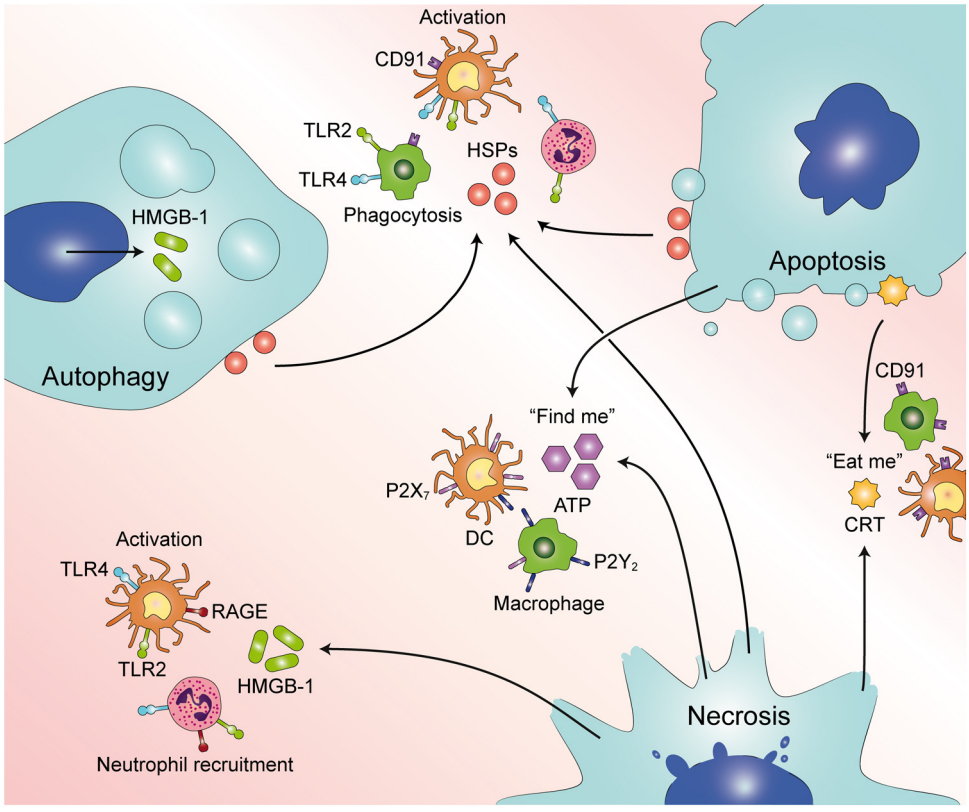

Fig. 5. Apoptotic cells (top right) expose and/or release heat shock protein 60 (HSP60) and HSP70. In addition, HSP70 is liberated by necrotic (bottom) and autophagic cells (top left). HSPs interact with immune cells *via* Toll-like receptor 2 (TLR2), TLR4, and CD91, which leads to immune cell activation. In addition, apoptotic cells express and/or release calreticulin (CRT), culminating in DC and macrophage activation *via* CD91. Necrotic cells release CRT as a result of membrane perturbation. Both apoptotic and necrotic cells release ATP that interacts with the $P2Y_2$ and $P2X_7$ receptor. Necrosis is accompanied by the release of high mobility group box-1 (HMGB-1), resulting in DC activation and neutrophil recruitment *via* TLR2, TLR4, and receptor for advanced glycation end products (RAGE) on these cells. In response to oxidative stress, HMGB-1 may act as an important regulator of autophagic cell death [385].

are associated with the extracellular release of HSPs such as HSP70 and HSP90 [116].

Calreticulin is a Ca^{2+}-binding protein that mainly resides in the lumen of the ER, where it functions as a chaperone and is involved in Ca^{2+} signaling [117,118]. Calreticulin exposed on the cell membrane (ecto-CRT) acts as an eat-me signal and engages in the recognition and phagocytic engulfment of apoptotic cells by APCs [119], a process mediated by CD91 on APCs [109]. Calreticulin also functions as one of the main DAMPs in immunogenic apoptosis (also termed immunogenic cell death, ICD) [120], as ecto-CRT facilitates the DC-mediated phagocytosis of cancer cells undergoing ICD, resulting in antigen presentation and an anti-tumor adaptive immune response [121]. Hypericin-PDT can for instance induce ICD through site-specific oxidative damage to the ER [122]. Both pre-apoptotic ecto-CRT and late apoptotic/secondary necrotic extracellularly released calreticulin have been found following hypericin-PDT *in vitro* [109,123,124].

High mobility group box-1 (HMGB-1) has been identified as a nuclear DNA-binding protein involved in DNA organization and gene transcription [125]. HMGB-1 can be actively secreted by immune cells [126,127] or passively released by necrotic cells [128,129]. Extracellular HMGB-1 acts as a DAMP by inducing inflammation [129], stimulating cytokine production [130,131], enhancing neutrophil recruitment [132], and activating DCs [133]. More recently, it has been demonstrated that apoptotic [134] and autophagic [135] cells also release HMGB-1. HMGB-1 exerts its pro-inflammatory functions through interactions with a range of receptors, including but not limited to receptor for advanced glycation end products (RAGE), TLR2, and TLR4 [136,137]. Very few studies have been conducted on the release of HMGB-1 from PDT-treated cells and the relative importance of this DAMP in the PDT-induced immune response. Korbelik et al. reported that PDT with porfimer sodium resulted in the release of HMGB-1 from necrotic cells into the blood stream of mice as early as 1 h post-PDT [138]. A study by Tracy et al. showed that HMGB-1 is one of the DAMPs released from necrotic cells treated with PDT using 2-(1-hexyloxyethyl)-2-devinylpyropheophorbide-a (HPPH, localizes to mitochondria) or HPPH-galactose (localizes to lysosomes) [116]. However, cells undergoing apoptotic cell death did not release significant amounts of HMGB-1 following PDT with HPPH or HPPH-galactose [116]. Moreover, no significant HMGB-1 release was detected from T24 cells treated with hypericin-PDT under ICD-inducing conditions [124], altogether suggesting that HMGB-1 signaling after PDT is dependent on the mode of cell death.

Extracellularly released ATP has been identified as a very potent find-me signal for monocytes, macrophages, and DCs [139]. Elliott et al. reported that the ATP/UTP receptor $P2Y_2$ on phagocytes is a critical sensor for extracellular ATP, which in turn promotes phagocyte recruitment [139]. Moreover, ATP has been identified as a ligand for $P2X_7$ purinergic receptors on DCs. ATP binding to this receptor can lead to the activation of the NLR family, pyrin domain containing 3 (NLRP3) inflammasome; a caspase 1 activation complex that stimulates DC maturation and subsequent secretion of IL-1β, an important chemokine for the priming of T cells and hence the induction of an anti-tumor adaptive immune response [140,141]. Garg et al. showed that hypericin-PDT-treated human bladder carcinoma (T24) cells undergoing ICD secrete ATP in the pre-apoptotic phase [109]. Unfortunately, the extracellular release of ATP following PDT has only been investigated using hypericin as PS in the paradigm of ICD [109,124]. It should be noted that oxidized ATP has been reported to act as an inhibitor of $P2RX_7$, thereby impeding proliferation and effector functions of T cells [142]. This means that ATP belongs to the class of redox-sensitive DAMPs such as HMGB-1, which are susceptible to oxidation-induced inactivation in terms of immunostimulatory properties.

2.4.3. Photodynamic therapy-induced anti-tumor immunity

The mechanisms whereby PDT activates and potentiates anti-tumor immunity have been extensively researched. However, the exact molecular mechanisms that lead to the PDT-induced enhancement of anti-tumor immunity have yet to be fully elucidated. Here, a brief overview of the mechanisms involved in the transition from focused, PDT-induced oxidative stress to a systemic anti-tumor immune response is addressed. For more detailed reports on PDT-induced anti-tumor immunity the readers are referred to other reviews [96,115,143–145].

PDT-induced oxidative stress results in extended tumor tissue injury. The host perceives this injury as localized trauma and is provoked to launch an inflammatory response mediated by the innate immune system [146]. DAMPs released by PDT-stressed cells act as danger signals intended to assist the host in recognizing the injured self. This PDT-induced activation of the innate immune system constitutes a multistep process that involves the initiation of a massive, acute, and sterile inflammatory response, cytokine release, complement activation, and recruitment and activation of innate immune cells (*e.g.*, neutrophils, DCs, macrophages) [96]. Different DAMPs play major roles in these processes (Section 2.4.2). Ultimately, this rapidly expanding, relatively non-specific innate immune response gives rise to the much slower developing adaptive immune response and hence anti-tumor immunity. The anti-tumor immune response is initiated by the presentation of TAAs, released from dying and dead cancer cells, by DCs to naive T cells, resulting in the generation of tumor-specific CTLs that attack and remove residual cancer cells. Moreover, the DAMPs interact with various receptors expressed by DCs (Fig. 5), which stimulates DC maturation that culminates in increased surface levels of major histocompatibility complex (MHC) classes I and II, and other co-stimulatory proteins [147], rendering fully mature DCs much more effective at presenting TAAs to T cells.

The involvement of CTLs in PDT-mediated anti-tumor immunity was first observed by Canti et al. [148]. In a subsequent study it was demonstrated that the growth inhibition of EMT6 tumors after porfimer sodium-mediated PDT is dependent on CTLs [149]. Recent studies showed that PDT-treated tumor cells stimulate DCs and their ability to present TAAs, resulting in the generation of tumor-specific CTLs [123,124].

The involvement of the adaptive immune system, and more specifically DCs and T cells, in PDT-induced tumor eradication enables the manifestation of abscopal effects, which is absolutely critical for good clinical outcomes of PDT given that PDT may not affect all cancer cells in a tumor equally (Section 2.1) and PDT-subjected cancer cells may activate survival pathways to revert cell death signaling (Section 2.5). The eradication of distant tumor cells that were not exposed to PDT has been observed not only in a murine syngeneic cancer model [149], but also in a clinical setting [150]. Other clinical studies that point towards the potency of PDT to induced anti-tumor immune responses have been published for vulval intraepithelial neoplasia [151], basal cell carcinoma [152], and both actinic keratosis and Bowen's disease [153].

2.5. Photosensitizer concentration- and light dosage-dependent cell responses

Two important factors in the cell's response to PDT are intracellular PS concentration and fluence rate (W/cm^2 in an infinitesimal tissue volume) and, by inference, the extent of ROS generation and consequent degree of oxidation. Tumor cells can cope with PDT-induced damage by activating one or more of several possible survival- and stress-response pathways, comprising (1) an immediate early stress response that promotes tumor cell proliferation, (2) an antioxidant response that results in *de novo* synthesis of antioxidants, (3) a hypoxia stress response that

restores energy homeostasis and induces angiogenesis, (4) a pro-inflammatory signaling response that governs angiogenesis and invasion, (5) an ER stress response that aims to restore ER homeostasis, and (6) autophagy that involves recycling of damaged cell components as part of promoting cell survival. The first five cell survival pathways have been reviewed in detail by Broekgaarden et al. in light of PDT [68]. The ER stress response following PDT [80,154] has not been completely characterized and likely applies predominantly to PSs that localize to or near the ER given the short diffusion distance of ROS/RNS. Consequently, the PS concentration- and light dose-dependent cell responses will be illustrated in the context of autophagy, which constitutes a better elucidated and more ubiquitous response mechanism than the ER stress response. For all responses, however, an oxidative damage threshold generally applies that governs the fate of a cell in that cells must possess sufficient residual metabolic capacity to remediate oxidative damage. When the oxidative damage threshold is crossed and the level of damage exceeds the restorative capacity, cells will typically actualize cell death programs.

Autophagy generally constitutes a cytoprotective mechanism through which cells recycle damaged and degraded organelles. Under certain conditions, autophagic pathways may be directed at promoting autophagic cell death upon continued exposure to stress conditions (reviewed in [155]). With respect to PDT, Kessel and Reiners [156] demonstrated that at lower PS dosages, PDT with CPO (targets to the ER) and mesochlorin (localizes to mitochondria) induced pro-survival autophagy, whereas both autophagic cell death and apoptosis were induced at higher dosages of either PS at equal radiant exposure. Cell death was presumably caused by loss of B-cell CLL/lymphoma 2 (BCL2) [157,158], which is confined to the mitochondria and/or ER, insofar as photo-oxidative loss of BCL2 can trigger both apoptosis and autophagy. As oxidative stress is known to be destructive to BCL2 [158,159], the oxidation-mediated release of autophagy-regulated protein beclin 1 (BECN1) from its BCL2 complex may induce autophagy following PDT [160,161] and consequent cell death.

Comparable results have been reported for the mode of autophagy as a function of light dosage. Low-dose PDT is typically associated with pro-survival autophagy, during which cells (L1210 cells, murine leukemia) recycle damaged and degraded cell organelles to remediate injury and facilitate survival [156,162]. Correspondingly, low-dose PDT with mitochondria- or ER-targeting PSs (CPO and mesochlorin, respectively) resulted in a greater degree of cell death when autophagy-related protein 7 (ATG7), a protein involved in autophagy induction, was silenced in a knockdown derivative cell line (L1210/Atg7^{-}) [156,163]. Conversely, higher-dose PDT induced autophagic cell death rather than survival and augmented the extent of photokilling [156,163]. It should be noted that these effects may in part be attributable to oxidative stress-dependent debilitation of autophagosome formation, particularly when ER- or mitochondria-targeted PSs are used [156,163].

Taken altogether, these findings indicate that autophagy contributes to cell survival after low-dose PDT but cell death after high-dose PDT. Since it has been postulated that there is an equilibrium state between apoptosis and autophagy [164,165], suppression of autophagy following PDT may exacerbate oxidative stress-induced cell demise.

3. Metallated phthalocyanines as photosensitizers for photodynamic therapy

3.1. Metallated phthalocyanines

Metallated PCs are synthetic second-generation PSs comprising a fully conjugated, symmetrical macrocyclic structure containing a centrally positioned, coordinated, multivalent metal cation such as Al^{3+}, Ga^{3+}, Zn^{2+}, Cu^{2+}, Fe^{2+}, or Co^{2+} (Fig. 6A–D). The type of metal dictates the photophysical properties of the PS [166]; closed-shell diamagnetic metal-containing PCs (Al^{3+}, Ga^{2+}, Zn^{2+}) exhibit higher triplet state quantum yields (Φ_T) and longer-lived triplet states than paramagnetic metal-containing PCs (Co^{2+}, Cu^{2+}, Fe^{2+}) [167].

The diamagnetic PCs, and particularly ZnPC and AlPC, are very suitable PSs for PDT due to several pronounced advantages. Firstly, these PCs have a molar absorptivity (ε) in the order of $\sim 10^5\ M^{-1}\ cm^{-1}$ and a strong Q-band in the mid-red wavelength range (absorption maximum at ~674 nm for AlPC and ZnPC), *i.e.*, well within the therapeutic window (650–850 nm) (Fig. 6E–I) [168]. Secondly, the non-functionalized diamagnetic PCs exhibit Φ_Ts of 0.3–0.5 [169] and triplet state lifetimes of >200 μs (reviewed in [170]). Moreover, the triplet states are amply energetic (1.21–1.31 eV) to generate $^1O_2$ (0.98 eV) [171], altogether accounting for considerable $^1O_2$ generation during PDT (Fig. 6J–M) relative to other PSs, and particularly the first-generation PSs. Thirdly, the synthesis of PCs is simple, cheap, and versatile in that any di- or tri-valent metal cation can be incorporated and the six-membered ring of the isoindole groups can be modified by conjugation of functional groups (*e.g.*, sulfonate) to alter the chemical properties (*e.g.*, log *P*) without drastically affecting the photophysical properties (Fig. 6A–E). In some instances, however, functionalization may change the photochemical properties, as was observed for tetrasulfonated ZnPC ($ZnPCS_4$) (Fig. 6L) but not for $AlPCS_4$ (Fig. 6 M).

3.2. Advantages of metallated phthalocyanines over conventional photosensitizers

An important advantage of metallated PCs over clinical first-generation PSs such as HpD, porfimer sodium, and 5-ALA as well as the second-generation PS mTHPC is that the PC Q-band maximum of ~675 nm lies more favorably in the therapeutic window (Fig. 3B and Fig. 6E), accounting for greater optical penetration depth and more homogeneous photon distribution throughout the target tissue. Diamagnetic PCs also exhibit an ε that is several orders of magnitude greater than that of traditional PSs (Fig. 2E), resulting in more effective photon absorption at a wavelength at which there is less competitive absorption and scattering by tissue [4]. A higher ε in combination with a larger Φ_T further lowers the intratumoral PS concentration that is required for a therapeutic response, thereby reducing PDT-related side effects such as phototoxicity as a lower PS dose suffices [172].

Another beneficial aspect of PCs is that they do not exhibit notable toxicity [173]. With respect to phototoxicity, it is well-documented that the clinically approved PSs elicit considerably longer photosensitivity, and thus potential phototoxicity, than the metallated PCs, which have not been associated with skin phototoxicity to date (Table 1). The photosensitivity of HpD and porfimer sodium, for example, extends to as much as 4–12 weeks after PS administration, which corresponds to the time patients must be kept away from light exposure. This is mainly due to a combination of factors, including long elimination half-life of the PSs (Table 1), long clearance times from the skin (Table 1), and a relatively unfavorable spectral overlap with sunlight (Fig. 3B) [174,175]. The photosensitivity of mTHPC is also quite extensive, namely 2–4 weeks, while that of 5-ALA is clinically manageable. However, the use of 5-ALA is associated with other drawbacks related to its photophysical properties (Fig. 2E) and unfavorable pharmacokinetics (*i.e.*, low tumor:healthy tissue ratio) after systemic administration (Table 1), as addressed below.

In regard to the toxicity profiles of the clinically approved PSs, Berlanda et al. studied the dark toxicity of mTHPC (both Foscan and its polyethylene glycol (PEG)-conjugated derivative, Fospeg), porfimer sodium, and 5-ALA, amongst others, in A431 cells

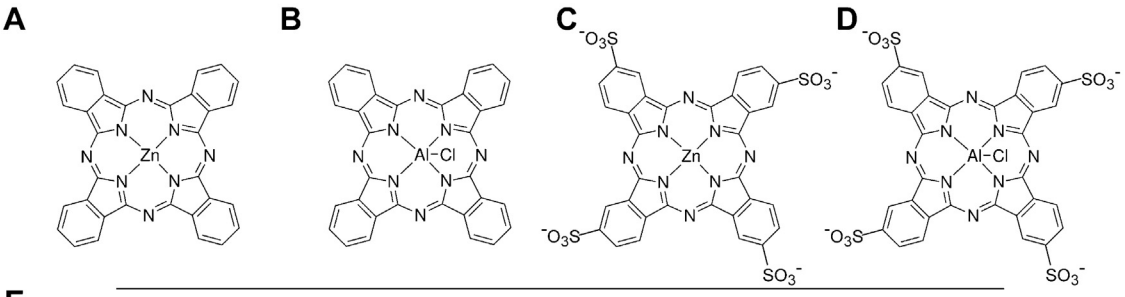

E

	Solubility	Log *P*	Q-band maximum [nm]	ε at Q-band maximum [$M^{-1} \cdot cm^{-1}$]	Triplet state quantum yield	Singlet oxygen quantum yield	[Ref]
(A) ZnPC	Lipophile	8.50 (±2.62)	674	274,000	0.57	0.70	[33, 86]
(B) AlPC	Lipophile	8.91 (±2.65)	680	126,000	0.41	0.34	[33, 254]
(C) $ZnPCS_4$	Hydrophile	-1.00 (±2.53)	690	295,000	0.47	0.43	[254, 256]
(D) $AlPCS_4$	Hydrophile	-0.74 (±2.65)	675	158,000	0.38	0.36	[36, 254, 256]

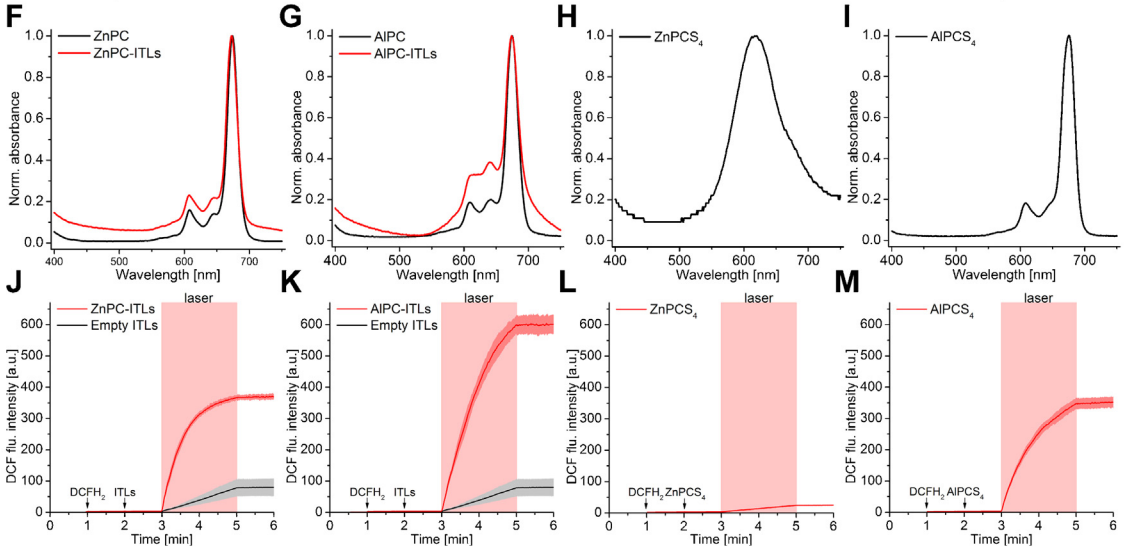

Fig. 6. Chemical structures of ZnPC (A), AlPC (B), tetrasulfonated ZnPC ($ZnPCS_4$) (C), and tetrasulfonated AlPC ($AlPCS_4$) (D). The physicochemical properties are provided in (E). Estimated octanol/water partition coefficients (log *P*) were obtained from [382]. Normalized absorption spectra are provided of ZnPC dissolved in pyridine and ZnPC encapsulated in liposomes (ZnPC-ITLs, composed of DPPC:DSPE-PEG (96:4, molar ratio) at a ZnPC:lipid ratio of 0.003) (F), AlPC dissolved in pyridine and AlPC encapsulated in liposomes (AlPC-ITLs, composed of DPPC:DSPE-PEG (96:4, molar ratio) at an AlPC:lipid ratio of 0.003) (G), tetrasulfonated ZnPC ($ZnPCS_4$) in MilliQ (H), and tetrasulfonated AlPC ($AlPCS_4$) in MilliQ (I), both at a 1.5-μM final PS concentration. The ROS-generating capacity of ZnPC-ITLs (J), AlPC-ITLs (K), $ZnPCS_4$ in physiological buffer [74] (L), and $AlPCS_4$ in physiological buffer (M) during PDT (pink area) was determined using the oxidation-sensitive fluorogenic probe 2′,7′-dichlorodihydrofluorescein ($DCFH_2$), prepared as described in [386]. The mean ± SD DCF fluorescence intensities are plotted for $n = 3$ experiments and the experiment was carried out according to [74].

[176]. The lethal 50% dose (LD_{50}) for non-irradiated Foscan, Fospeg, porfimer sodium, and 5-ALA was 8, 246, 5, and 9040 μM, respectively. The LD_{50} value for $AlPCS_4$ could not be calculated as its dark toxicity did not fall below 50% at concentrations up to 200 μM. Similarly, Amin et al. found no dark toxicity of $AlPCS_4$ up to a concentration of 500 μM in bladder cancer (T24) cells [177]. A summary of the dark toxicity LD_{50} values is provided in Table 1. In addition, PCs appear to be non-genotoxic compounds. PDT with AlPC induced considerable oxidative damage and cell death in human oral keratinocytes *in vitro*, but without inducing a genotoxic response, as confirmed by the comet assay [178]. These results were corroborated in another study employing AlPC-PDT [179]. Similarly, $ZnPCS_4$ is not genotoxic upon PDT *in vitro* [180], although its utility in PDT is limited due to the relatively poor ROS-generating capacity (Fig. 6L).

With respect to clinically approved PSs, mTHPC did not induce DNA damage in human myeloid leukemia (K562) and nasopharyngeal carcinoma (CNE2 and HK1) cells under dark conditions or following PDT [181,182]. In contrast, considerable DNA damage was observed in K562 cells after HpD-PDT [181]. Other *in vitro* studies showed that treatment of cells with 5-ALA resulted in mutagenic effects after exposure to visible light [183]. Chromosomal aberrations and formation of micronuclei were also detected under dark conditions [184]. Of note, as the photoactive product of 5-ALA, namely PpIX, is produced in mitochondria, it is conceivable that most of the genomic aberrations might be confined to

mitochondrial DNA, which is a typical target for DNA modifications, even during regular energy metabolism [185].

The safety:efficacy ratio of a compound is also an important parameter in pharmacology, as it reflects the 'clinical worthwhileness' of a drug. In case of PDT, this ratio can be calculated by dividing the PS LD_{50} (*i.e.*, dark toxicity) by the PS LD_{50} following PDT. The safety:efficacy values for Foscan, Fospeg, porfimer sodium, and 5-ALA in A431 cells were 268, 4695, 3, and 23, respectively [176], whereby the lower values indicate a less favorable balance between dark toxicity and PDT efficacy. The safety:efficacy ratio of $AlPCS_4$ could not be derived in this study, as the dark toxicity was too low to calculate an LD_{50} value. The safety:efficacy ratio of Foscan in two biliary tract cancer cell lines (gall bladder cancer and bile duct cancer cells) was 356 and 410, respectively [186].

Moreover, the tumor:healthy tissue ratio is a critical *in vivo* pharmacokinetic parameter because it relates PDT efficacy to biodistribution and potential (photo)toxicity. Theoretically, a high tumor:healthy tissue ratio is likely to improve therapeutic outcome and reduce drug accumulation in healthy tissue, which is inherently proportional to the level of undesired side effects. For example, porfimer sodium exhibited a tumor:skin ratio of only 1.7:1 in a hamster melanoma model [187]. Similarly, intravenously or intravesically injected 5-ALA resulted in a tumor:bladder wall ratio of 2:1 in an orthotopic rat bladder tumor model [188]. Slightly higher tumor:normal adjacent mucosa ratios of 2–3:1 were observed for mTHPC after intravenous injection in patients with different types of solid cancer [189]. In case of diamagnetic PCs, the majority of studies on these PSs have employed liposomal formulations (discussed in the next section) as a delivery vehicle. In a fibrosarcoma mouse model using ZnPC liposomes, tumor:muscle ratios (muscle tissue adjacent to the fibrosarcoma) of 7.5:1 [190] and 9:1 [191] were found 18 to 24 h post-injection, respectively. Furthermore, Chan and colleagues showed that the uptake of sulfonated AlPC in Colo 26 tumor-bearing mice was dependent on the degree of sulfonation [33]. Whereas $AlPCS_4$ accumulated in tumors at a 10:1 tumor:adjacent tissue ratio, lower ratios were observed with a lower degree of sulfonation. Accordingly, monosulfonated AlPC appeared to have the lowest tumor:adjacent tissue ratio (*i.e.*, <2:1). Similar tumor:tissue ratios (*i.e.*, 10:1) for $AlPCS_4$ were observed in mice bearing melanoma tumors, which peaked 18 h after systemic administration [192]. The tumor:tissue ratios of the most common clinical and experimental PSs are listed in Table 1.

Lastly, the high log*P* value of metallated PCs (Fig. 6E) is responsible for the distribution of these PSs to a wide variety of lipophilic compartments (Sections 2.2.2 and 4.4.2). PDT of metallated PC-containing cells will therefore induce oxidative damage at multiple intracellular sites that are critical to cell viability and function (Section 2.3). As addressed in Section 2.3.1, the mode of cell death depends on intracellular PS localization and thus the origin of PDT-induced damage. Given that metallated PCs localize to multiple intracellular sites, PDT with these PSs will activate different modes of cell death that will ultimately result in necrotic, apoptotic, necroptotic, and/or autophagic cell death. The concomitant activation of different cell death pathways will therefore increase the probability that a tumor cell is terminated after PDT through the 'cumulative cell death induction effect' rather than salvaged by activated survival and/or stress response mechanisms [68]. Consequently, the cytotoxic potential of irradiated PCs is theoretically higher per mole compound in a cell than for PSs that target to a single location, such as lutetium texaphyrin [193], verteporfin [194], and hypericin [79], where only one specific cell death induction pathway dominates.

In the final analysis, compared to clinically approved PSs, diamagnetic PCs have a more red-shifted Q-band maximum and superior molar absorptivity, which facilitates deeper light penetration, a higher efficiency of light absorption at clinically relevant wavelengths, and extensive ROS generation at comparably lower intratumoral PS concentrations. The generation of ROS occurs at multiple cellular locations, which enables optimal PDT efficacy due to the cumulative cell death induction effect. Moreover, diamagnetic PCs exhibit no dark toxicity or genotoxicity, even after irradiation. Lastly, the diamagnetic PCs are associated with a higher safety:efficacy ratio and tumor:healthy tissue ratio, altogether making these metallated PCs more suitable for PDT compared to conventional PSs. Unfortunately, a direct comparison regarding the therapeutic efficacy of clinical PSs and diamagnetic PCs could not be made inasmuch as the effectiveness (*e.g.*, LD_{50} value) is dependent on several variables such as irradiance, cumulative radiant exposure, wavelength/molar absorptivity, and cell/tumor tissue type, which widely differ among studies.

4. Multi-targeted photosensitizer-encapsulating nanoparticulate delivery systems for photodynamic therapy

A major obstacle in oncopharmacology is specific delivery of drugs to the tumor, as is for instance problematic with most orally or intravenously administered chemotherapeutics. The unspecific uptake of chemotherapeutic agents by healthy tissue causes all sorts of sequelae that impose a significant burden on patient well-being and quality of life. As a result, numerous chemotherapeutic agents have been encapsulated in nanoparticulate drug delivery systems to improve drug solubility, to ensure improved delivery to the tumor and enhanced therapeutic efficacy, and to reduce chemotherapy-associated side effects (reviewed in [195]).

4.1. Non-liposomal photosensitizer carrier and delivery systems

Nanoparticulate PS delivery systems can be classified into lipid-based and non-lipid based delivery systems. Both types of delivery systems are described in Table 2, including the physico-chemical attributes as well as the advantages and disadvantages in terms of PS delivery. The lipid-based delivery systems include LDL, micelles, and solid lipid nanoparticles, all of which are water-compatible carriers suitable for the encapsulation of hydrophobic PSs (Table 2). LDL is an endogenous blood-borne particle composed of (free and esterified) cholesterol, phospholipids, triglycerides, and a single apoliporotein B-100 that the body uses for the transport of lipophilic biomolecules (*e.g.*, cholesterol) to cells. Micelles comprise small-diameter particles composed of a phospholipid monolayer that, in case of normal-phase micelles, contain an acyl chain-based core and the hydrophilic head groups positioned at the phospholipid–water interface. Solid lipid nanoparticles are composed of a solid lipid core that is stabilized by a surfactant layer, albeit the composition can be highly variable. The micelles and solid lipid nanoparticles can be functionally modified to accommodate a specific pharmacokinetic purpose, including PEGylation to enhance circulation half-life [196,197] and the conjugation of ligands for *e.g.*, immunotargeting [198,199], whereas this is less applicable to LDL due to its intrinsic targeting properties. LDL has been employed for intratumoral PS delivery [200,201] *via* its cognate LDL receptor (LDLR). However, this delivery system may lack targeting specificity inasmuch as the LDLR is not exclusively present on tumor cells and a variety of malignant tissues lack overexpression of LDLR (reviewed in [202]).

Of the non-lipid based nanoparticles, dendrimers, polymeric micelles, and polymers are capable of encapsulating hydrophobic as well as hydrophilic PSs (Table 2). Dendrimers are supramolecular assemblies typically composed of branched polyaminoamides that can be synthesized in a controlled manner with a high monodispersity (reviewed in [203,204]). However, the *in vivo* toxicity data for dendrimers is currently unavailable, which limits

Table 2
Overview of lipid- and non-lipid-based nanoparticles that have been used for the delivery of photosensitizers. Abbreviations: $AlPCS_4$, tetrasulfonated chloroaluminumphthalocyanine; Cl_2SiPC, dichlorosilicon phthalocyanine; HexSiPc, bis(tri-*n*-hexylsiloxy)silicon phthalocyanine; LDLR, low-density lipoprotein receptor; Pc 4, silicon phthalocyanine 4; SiPC, silicon phthalocyanine.

Lipid-based	Size	Carrier material	Encapsulated PS	(Dis) advantages	[Ref]
Liposomes	15–1000 nm	Hydrophobic Hydrophilic	5-ALA [321], AlPC [255], $AlPCS_4$ [257], mTHPC [236], porfimer sodium [322], temocene [323], ZnPC [74]	+ Versatility + Non-toxic + Payload – Stability – PS transfer	[324]
Low-density lipoprotein	18–25 nm	Hydrophobic	Bacteriochlorin e6 bisoleate [325], hematoporphyrin [200], SiPC [326], ZnPC [201]	+ Endogenous carrier + Drugs are protected + Circulation time – Specificity – Requires overexpression of LDLR	[202]
Micelles	2–20 nm	Hydrophobic	Cl_2SiPC [327], HexSiPC [327], temocene [328], ZnPC [329]	+ Synthesis + Shelf-life + Low viscosity – Low solubilization – Potential surfactant toxicity	[330]
Solid lipid nanoparticles	50–1000 nm	Hydrophobic	Hypericin [331], mTHPC [332]	+ Easy to scale up + Water-based technology + Biocompatibility – Particle growth – Drug loading capacity	[333]
Other					
Dendrimers	1–100 nm	Hydrophobic Hydrophilic	5-ALA [334], SiPC [335]	+ Monodispersity + Versatility + High payload – Lack of in vivo toxicity data – Preparation is laborious	[203]
Gold nanoparticles	1–100 nm	Hydrophobic Hydrophilic	5-ALA [336], PpIX [337], ZnPC [338]	+ Physico-chemical properties of gold + Synthesis + Versatility – Potential toxicity – Costs	[339]
Polymeric micelles	10–100 nm	Hydrophobic Hydrophilic	mTHPC [340], Pc 4 [341], porfimer sodium [342], ZnPC [343]	+ Structural stability + Payload + Low toxicity – Synthesis – No universal incorporation method	[344]
Polymeric nanoparticles	10–1000 nm	Hydrophobic Hydrophilic	5-ALA [345], mesochlorin e6 [346]	+ Versatility + Biocompatibility + Synthesis – Encapsulation efficiency – Stability	[208]
Quantum dots	2–100 nm	Hydrophobic Hydrophilic	$AlPCS_4$ [214], chlorin e6 [347], PpIX [348], Rose Bengal [349]	+ Unique optical properties + Tunable surface properties – Limited knowledge on clinical use – Potential toxicity – Compatibility in biological environments	[350]

the prospects for clinical applicability. Polymeric micelles are nanoparticles that are usually composed of amphiphilic polymers, including PEG-based phospholipid conjugates and poloxamers [205]. Although polymeric micelles have a high structural stability and low toxicity (Table 2), the development of these nanoparticles may be hampered by technical difficulties in specific polymer synthesis and efficient drug incorporation methods on an industrial-scale basis [206]. Alternatively, polymeric nanoparticles are generally composed of biodegradable polymers, including polyglycolic acid, polylactic acid, and poly(lactic-*co*-glycolic acid), which are generally non-toxic [207]. Although polymeric nanoparticles may be attractive as a delivery vehicle, there are still some difficulties to overcome, including a poor encapsulation efficiency [208,209] and a poor PS stability in solution [210].

In contrast, gold nanoparticles and quantum dots are nanoparticles with unique physico-chemical and optical properties, respectively [211]. Gold nanoparticles that are coupled to PSs have been associated with increased $^1O_2$ upon irradiation as a result of surface plasmon resonance (reviewed in [212]), allowing these particles to be used for PDT as well as photothermal therapy. Moreover, the excitation wavelength is tunable to wavelengths in the far red [213], enabling deep light penetration and relatively homogenous irradiation of bulkier tumors. Quantum dots are semiconductor nanocrystals that function as light acceptor for subsequent PS activation *via* fluorescence resonance energy transfer [214]; the PS therefore has to be conjugated to the quantum dots in order to achieve a photodynamic effect. Although gold nanoparticles and quantum dots are attractive for PDT, the nanoparticles may be quite toxic (Table 2) and therefore limited in terms of clinical applicability.

Inasmuch as the nanoparticulate PS delivery systems addressed in this section may not be ideal for clinical PDT (Table 2), the

following sections will focus on liposomes for intratumoral PS delivery. Although liposomes are not superior to the above-mentioned PS delivery systems per se, the combination of advantages (next section) makes liposomes very suitable for PS targeting to tumors.

4.2. Liposomal photosensitizer carrier and delivery systems

To date, the Food and Drug Administration has approved liposomal formulations of two anti-cancer drugs, daunorubicin and doxorubicin, and various anti-cancer formulations are under evaluation in clinical trials [215,216]. It is somewhat surprising that none of these drugs include a PS, given the fact that the clinical implementation of PDT is primarily hampered by ethical issues related to phototoxicity (which can be alleviated by encapsulation) while the therapy is very effective for several cancer types (Section 1). At this moment, clinical phase I/II trials with liposome-encapsulated PSs are being conducted exclusively with verteporfin (Fospeg). Of note, it is not expected that PDT with liposome-encapsulated first-generation PSs will result in better therapeutic outcomes compared to liposome-encapsulated second-generation PSs, given that the majority of drawbacks of the first-generation PSs as addressed in Section 3.2 will remain an issue.

In case of PDT with second-generation PSs (metallated PCs), liposomal encapsulation (in which case it is referred to as a third-generation PS) is advantageous [217] for several reasons. First, liposomes are able to encapsulate hydrophilic and lipophilic molecules and hence render the highly lipophilic second-generation PSs compatible with plasma. Second, liposomal incorporation resolves PS aggregation in aqueous solutions such as biological fluids, which negatively affects Φ_T and ROS generation [218–220]. Third, due to the high payload, a single liposome could theoretically deliver a sufficient amount of PS to a cell to cause lethal oxidative stress following PDT. As a result, less liposomal PS can be administered to patients to achieve equal intratumoral PS levels compared to unencapsulated PS. Moreover, unencapsulated PSs have a tendency to extravasate and accumulate in the skin. Liposomal encapsulation minimizes PS accumulation in the skin [221,222], which will not only reduce phototoxicity but also further improve PS bioavailability for tumor targeting. Fourth, additional pharmacological compounds can be co-encapsulated in a single delivery system (in which case it is referred to as a fourth-generation PS) for further improvement of therapeutic efficacy. Finally, in addition to the inherent non-toxicity of neutral phospholipids [223,224], *i.e.*, typically the main lipid constituents of liposomal drug delivery systems [225], liposomes can easily be modified compositionally to facilitate the unique prerequisites of the drug delivery system and to accommodate a specific physiological context. For instance, liposome uptake by cells of the mononuclear phagocyte system can be considerably forestalled by proper sizing [226] and by the conjugation of PEG to component phospholipids, usually phosphatidylethanolamine [227–230]. It has been proposed that (1) the presence of a "dense conformational cloud" by the PEG polymers over the liposome surface [231], (2) the repulsive interactions between PEG-grafted membranes and blood constituents [232], (3) the hydrophilicity of

Table 3
Summary of experimental *in vivo* studies with immunoliposomes. Abbreviations: CHEMS, cholesteryl hemisuccinate; Chol, cholesterol; DOPE, dioleoyl phosphatidylethanolamine; DSPC, distearoyl phosphatidylcholine; EGFR, epidermal growth factor receptor (HER1); EPC, egg phosphatidylcholine; Fab antigen-binding fragment; GD2, ganglioside GD2; HBEGF, heparin-binding EGF-like growth factor; HPTS, 8-hydroxypyrene-1,3,6-trisulphonic acid; HSPC, hydrogenated soy phosphatidylcholine; IGF-1R; insulin-like growth factor 1 receptor; ILs, immunoliposomes; mAb, monoclonal antibody; mPEG, methoxy polyethylene glycol; MT1-MMP, membrane type-1 matrix metalloproteinase; PC, phosphatidylcholine; PDP-PEG-DOPE, 3-(2-pyridyldithio)propionic acid-polyethylene glycol-DOPE; PEG-PE, polyethyleneglycol-phosphatidylethanolamine; POPC, palmitoyloleoyl phosphatidylcholine; scFV, single-chain variable fragment; SM, egg sphingomyelin; VCAM-1, vascular cell adhesion molecule 1; VEGFR, vascular endothelial growth factor receptor.

Target	Antibody	Cancer subtype	Liposomal composition	Drug	Response	[Ref]
CD19	Anti-CD19 mAb	B-cell lymphoma	HSPC:Chol:mPEG	Doxorubicin	Improved survival compared to untargeted liposomes.	[351]
CD19	Anti-CD19 mAb Anti-CD19 Fab	B-cell lymphoma	SM:Chol:mPEG	Doxorubicin Vincristin	Significantly more effective than untargeted liposomes or free drug.	[352]
EGFR	IMC-C225 Fab	Breast cancer	DSPC:Chol:mPEG	Various	Significant anti-tumor effects and superior to untargeted liposomes.	[264]
EGFR	EMD72000 Fab IMC-C225 Fab	Breast cancer, colorectal cancer	DSPC:Chol:mPEG	Doxorubicin	High uptake in various EGFR-overexpressing cell lines.	[353]
EGFR	EGFR mAb	Non-small cell lung cancer	DOPE:CHEMS:PDP-PEG-DOPE	Gemcitabine	Significant tumor reduction in A549 tumor-bearing nude mice.	[354]
EGFR	EGFR mAb	Glioblastoma multiforme	Soy PC:Chol:mPEG: PEG-PE		Significantly enhanced accumulation and uptake.	[355]
EGFR	EGFR mAb	Ovarian carcinoma	HSPC:Chol:mPEG	Doxorubicin	Accumulation was comparable to control liposomes.	[356]
GD2	Anti-GD2 mAb Anti-GD2 Fab	Neuroblastoma	HSPC:Chol:mPEG	Doxorubicin	Complete inhibition of metastatic growth in a nude mouse model.	[357]
HBEGF	Anti-HBEGF Fab	Breast cancer	HSPC:Chol:mPEG	Doxorubicin	Tumor regression in MDA-MB-231 tumor-bearing mice.	[266]
HER-2	Anti-HER2 scFV	Breast cancer	POPC:Chol:mPEG	Doxorubicin	Significant decrease in tumor size compared to untargeted liposomes.	[358]
HER-2	Anti-HER2 Fab	Breast cancer	EPC:Chol:mPEG	PE38KDEL	Receptor-specific binding and internalization *in vitro*.	[359]
HER-2	Anti-HER2 Fab	Breast cancer	POPC:Chol:mPEG	HPTS (probe)	The uptake correlated with the cell surface expression of HER2 *in vitro*.	[360]
IGF-1R	1H7 mAb	Pancreatic carcinoid cancer	HSPC:Chol:mPEG	Doxorubicin	Superior antitumor efficacy compared to control liposomes.	[361]
MT1-MMP	222-1D8 Fab	Fibrosarcoma	HSPC:Chol:mPEG	Doxorubicin	Significant suppression of tumor growth, independent of tumor accumulation.	[362]
VCAM-1	Anti-VCAM-1 mAb	Multiple myeloma	Soy PC:Chol: cyanur-PEG-PE		Selective targeting of tumor vessels.	[363]
VEGFR	DC101 Fab	Hepatocellular carcinoma	PC:mPEG	Doxorubicin	Significant delay of tumor growth up to 7 weeks.	[364]
VEGFR	DC101 Fab	Colon cancer, breast cancer, pancreatic cancer	DSPC:Chol:mPEG	Doxorubicin	Superior therapeutic efficacy and selective abolishment of the tumor vasculature.	[365]

PEGylated formulations [233], and (4) the decreased rate of plasma protein adsorption on the hydrophilic surface of PEGylated liposomes [234] impose so-called 'stealth' properties [235]. Consequently, PEGylated liposomes are targeted to tumors by means of the EPR effect, which facilitates higher tumor:healthy tissue ratios and tumor killing capacity compared to their unencapsulated equivalents [236,237]. Inclusion of PEG chains further enables the design of immunoliposomes capable of homing to the target site through the attachment of antibodies, antigen-binding fragments (Fab' fragments), or nanobodies to a chemically modified distal end of a liposome-grafted PEG chain [238–241]. As for the stealth liposomes, the use of drug-encapsulating immunoliposomes is associated with greater *in vivo* target selectivity and improved cytostatic efficacy (Table 3). More detailed information on the utility of PS encapsulation into lipid-based delivery systems is available elsewhere [21].

In light of the advantages of liposomal encapsulation of metallated PCs and the proven *in vivo* efficacy of stealth liposomes and immunoliposomes, the remainder of this review will mainly focus on second-generation PC-encapsulating liposomes for the treatment of solid tumors. Three different liposomal formulations will be addressed from the perspective of a comprehensive multi-targeting modality. Inasmuch as diamagnetic PCs exhibit similar photochemical and photophysical properties (Section 3.1), ZnPC is used as a model PS in many instances.

4.3. Phthalocyanine-encapsulating liposomes

Metallated PC-containing liposomes have been employed for a broad array of clinical applications, including the treatment of cutaneous leishmaniasis [242], antineoplastic therapy [190,243,244], and diagnostic applications in atherosclerosis [245]. For the treatment of solid cancers, ZnPC has been conjugated to LDL [201] and serum albumin for systemic administration [246], encapsulated into various nanoparticulate drug delivery systems for intravenous infusion [244,247–249], and formulated in a mixture of oleic acid and propylene glycol for topical administration [250]. With respect to liposomal formulations, *in vivo* studies demonstrated accumulation of liposomal ZnPC in tumors, the subsequent irradiation of which led to a significant reduction in tumor size [201]. A liposomal formulation of ZnPC (CGP-55847, Ciba-Geigy) was evaluated in a phase I/II clinical trial for the treatment of squamous cell carcinoma in the upper digestive tract [172]. However, the clinical trial with CGP-55847 was discontinued due to reasons not publicly disclosed.

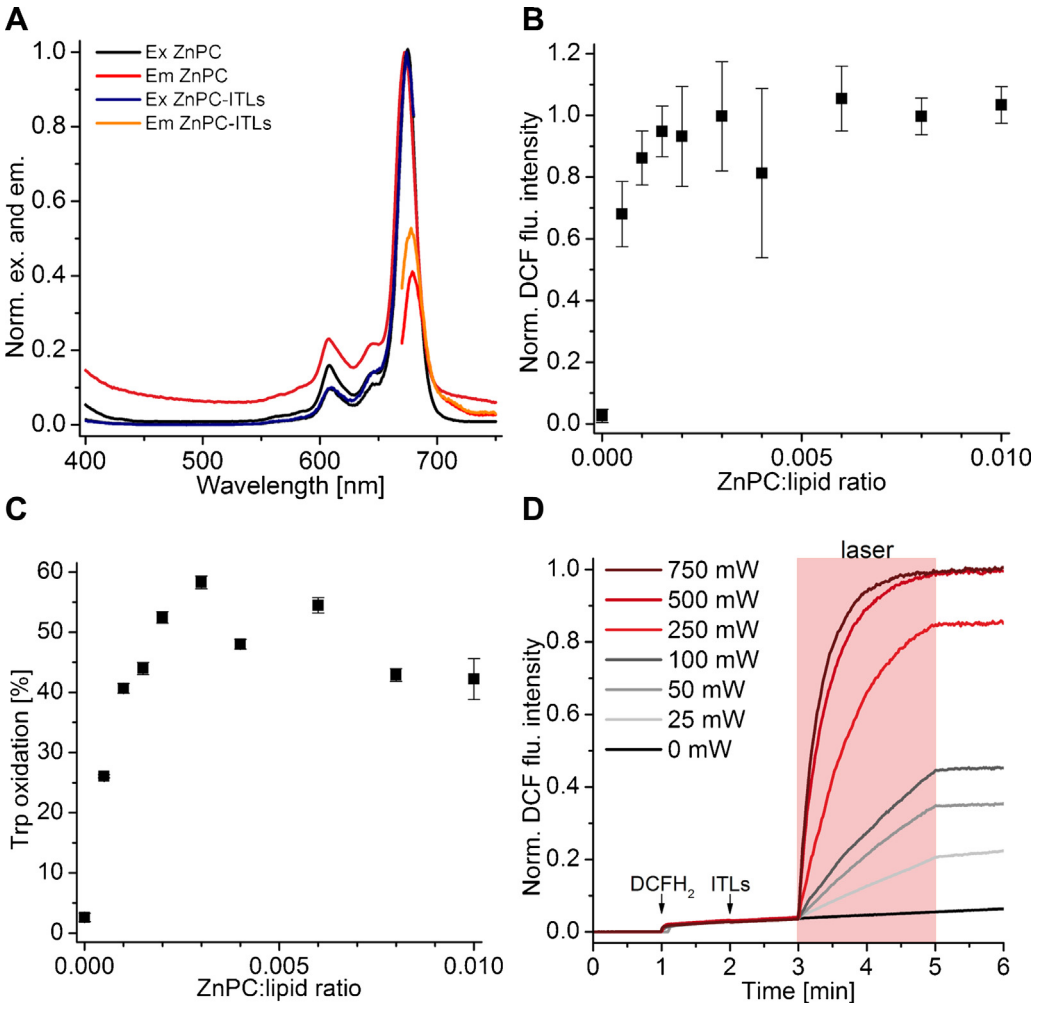

Fig. 7. (A) Normalized fluorescence emission (Em) and excitation (Ex) spectra of unencapsulated ZnPC and ZnPC-containing liposomes (ZnPC–ITLs) consisting of DPPC: cholesterol:DSPE-PEG (66:30:4 molar ratio) in physiological buffer. (B) ZnPC:lipid ratio-dependent ROS generation following PDT with ZnPC-ITLs. ROS production was assayed with 2′,7′-dichlorodihydrofluorescein ($DCFH_2$). The protocol is described in [74]. (C) ZnPC:lipid ratio-dependent oxidation of tryptophan (Trp) residues in bovine serum albumin following PDT with ZnPC–ITLs. The protocol is described in [74]. (D) Laser power-dependent oxidation kinetics of $DCFH_2$ during PDT with ZnPC–ITLs. The protocol is described in [74].

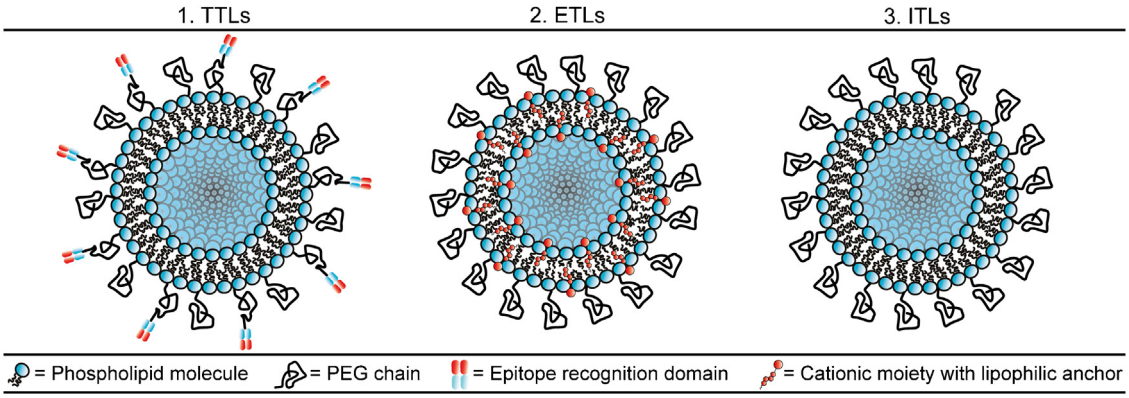

Fig. 8. (1) Tumor cell-targeting liposomes (TTLs) contain specific epitope recognition domains (*e.g.* antibodies, Fab' fragments, nanobodies, or peptides) that are conjugated to an anchor molecule such as a lipid-conjugated, distally modified polyethylene glycol (PEG) chain. (2) Endothelial cell-targeting liposomes (ETLs) are typically cationic liposomes that exhibit a strong affinity for the negatively charged tumor endothelium. (3) Interstitially-targeted liposomes (ITLs) passively accumulate in the tumor interstitium by exploiting the enhanced permeability and retention (EPR) effect and poor lymphatic drainage in solid tumors. PEGylation of the liposomes imparts 'stealth' properties in that unspecific liposome uptake by the mononuclear phagocyte system is considerably forestalled.

An advantage of liposomal ZnPC, on top of the previously addressed benefits of liposomal encapsulation (Section 4.2), is that incorporation into a lipid bilayer does not negatively affect the photochemical properties of ZnPC (Figs. 6F and 7). The electronic transition states of π-electrons are susceptible to changes in chemical environment (*e.g.*, solvent or polarity effects), which could impact the peak position of the absorption/excitation spectrum of a molecule as well as its singlet and triplet state quantum yield [251]. As shown in Fig. 6F, the main absorption bands of ZnPC in pyridine and liposomal ZnPC fully overlap, indicating that the Q-band electronic transition states are not influenced by the lipid bilayer. Moreover, the fluorescence excitation and emission spectra of ZnPC in pyridine are entirely superimposable on the spectra of liposomal ZnPC, attesting to the fact that the singlet state is not influenced by the lipid bilayer (Fig. 7A) [74]. Fig. 7B and C further show that liposomal ZnPC produces ROS upon PDT that oxidize small molecules (2′,7′-dichlorodihydrofluorescein) and large biomolecules (albumin), respectively [74]. The generation of ROS proceeds in a PS:lipid molar ratio- (Fig. 7B and C) and irradiance-dependent manner (Fig. 7D) [74], and the extent of oxidation of extraliposomal compounds is hampered by the presence of antioxidants in the membrane, such as cholesterol [252], α-tocopherol [253], and (poly)unsaturated fatty acids [254]. Although the amount of ROS generation is linearly proportional to the amount of ZnPC in the membrane, there is an optimal PS:lipid molar ratio beyond which the extent of ROS generation plateaus and abandons linearity, despite an increased ZnPC bilayer density (Fig. 7B and C) [74]. At a PS:lipid molar ratio of >0.003, ZnPC starts forming aggregates [255] that, due to altered relaxation mechanisms in excited PS dimers/multimers [219] and/or reduced oxygen availability in these aggregates [218], results in impaired $^1O_2$ generation. Similar effects have been described for AlPC [255].

The main implication of these findings is that ZnPC retains its photophysical and photochemical properties once it has entered a cell, where it will distribute to the cell- and subcellular membranes as elaborated in Section 2.2.2. PDT with liposomally delivered ZnPC will induce (per)oxidation of proximal cellular constituents (Fig. 7B and C), particularly membrane-embedded molecules and bilayer constituents. The (per)oxidation of intra/transmembrane molecules and unsaturated lipids causes membrane perturbation and leakage of intracellular content, which has been demonstrated with PDT-subjected cell phantoms containing ZnPC in the bilayer [74]. The biological consequences of membrane permeabilization have been addressed in Section 2.3 and ultimately result in cell death, as experimentally demonstrated in the following sections.

4.4. Targeting photosensitizer-encapsulating liposomes to solid tumors

4.4.1. Comprehensive tumor-targeting strategy

The microenvironment of solid cancers can essentially be classified into three pharmacologically relevant target areas: the tumor cells that make up the bulk of the cancer, the endothelial cells that line the intratumoral vasculature, and the interstitial space that is comprised of stromal proteins, fibroblasts, and immune cells (macrophages and dendritic cells). PS-encapsulating liposomes for systemic administration can be prepared that preferentially accumulate in one of the three target areas. The generic make-up of the liposomes is presented in Fig. 8, and each formulation, namely tumor-targeting liposomes (TTLs), tumor endothelium-targeting liposomes (ETLs), and interstitially-targeted liposomes (ITLs) is discussed separately in Sections 4.4.2 through 4.4.4.

Principally, each formulation can be employed individually for PDT, whereby the TTLs and ETLs have proven most effective *in vitro* in terms of tumor killing potential [256,257]. However, the implementation of a combinatorial, multi-targeting modality for PDT as illustrated in Fig. 9 is advocated for two important reasons. First, the generation of oxidative damage at multiple intratumoral locations will translate to more extensive interference with post-treatment biological and biochemical processes and hence exacerbate the degree of tumor cell death. For example, if only the tumor cells are targeted, which is usually the case, the PDT-induced activation of cell death mechanisms may be reverted due to co-activation of cell survival and stress response pathways [68], leading to increased cancer cell survival following PDT. When, however, the TTL-induced damage profile is complemented by concomitant ETL-mediated vascular shutdown and consequent intratumoral anoxia, the chances that partially viable cells survive as a result of survival and recovery programs will considerably diminish. Second, the induction of damage in a greater tumor volume (*i.e.*, tumor parenchyma + vasculature + stroma *versus* parenchyma only) is expected to trigger more extensive DAMP release with a broader spectrum of DAMP molecules, which will result in a more profound immune response. As addressed in Fig. 1 and Section 2.4, the PDT-induced immune response is critical for tumor removal through immunogenic apoptosis and immunological processing of tumor cells.

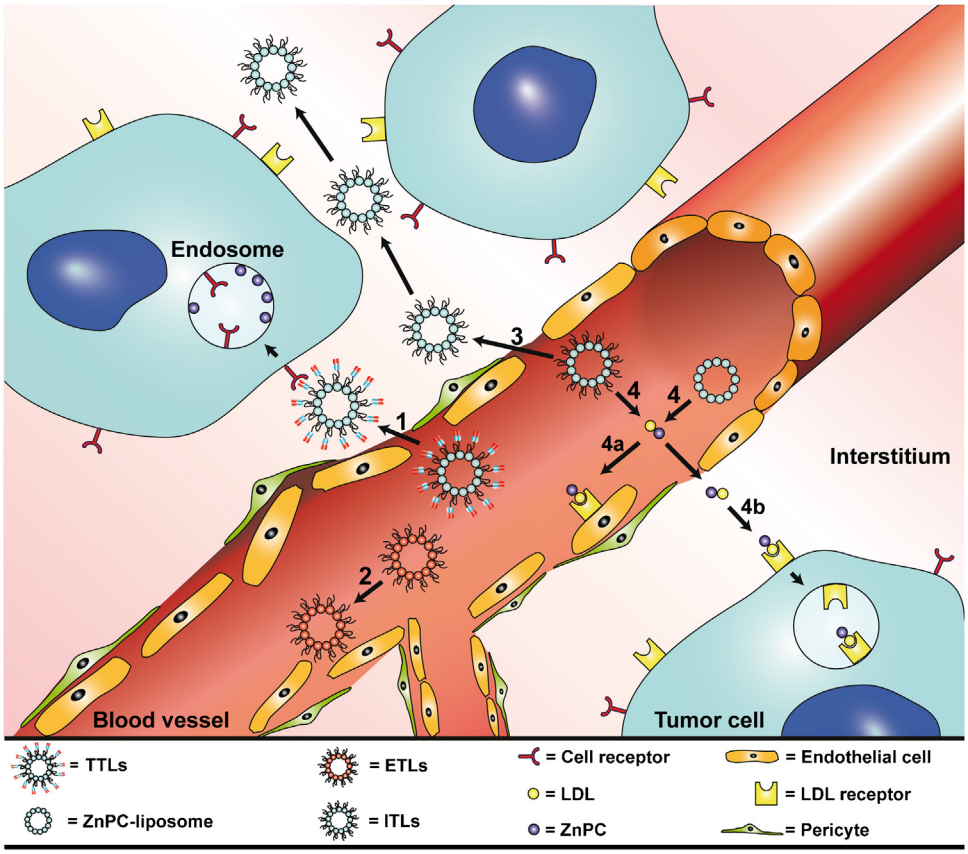

Fig. 9. *In vivo* pharmacokinetics of the liposomal PS-encapsulating formulations for tumor targeting (illustrated in Fig. 8). Route 1 (Section 4.4.2): tumor-targeting liposomes (TTLs) extravasate and bind to the corresponding receptor on a tumor cell. Route 2 (Section 4.4.3): cationic liposomes (ETLs) have a propensity to bind inflamed and angiogenic endothelium. Route 3 (Section 4.4.4): sterically stabilized liposomes (ITLs) extravasate into the interstitium, enter the interstitial space, and accumulate due to the EPR effect. Route 4 (Section 4.4.4): transfer of hydrophobic PSs from non-PEGylated liposomes to LDL particles. Consequently, the PS-LDL complexes (4a) bind to LDL receptors that are typically replete on endothelial cells lining the tumor vasculature or (4b) extravasate, bind to LDL receptors that are abundantly present on tumor cells, and enter the cells *via* endocytosis.

4.4.2. Photosensitizer-encapsulating tumor cell-targeting liposomes

Tumor cells constitute a primary target for second-generation lipophilic PSs such as ZnPC because their high log *P* value (Fig. 6E) causes the PS to localize to the cell and organelle membranes, including those of mitochondria and the Golgi apparatus (ZnPC) [61,258]. Consequently, PDT with PC-TTLs will induce oxidative damage at multiple critical sites, which will culminate in the execution of different cell death pathways as elaborated in Section 2.3.1. Extensive cell damage and death is not only imperative for optimal therapeutic efficacy, but also for minimizing the number of residual tumor cells that could mediate cancer recurrence, for optimally deterring the execution of cell survival pathways [68], and for maximally reducing post-treatment tumor sustenance through the processes related to the hallmarks of cancer [259,260]. Moreover, tumor cells are the source of TAAs and DAMPs, which are released as a result of oxidation of membrane constituents or cell death signaling, that mediate the anti-tumor immune response (Fig. 1, Section 2.4) [96]. The extent to which these signaling molecules are liberated in the treated tissue, and hence the magnitude of the anti-tumor immune response, is proportional to the degree of induced damage. Accordingly, PDT with PC-TTLs is expected to induce widespread and pleiotropic oxidative damage that results in extensive cell death, a prolific anti-tumor immune response, and, in fully treated tumors, minimal probability of tumor recurrence.

TTLs (Fig. 8) are generally composed of phosphatidylcholines and a molar fraction of PEGylated lipids to which a ligand/epitope recognition molecule has been conjugated, such as an antibody, Fab' fragment, nanobody, or peptide (reviewed in [21,217,261]). The ligand/epitope recognition molecules typically bind to antigens that are abundantly expressed on the outer membrane of cancer cells but not or only minimally expressed by healthy cells. The different immunoliposome formulations and the ligand/epitope recognition molecules that have been investigated to date are summarized in Table 3 and the ligands/epitopes that constitute viable targets for PS-containing immunoliposomes specifically developed for the treatment of PDT-recalcitrant tumors (Section 1) are provided in Table 4.

The utility of immunoliposomes for the delivery of pharmacological agents has been demonstrated in numerous *in vitro* and *in vivo* studies. In mice, Song et al. [262] showed that systemically infused, sterically stabilized epidermal growth factor receptor (EGFR)-targeted liposomes were able to extravasate from the intratumoral microcirculation and specifically and efficiently bind to xenotransplanted EGFR-overexpressing human non-small cell lung carcinoma (H1299) cells, after which the TTLs were internalized *via* an ATP-dependent process. Corroboratively, our group found that anti-EGFR nanobody-conjugated TTLs (1,2-dipalmitoyl-*sn*-glycero-3-phosphocholine (DPPC):cholesterol:1,2-distearoyl-*sn*-glycero-3-phosphoethanolamine-*N*-[methoxy (PEG)-2000] (DSPE-PEG), 66:30:4 molar ratio) extensively bound to and were taken up by human EGFR-transfected murine (HER14) fibroblasts (Fig. 10A and B) and A431 cells [21]. The *in vitro* and *in vivo* PDT efficacy of these TTLs will be published elsewhere [21,263]. Mamot et al. [264] demonstrated that anti-EGFR TTLs exhibit a 6-fold higher uptake by EGFR-transfected human primary

Table 4
Potential targets of PDT-recalcitrant tumor types for immunoliposomes. An immunohistochemical expression score of ≥2 (scale 0–3) was considered overexpression. Positive staining was defined as followed: * staining index of ≥1.5 (staining intensity (0–3) × (number of positively stained cells/total number of cells counted)), ** staining in ≥10% of tumor cells, and *** >10% cytoplasm and membrane staining in all tumor cells. Abbreviations: EGFR, epidermal growth factor receptor; HER-1/2, human epidermal growth factor receptor 1/2; MUC-1, mucin 1, cell surface associated; IGF-1R, insulin-like growth factor 1 receptor.

Cancer type	Target ligand/epitope	Overexpression (OE) or positive staining (PS) [range]	[Ref]
Superficial recurrent urothelial carcinoma	EGFR/HER-1	23.6% (OE)	[366]
	EGFR/HER-1	100% (PS)*	[367]
	HER-2	12.4% (OE)	[368]
	MUC-1	44.1% (OE)	[369]
Nasopharyngeal carcinoma	EGFR/HER-1	62.7% [43.2–83.3] (OE)	[370–373]
	HER-2	50.7% (PS)**	[371]
	IGF-1R	56% (OE)	[374]
Extrahepatic cholangiocarcinoma	EGFR/HER-1	33.7% [15.8–57.9] (OE)	[375–378]
	HER-2	23.2% [8.5–31.3] (OE)	[375–380]
	HER-2	80% (PS)***	[381]

glioblastomas (U87) in mice *versus* non-targeted (anti-EGFR C225 Fab-lacking) liposomes. The TTLs were presumably internalized *via* receptor-mediated endocytosis. Park et al. [265] found that systemic administration of either sterically stabilized liposomes (comparable to ITLs, Section 4.4.4) or anti-human epidermal growth factor receptor 2 (HER-2)-conjugated TTLs resulted in equivalent levels of accumulation in xenografted breast cancer (BT-474, MDA-MB-453, MCF-7/HER2) tumors in mice, but the intratumoral distribution and internalization pattern clearly differed between the formulations. Whereas sterically stabilized liposomes accumulated extracellularly, the PEGylated anti-HER2 TTLs predominantly distributed in the cytoplasm of tumor cells. Of note, the conjugation of antibodies or fragments thereof to *e.g.*, PEG chains appear not to alter the size, surface charge, or pharmacokinetic properties of the liposomes compared to non-targeted, PEGylated liposomes [264,266].

Due to the selective uptake of PS-TTLs, intracellular PS levels are generally higher than for their non-targeted counterparts, causing the TTLs to be more potent in terms of phototoxicity. Gijsens et al. [257] demonstrated that $AlPCS_4$-encapsulating transferrin-conjugated liposomes exhibit a 10-fold lower IC_{50} value than non-targeted liposomes in HeLa cells treated with PDT (0.63 μM *versus* 6.3 μM $AlPCS_4$, respectively). Moreover, the intracellular accumulation of transferrin-conjugated TTLs was significantly higher than free $AlPCS_4$ or non-targeted liposomes. García-Diaz et al. used folate-conjugated liposomes containing zinc tetraphenyl porphyrin (ZnTPP) to treat folate receptor-expressing HeLa cells [267]. At a concentration of 1 μM ZnTPP and a radiant exposure of 10 J/cm^2, the non-targeted liposomes induced cell death in 65% of HeLa cells, whereas folate-conjugated liposomes led to a 94% mortality rate 24 h post-PDT. In line with previous findings, human ovarian carcinoma (Ovcar-5) cells treated with verteporfin-containing anti-EGFR TTLs exhibited significantly lower cell viability than non-targeted liposomes [268].

The data presented in this section indicate that the overexpression of specific surface recognition domains (*e.g.*, transferrin

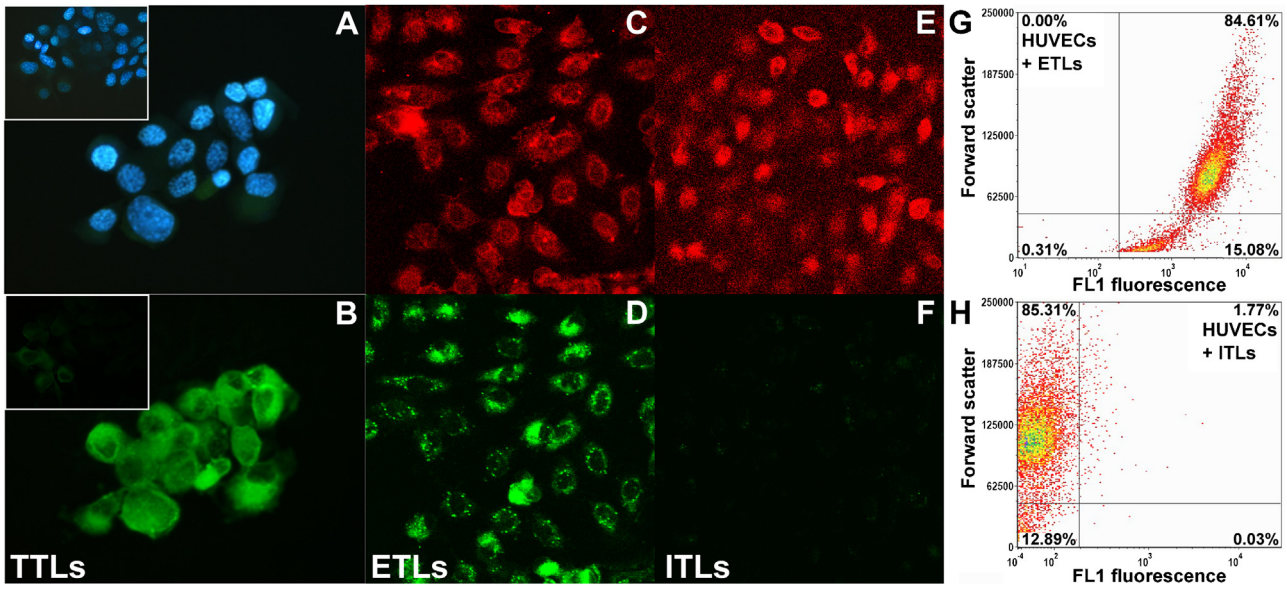

Fig. 10. Confocal images of DAPI-stained (in blue) EGFR-overexpressing HER14 cells (A) that have taken up anti-EGFR nanobody-conjugated TTLs (composed of DPPC:cholesterol:DSPE-PEG:NBD-PC (62:30:4:4 molar ratio)) fluorescently labeled with nitrobenzoxadiazole (NBD, green fluorescence) (B). The inserts in (A, B) are comparable images of HER14 cells incubated with fluorescently labeled control liposomes. Human umbilical vein endothelial cells (HUVECs) (isolated as described in [387]) were stained with ToPro3 (C, E) and incubated with NBD-labeled ETLs (composed of DPPC:DC-cholesterol:cholesterol:DSPE-PEG:NBD-DPPC (60:25:5:5:5 molar ratio)) (D) or ITLs (composed of DPPC:cholesterol:DSPE-PEG:NBD-DPPC (60:30:5:5 molar ratio)) (F). The uptake of NBD-labeled ETLs (G) and the lack of uptake of NBD-labeled ITLs (H) by HUVECs was confirmed by flow cytometry (protocol described in [74]). NBD fluorescence was measured in the FL1 fluorescence channel of the flow cytometer.

receptor, EGFR) by tumor cells can be exploited for tumor cell targeting. High intracellular PS concentrations are subsequently achieved *via* endocytosis. Consequently, as has been determined in a variety of studies, this PDT strategy is expected to produce increased levels of phototoxicity compared to unencapsulated PSs or PS-encapsulating non-targeted liposomes.

4.4.3. Photosensitizer-encapsulating endothelial cell-targeting liposomes

It is widely accepted that intratumoral vasculature plays a pivotal role in tumor sustenance and progression, as it provides the tumor with oxygen and nutrients. Correspondingly, photodestruction of tumor vasculature is a decisive therapeutic outcome of PDT [249,269–272]. It has been shown in mice that PDT with the systemically infused PS MV6401 resulted in acute vasoconstriction and thrombosis 3 h after PDT [273]. Fingar et al. [274] reported that verteporfin-mediated PDT of chondrosarcomas in rats resulted in selective destruction of tumor vasculature, which was associated with thrombus formation, hemostasis, and long-term tumor regression.

Blood vessels constitute an ideal target for PDT inasmuch as the relatively high local oxygen tension (in blood vessels and endothelium) as well as the physiologically abundant presence of the radical nitric oxide contribute to exacerbated ROS/RNS production upon PS excitation. Photochemical affliction of tumor microvasculature leads to acute tumor infarction, culminating in a local anoxic/hypoxic and malnourished environment that is associated with stalled tumor growth in case of sustained hemostasis [273]. Moreover, thrombi are potent chemoattractants for cells of the innate immune systems (neutrophils andmonocytes/macrophages) that, when activated, propagate thrombus/vascular remodeling by releasing cytokines and chemokines to attract additional immune cells to the thrombostatic vasculature [275,276]. Accordingly, PC-ETLs are potentially effective in PDT of particularly hypervascularized tumors by inducing cessation of oxygen and nutrient supply and corollary cell death [273,277,278], retarding tumor growth [273], and triggering pro-inflammatory signaling that leads to an anti-tumor immune response (Section 2.4) and removal of PDT-afflicted tissue (reviewed in [96]).

The uptake of PC-ETLs by intratumoral endothelial cells can be achieved by coating the liposomes with specific endothelium-recognizing epitopes or by imparting a positive surface charge on the liposomes. In case of the former, a variety of epitopes that are abundantly present on tumor cells can also be used to target the tumor endothelium, as elaborately described in [279] and summarized in Tables 3 and 4. These includes vascular cell adhesion molecule-1 (VCAM-1), membrane type-1-matrix metalloproteinase (MT1-MMP), integrins $\alpha_{v\beta}3$, $\alpha_{v\beta}5$, and $\alpha5\beta1$ (*e.g.*, by employing arginine-glycine-aspartic acid (RGD)-peptides), and asparagine-glycine-arginine (NGR) peptides that target aminopeptidase N.

Alternatively, cationic liposomes have been employed to target the tumor vessels. Generally, cationic liposomes are partly composed of (phospho)lipids with a positively charged head group, frequently complemented by neutral lipids such as phosphatidylcholines and cholesterol (summarized in [280]). Alternatively, a non-to-minimally toxic cationic moiety with a lipophilic anchor, such as 3β-[*N*-(*N*′,*N*′-dimethylaminoethane)-carbamoyl] cholesterol (DC-chol) [281], can be used in conjunction with neutral lipids. It is believed that cationic liposomes electrostatically associate with the negatively charged glycocalyx of inflamed or angiogenic endothelial cells [282], as evidenced by their propensity to accumulate more extensively in tumor vessels (~25–28% of the total administered dose) than in normal vessels (~4% of the total administered dose) [283]. This binding specificity may be in part explained by the lethargic and irregular blood flow in the tumor environment, as a result of which a greater probability of ETL–glycocalyx interactions exists that in turn enables more profound accumulation of ETLs in the tumor vasculature. Another factor that may contribute to this phenomenon is the typical upregulation and overexpression of negatively charged surface glycoproteins (*e.g.*, sialic acid-rich glycoproteins) by tumor endothelium [284].

Presently, relatively limited *in vitro* and *in vivo* data is available on the utility of ETLs for PDT. The cationic ETLs are believed to be internalized by endothelial cells *via* endocytosis [282]; cationic PEGylated ZnPC–ETLs, but not their neutral controls (*i.e.*, ZnPC–ITLs, Section 4.4.4), are indeed taken up by cultured human umbilical vein endothelial cells (HUVECs) (Fig. 10C–F). Campbell et al. [283] showed that cationic ETLs (1,2-dioleoyl-3-trimethylammonium-propane (DOTAP)) specifically targeted to the vasculature of xenografted human colon carcinoma (LS174T) tumors in mice. The cationic ETLs exhibited heterogeneous vascular distribution and accumulated predominantly in vessel branches. In addition, Thurston et al. demonstrated that ETLs specifically accumulated in RIP-Tag2 tumor-bearing mice (Fig. 11) and that the degree of accumulation was associated with the developmental

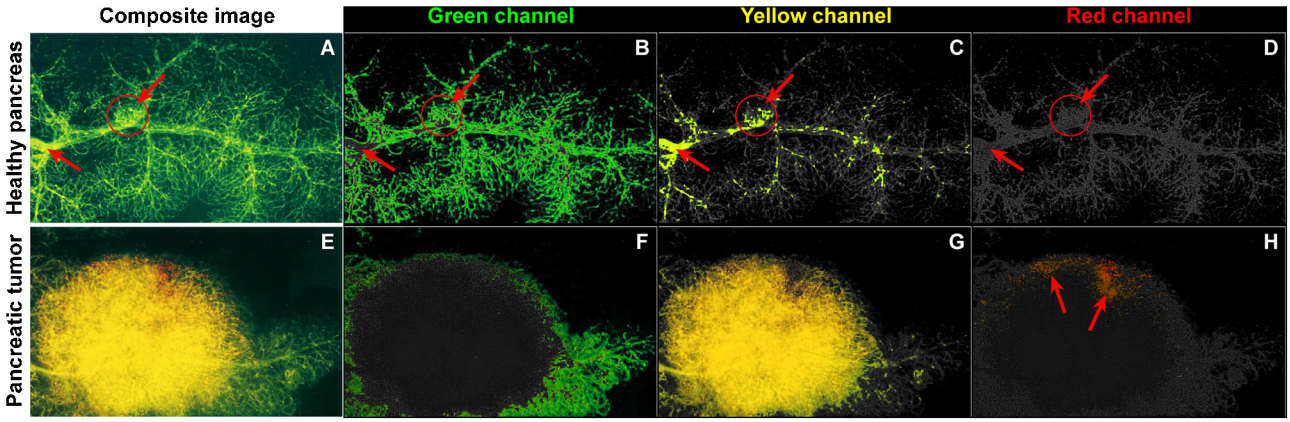

Fig. 11. *In vivo* proof-of-concept of cationic liposome targeting to intratumoral vasculature. Fluorescently labeled cationic liposomes (1,2-dioleoyl-3-trimethylammonium propane:cholesterol:Texas red-conjugated 1,2-dihexadecanoyl-*sn*-glycero-3-phosphoethanolamine, 55:45:0.2 molar ratio, in red) were systemically infused into wild-type mice (A–D) and RIP-Tag2 mice (E–H). The vasculature was stained with fluorescein-labeled lectin (in green) and yellow fluorescence indicates colocalization of cationic liposomes with (intratumoral) blood vessels (C, G). Images were modified from [282] and used with permission from Dr. Gavin Thurston.

stage of the tumor [282]. In terms of *in vitro* efficacy, we have shown that ZnPC–ETLs (composed of DPPC:DC-chol:cholesterol: DSPE-PEG (66:25:5:4, molar ratio) and a ZnPC:lipid ratio of 0.003) exhibit no dark toxicity in HUVECs and respond to PDT in a PS concentration-dependent manner [285]. With respect to *in vivo* efficacy studies, Gross et al. [286] encapsulated verteporfin in ETLs (DOTAP) and performed PDT on laser-induced choroidal neovasculature in mice. The unencapsulated and ETL-encapsulated verteporfin were equally effective and significantly decreased the size of the choroidal neovessels, although the cationic ETLs demonstrated higher selectivity and reduced PS-associated side effects. However, choroidal neovessels are not equivalent to intratumoral vasculature, so the results are not *per se* extrapolatable to the responsiveness of solid tumors to ETL-mediated PDT. Nevertheless, the data collectively suggest that cationic ETLs can selectively deliver PSs to intratumoral vasculature and that PDT will result in vascular shutdown, tumor cell death, and retardation of tumor growth. Evidently, more *in vivo* studies are needed to establish pharmacokinetic-, pharmacodynamic-, and toxicological profiles of PC-containing ETLs.

4.4.4. Photosensitizer-encapsulating interstitially targeted liposomes

The interstitial compartment of a tumor contains tumor-associated fibroblasts and immune cells that continuously remodel the tumor extracellular matrix (stroma), which entails neovascularization, activation of extracellular matrix-bound growth factors, and tumor cell invasion following proteolytic degradation of extracellular matrix components. Stromal remodeling is also required for tumor metastasis (reviewed in [287–289]). Consequently, PS delivery to the tumor interstitium may constitute a useful means to inflict considerable damage to the tumor [290,291]. The mechanisms that stand at the basis of PDT efficacy in the stromal environment include: (1) oxidation of cell membranes, either by primary ROS or by secondary or tertiary ROS (*e.g.*, $^{\bullet}$OH [2]) that are formed from type I reactions in the tumor microenvironment, and (2) activation of immune cells by (a) direct oxidation of cellular constituents following PDT of PS-ITLs that have been taken up by the immune cells (*e.g.*, tumor-resident macrophages) and/or (b) by oxidized extracellular biomolecules [276] (*e.g.*, stromal proteins or glycocalyx degradation products [2]) that bind to immune receptors (*e.g.*, TLR-2, TLR-4, CD44) or are taken up by the immune cells following PDT [292].

The targeting of ITLs to the tumor interstitium and their retention proceeds passively *via* the EPR effect. For these purposes, liposomes are generally composed of neutral (zwitterionic) phospholipids (mostly phosphatidylcholines) and a molar fraction (4–6%) of PEGylated lipids for steric stabilization and to impart stealth properties [293]. Alternatively, ITLs may be sterically stabilized by other types of non-to-low immunogenic (block co-) polymers, including polyacrylamide (PAA), poly(vinylpyrrolidone) (PVP), and poly(acryloyl morpholine) (PAcM) (reviewed in [294]). Proper sizing is also important, as the ITLs must have a smaller diameter than the length of the inter-endothelial cell fenestrations in the tumor vasculature, *i.e.*, <200 nm [295], to extravasate. Moreover, particles <160 nm are profoundly taken up by the liver in rabbits, whereas particles >210 nm are avidly taken up by both the spleen and the liver [226]. Consequently, the diameter of ITLs should be between 160 and 210 nm. Steric stabilization in combination with proper sizing considerably prolongs the circulation time, as a result of which the ITLs will have ample time to passively diffuse into the tumor interstitium. Accordingly, Wu et al. [296] demonstrated that, in rats, sterically stabilized liposomes rapidly accumulated in the interstitial compartment of xenografted rat breast adenocarcinomas (R3230Ac) following infusion, which was 3–4 fold more extensive than their non-PEGylated counterparts.

With respect to *in vitro* PDT studies, our group has demonstrated that ITLs encapsulating ZnPC exhibited no dark toxicity, but became cytotoxic upon irradiation of extrahepatic cholangiocarcinoma (Sk-Cha1) cells in a lipid concentration-dependent manner (at a constant ZnPC:lipid ratio of 0.003) [74]. The mode of cell death comprised both apoptosis and necrosis, whereby necrosis was the predominant mode of cell death, most likely because a small fraction of the ITLs was internalized by the cells [74]. Moreover, the ITLs were not taken up by HUVECs, which suggests that these liposomes will not be cleared by endothelial-like cells following intravenous infusion (Fig. 10E, F, and H). *In vivo* studies in mice bearing human fibrosarcoma (MS-2) tumors demonstrated that ZnPC-encapsulating non-PEGylated ITLs accumulated in the tumors at tumor:healthy tissue ratios of 7.5:1–9:1 24 h after systemic administration [190,191], which is in agreement with the previously cited findings by Wu et al. [296] regarding interstitial ITL accumulation. Furthermore, Oku et al. [297] performed PDT with glucuronidated ITLs containing verteporfin and achieved a complete response rate in 80% of the Meth A sarcoma-bearing mice. In contrast, a 20% complete response rate was observed with free PS or verteporfin encapsulated in conventional anionic liposomes (DPPC:1-palmitoyl-2-oleoyl-*sn*-glycero-3-phosphocholine (POPC):cholesterol:1,2-dipalmitoyl-*sn*-glycero-3-phosphoglycerol (DPPG)). These data clearly indicate that the tumor interstitium comprises a viable target for PDT-mediated tumor eradication using PS-ITLs.

Alternatively, LDL can serve as an additional vehicle for the transfer of lipophilic PCs from the ITLs to blood-borne LDL and subsequently to tumor cells (Fig. 9). Various studies have found that ZnPC incorporated in non-PEGylated lipid-based delivery vehicles can transfer to plasma proteins, including LDL and high-density lipoprotein (HDL) [49,298]. As demonstrated by Reddi et al. [201], intravenous infusion of *in vitro* prepared ZnPC–LDL complexes resulted in selective accumulation of these complexes in the tumor, as evidenced by a maximal tumor:healthy tissue ratio of 5.7, 24 h post-injection. None of the studies examined the effect of PEGylation on the transfer kinetics of ZnPC from ITLs to plasma proteins. Such studies have only been conducted with mTHPC [299,300], showing that 42% of mTHPC was transferred from PEGylated ITLs to plasma proteins 30 minutes after incubation, which progressively increased to 74% after 24 h [300]. Inasmuch as mTHPC and metallated PCs are chemically comparable (Fig. 2D and Fig. 6A–D) and the PCs are typically encapsulated in lipid formulations that resemble the formulations used in [299,300], it is expected that ZnPC will exhibit similar transfer behavior. Accordingly, the transfer of PC molecules from (PEGylated) ITLs to LDL will lead to tumor-specific PC accumulation [301]. Based on *in vitro* results it appears that the ZnPC–LDL conjugates enter the cells *via* non-specific endocytosis [302]. The ZnPC–LDL complexes are not internalized *via* receptor-mediated endocytosis, since the association of PCs with LDL slightly distorts the molecular structure of apoprotein B [302] that is responsible for LDL receptor binding [303].

This section summarized the importance of targeting the stromal environment inasmuch as the tumor stroma is responsible for neovascularization and metastatic spread of tumor cells and contains oxidizable cellular and molecular constituents with immunogenic potential. PEGylated ITLs generally exhibit better pharmacokinetics, tumor-accumulating capacity, and hence therapeutic outcomes than their non-PEGylated equivalents. The transfer of ZnPC from ITLs to endogenous lipid-based nanocarriers such as LDL constitutes an alternative way to augment ZnPC accumulation in the tumor stroma.

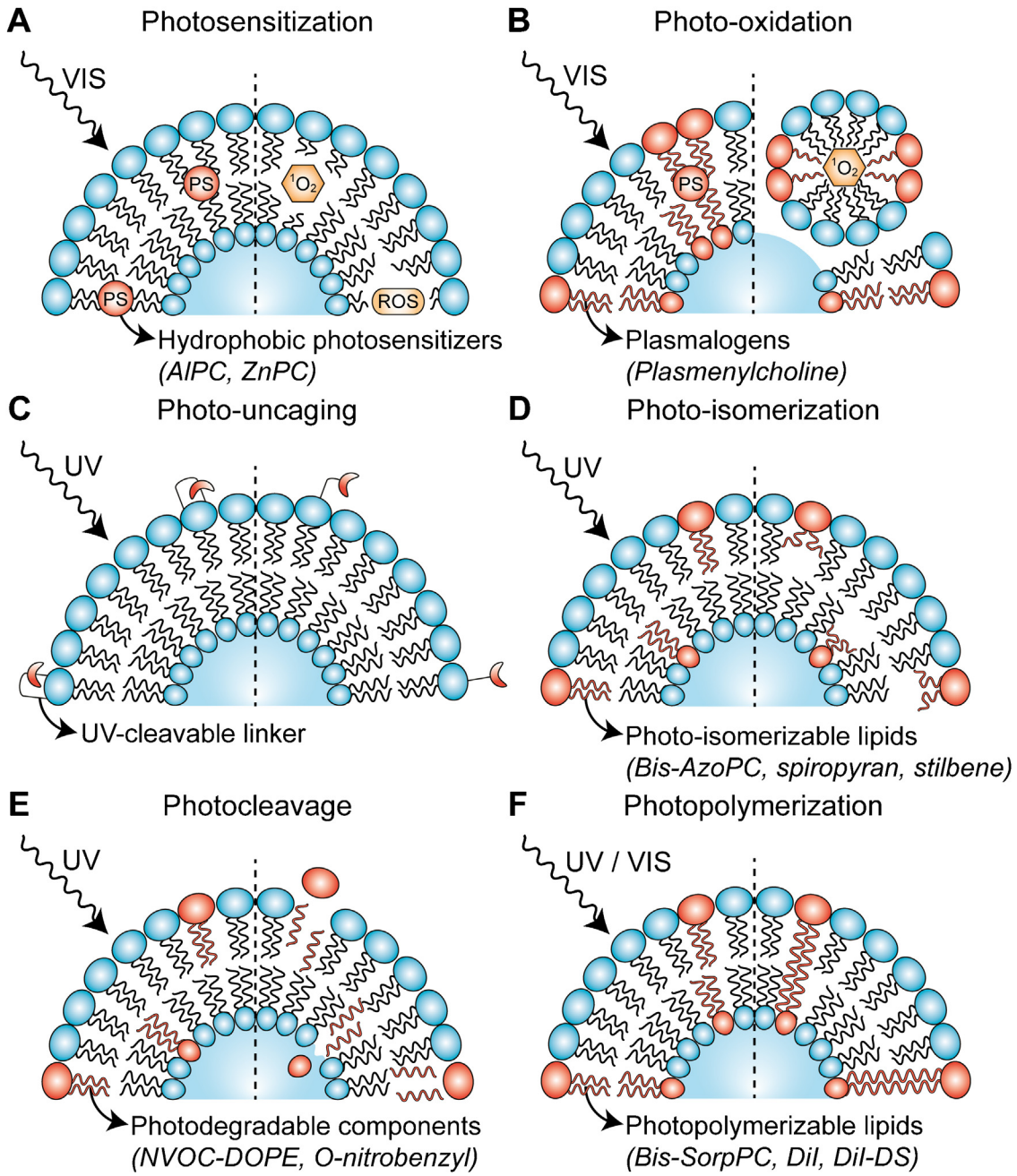

Fig. 12. Summary of methods for photochemically triggered drug release. Light-induced release of water-soluble compounds can be achieved by photosensitization (A), a process that involves ROS-mediated destabilization of the lipid bilayer, photo-oxidation of plasmalogens that drives micelle formation (B), photo-uncaging of recognition molecules that enable tumor cell uptake (C), photo-isomerization of lipids that switch from an extended form (*trans*) to a twisted form (*cis*) (D), light-induced degradation of lipid components (E), and light-induced cross-linking of photopolymerizable lipids (F). All processes, except for photo-uncaging, cause destabilization of the lipid bilayer that enables efflux of the liposomal cargo. Abbreviations: VIS, visible light; UV, ultraviolet light; bis-AzoPC, 1,2-bis[4-4(4-*n*-butylphenylazo)phenylbutyroyl] phosphatidylcholine; NVOC-DOPE, 6-nitroveratryloxycarbonylated 1,2-dioleoyl-*sn*-glycero-3-phosphoethanolamine; bis-SorpPC, 1,2-bis[10-(2′,4′-hexadienoyloxy)-decanoyl]-*sn*-phosphatidylcholine; DiI, 1,1′-dioctadecyl-3,3,3′,3′-tetramethylindocarbocyanine; DiI-DS, 1,1′-dioctadecyl-3,3,3,3′-tetramethylindocarbocyanine disulfonic acid.

4.5. Phototriggered release modalities for liposome-delivered anti-cancer agents

In addition to the delivery of PSs, liposomes may also be used for the delivery of water-soluble compounds to the tumor site rather than the tumor cells *per se*. With such modalities, the liposomal encapsulants may accumulate in the tumor interstitial space and undergo local release into the tumor microenvironment upon irradiation. Upon their release, these compounds essentially aid in the tumor eradication process.

The triggered release of the hydrophilic encapsulants can be integrated into the photodynamic process by the inclusion of photo-labile constituents such as photodegradable phospholipids. These constituents are chemically modified upon light irradiation, leading to a change in chemical properties or degradation, consequent perturbation/destabilization of the particle, and corollary release of the hydrophilic encapsulants. A complete

overview of the phototriggered release mechanisms is provided in Fig. 12. Detailed reviews on these mechanisms are available elsewhere [304–306]. Unfortunately, a multitude of the photochemical triggering methods rely on UV light, which may have limited clinical applicability due to its low optical penetration depth and harmful effects. As such, novel methods or optimized methods are required that are compatible with wavelengths in the therapeutic window (Fig. 3B).

5. Concluding remarks

PDT is an attractive treatment modality for a variety of diseases, including anti-neoplastic treatment, has yielded promising clinical results at relatively low cost, and can be carried out in a non-invasive and patient-friendly manner. However, contemporary PDT strategies lack effectiveness in various solid cancer subtypes and are associated with a substantial amount of photosensitivity. To circumvent these issues, the application of diamagnetic PCs is expected to improve clinical outcome and lower the degree of photosensitivity and phototoxic reactions. The encapsulation of diamagnetic PCs into liposomes provides a sophisticated PS delivery platform for the targeting of pharmacologically important intratumoral sites, including the tumor interstitium, tumor endothelium, and tumor cells. Future *in vivo* and clinical research should determine whether this multi-faceted tumor targeting strategy improves therapeutic efficacy in PDT-recalcitrant tumors while reducing side effects. Besides our proposed cancer treatment strategy, the versatility of this delivery platform offers researchers many new applications, varying from the delivery of contrast agents for tumor imaging to delivery of pharmaceutical agents for therapy.

Acknowledgements

The authors thank Dr. Gavin Thurston for his permission to publish the *in vivo* localization of cationic liposomes and Prof. Dr. Bing Tan for providing Foscan. This study was supported by grants from the Dutch Anti-Cancer Foundation (Stichting Nationaal Fonds Tegen Kanker, Amsterdam, the Netherlands), the Phospholipid Research Center (Heidelberg, Germany), and the Nijbakker-Morra Foundation (Leiden, the Netherlands) to MH.

References

[1] K. Plaetzer, B. Krammer, J. Berlanda, F. Berr, T. Kiesslich, Photophysics and photochemistry of photodynamic therapy: fundamental aspects, Lasers Med. Sci. 24 (2009) 259–268.
[2] R.F. van Golen, T.M. van Gulik, M. Heger, Mechanistic overview of reactive species-induced degradation of the endothelial glycocalyx during hepatic ischemia/reperfusion injury, Free Rad. Biol. Med. 52 (2012) 1382–1402.
[3] B.W. Henderson, T.J. Dougherty, How does photodynamic therapy work? Photochem. Photobiol. 55 (1992) 145–157.
[4] M. Triesscheijn, P. Baas, J.H. Schellens, F.A. Stewart, Photodynamic therapy in oncology, Oncologist 11 (2006) 1034–1044.
[5] R.C. Benson, Jr., Laser photodynamic therapy for bladder cancer, Mayo Clin. Proc. 61 (1986) 859–864.
[6] M.P. Copper, I.B. Tan, H. Oppelaar, M.C. Ruevekamp, F.A. Stewart, Meta-tetra (hydroxyphenyl) chlorin photodynamic therapy in early-stage squamous cell carcinoma of the head and neck, Arch. Otolaryngol. Head Neck Surg. 129 (2003) 709–711.
[7] T.J. Dougherty, Photodynamic therapy (PDT) of malignant tumors, Crit. Rev. Oncol. Hematol. 2 (1984) 83–116.
[8] A.C. Kubler, C.J. de, C. Hopper, A.G. Leonard, G. Putnam, Treatment of squamous cell carcinoma of the lip using Foscan-mediated photodynamic therapy, Int. J. Oral Maxillofac. Surg. 30 (2001) 504–509.
[9] G.D. Mackenzie, J.M. Dunn, C.R. Selvasekar, C.A. Mosse, S.M. Thorpe, M.R. Novelli, S.G. Bown, L.B. Lovat, Optimal conditions for successful ablation of high-grade dysplasia in Barrett's oesophagus using aminolaevulinic acid photodynamic therapy, Lasers Med. Sci. 24 (2009) 729–734.
[10] A. Morales, Treatment of superficial bladder cancer, Can. Med. Assoc. J. 122 (1980) 1133–1138.
[11] C.A. Morton, C. Whitehurst, H. Moseley, J.H. McColl, J.V. Moore, R.M. Mackie, Comparison of photodynamic therapy with cryotherapy in the treatment of Bowen's disease, Br. J. Dermatol. 135 (1996) 766–771.
[12] S.J. Rosenberg, R.D. Williams, Photodynamic therapy of bladder carcinoma, Urol. Clin. North Am. 13 (1986) 435–444.
[13] A. Sibille, R. Lambert, J.C. Souquet, G. Sabben, F. Descos, Long-term survival after photodynamic therapy for esophageal cancer, Gastroenterology 108 (1995) 337–344.
[14] N.C. Zeitouni, S. Shieh, A.R. Oseroff, Laser and photodynamic therapy in the management of cutaneous malignancies, Clin. Dermatol. 19 (2001) 328–338.
[15] U.O. Nseyo, B. Shumaker, E.A. Klein, K. Sutherland, Photodynamic therapy using porfimer sodium as an alternative to cystectomy in patients with refractory transitional cell carcinoma in situ of the bladder. Bladder Photofrin Study Group, J. Urol. 160 (1998) 39–44.
[16] Z.Q. Sun, Photodynamic therapy of nasopharyngeal carcinoma by argon or dye laser—an analysis of 137 cases, Zhonghua Zhong Liu Za Zhi 14 (1992) 290–292.
[17] F.L. Dumoulin, T. Gerhardt, S. Fuchs, C. Scheurlen, M. Neubrand, G. Layer, T. Sauerbruch, Phase II study of photodynamic therapy and metal stent as palliative treatment for nonresectable hilar cholangiocarcinoma, Gastrointest. Endosc. 57 (2003) 860–867.
[18] M. Wiedmann, F. Berr, I. Schiefke, H. Witzigmann, K. Kohlhaw, J. Mossner, K. Caca, Photodynamic therapy in patients with non-resectable hilar cholangiocarcinoma: 5-year follow-up of a prospective phase II study, Gastrointest. Endosc. 60 (2004) 68–75.
[19] E.A.J. Rauws, Photodynamic therapy and Klatskin tumour: an overview, Scand. J. Gastroenterol. 41 (2006) 135–138.
[20] N. Oku, Y. Namba, S. Okada, Tumor accumulation of novel RES-avoiding liposomes, Biochim. Biophys. Acta 1126 (1992) 255–260.
[21] R.T. van Kooten, W. Perini, L.G. Dijkstra, S.R. Veldkamp, A.K. Warps, E. van Elsäcker, M. Hafdi, Q. Hofsink, M. Kos, M. Broekgaarden, R. Weijer, R. van Vught, S. Oliveira, Y. Liu, Y. Nie, Z. Gu, J. Birkhoff, I.B. Tan, G. Storm, M. Heger, Lipid-based nanoparticulate drug delivery systems for photodynamic therapy of solid cancers: the utility of photosensitizer encapsulation. Manuscript in preparation (2015).
[22] R.R. Allison, G.H. Downie, R. Cuenca, X.H. Hu, C.J. Childs, C.H. Sibata, Photosensitizers in clinical PDT, Photodiagn. Photodyn. Ther. 1 (2004) 27–42.
[23] R.S. Wooten, K.C. Smith, D.A. Ahlquist, S.A. Muller, R.K. Balm, Prospective study of cutaneous phototoxicity after systemic hematoporphyrin derivative, Lasers Surg. Med. 8 (1988) 294–300.
[24] A.R. Oseroff, L.R. Blumenson, B.D. Wilson, T.S. Mang, D.A. Bellnier, J.C. Parsons, N. Frawley, M. Cooper, N. Zeitouni, T.J. Dougherty, A dose ranging study, of photodynamic therapy with porfimer sodium (Photofrin) for treatment of basal cell carcinoma, Lasers Surg. Med. 38 (2006) 417–426.
[25] J. Regula, A.J. MacRobert, A. Gorchein, G.A. Buonaccorsi, S.M. Thorpe, G.M. Spencer, A.R.W. Hatfield, S.G. Bown, Photosensitization and photodynamic therapy of esophageal, duodenal, and colorectal tumors using 5-aminolevulinic acid-induced protoporphyrin-IX—a pilot-study, Gut 36 (1995) 67–75.
[26] G. Wagnieres, C. Hadjur, P. Grosjean, D. Braichotte, J.F. Savary, P. Monnier, H. van den Bergh, Clinical evaluation of the cutaneous phototoxicity of 5,10,15,20-tetra(*m*-hydroxyphenyl) chlorin, Photochem. Photobiol. 68 (1998) 382–387.
[27] Q. Peng, J.M. Nesland, J. Moan, J.F. Evensen, M. Kongshaug, C. Rimington, Localization of fluorescent Photofrin-II and aluminum phthalocyanine tetrasulfonate in transplanted human malignant tumor LOX and normal tissues of nude mice using highly light-sensitive video intensification microscopy, Int. J. Cancer 45 (1990) 972–979.
[28] D.G. Boyle, W.R. Potter, Photobleaching of Photofrin II as a means of eliminating skin photosensitivity, Photochem. Photobiol. 46 (1987) 997–1001.
[29] S.L. Jacques, How tissue optics affect dosimetry of photodynamic therapy, J. Biomed. Opt. 15 (2010) 51608.
[30] H. Maeda, The enhanced permeability and retention (EPR) effect in tumor vasculature: the key role of tumor-selective macromolecular drug targeting, Adv. Enzyme Regul. 41 (2001) 189–207.
[31] D.A. Bellnier, Y.K. Ho, R.K. Pandey, J.R. Missert, T.J. Dougherty, Distribution and elimination of Photofrin II in mice, Photochem. Photobiol. 50 (1989) 221–228.
[32] C.J. Gomer, A. Ferrario, Tissue distribution and photosensitizing properties of mono-L-aspartyl chlorin e6 in a mouse tumor model, Cancer Res. 50 (1990) 3985–3990.
[33] W.S. Chan, J.F. Marshall, R. Svensen, J. Bedwell, I.R. Hart, Effect of sulfonation on the cell and tissue distribution of the photosensitizer aluminum phthalocyanine, Cancer Res. 50 (1990) 4533–4538.
[34] M. Van de Putte, T. Roskams, G. Bormans, A. Verbruggen, P.A.M. de Witte, The impact of aggregation on the biodistribution of hypericin, Int. J. Oncol. 28 (2006) 655–660.
[35] A. Barel, G. Jori, A. Perin, P. Romandini, A. Pagnan, S. Biffanti, Role of high-density, low-density and very low-density lipoproteins in the transport and tumor-delivery of hematoporphyrin in vivo, Cancer Lett. 32 (1986) 145–150.
[36] M.A. Elfar, N.R. Pimstone, Tumor-localization of uroporphyrin isomer-I and isomer-III and their correlation to albumin and serum-protein binding, Cell Biochem. Funct. 1 (1983) 156–160.
[37] I. Freitas, Lipid accumulation: the common feature to photosensitizer-retaining normal and malignant tissues, J. Photochem. Photobiol. B 7 (1990) 359–361.

[38] P.J. Bugelski, C.W. Porter, T.J. Dougherty, Autoradiographic distribution of hematoporphyrin derivative in normal and tumor tissue of the mouse, Cancer Res. 41 (1981) 4606–4612.
[39] Q. Peng, J. Moan, L.S. Cheng, The effect of glucose administration on the uptake of Photofrin-II in a human tumor xenograft, Cancer Lett. 58 (1991) 29–35.
[40] M. Korbelik, G. Krosl, P.L. Olive, D.J. Chaplin, Distribution of Photofrin between tumor cells and tumor-associated macrophages, Br. J. Cancer 64 (1991) 508–512.
[41] G. Jori, In vivo transport and pharmacokinetic behavior of tumour photosensitizers, Ciba Found. Symp. 146 (1989) 78–86.
[42] M. Chopp, M.O. Dereski, L. Madigan, F. Jiang, B. Logie, Sensitivity of 9L gliosarcomas to photodynamic therapy, Radiat. Res. 146 (1996) 461–465.
[43] B. Chen, B.W. Pogue, P.J. Hoopes, T. Hasan, Vascular and cellular targeting for photodynamic therapy, Crit. Rev. Eukaryot. Gene Expr. 16 (2006) 279–305.
[44] K.C. Gatter, G. Brown, I.S. Trowbridge, R.E. Woolston, D.Y. Mason, Transferrin receptors in human tissues: their distribution and possible clinical relevance, J. Clin. Pathol. 36 (1983) 539–545.
[45] S. Vitols, G. Gahrton, A. Ost, C. Peterson, Elevated low-density lipoprotein receptor activity in leukemic cells with monocytic differentiation, Blood 63 (1984) 1186–1193.
[46] G. Stehle, H. Sinn, A. Wunder, H.H. Schrenk, J.C.M. Stewart, G. Hartung, W. MaierBorst, D.L. Heene, Plasma protein (albumin) catabolism by the tumor itself—implications for tumor metabolism and the genesis of cachexia, Crit. Rev. Oncol. Hematol. 26 (1997) 77–100.
[47] S. Nakajima, T. Takemura, I. Sakata, Tumor-localizing activity of porphyrin and its affinity to LDL, transferrin, Cancer Lett. 92 (1995) 113–118.
[48] D. Kessel, Porphyrin-lipoprotein association as a factor in porphyrin localization, Cancer Lett. 33 (1986) 183–188.
[49] F. Ginevra, S. Biffanti, A. Pagnan, R. Biolo, E. Reddi, G. Jori, Delivery of the tumor photosensitizer zinc(II)-phthalocyanine to serum proteins by different liposomes—studies in vitro and in vivo, Cancer Lett. 49 (1990) 59–65.
[50] E. Alarcon, A.M. Edwards, A.M. Garcia, M. Munoz, A. Aspee, C.D. Borsarelli, E.A. Lissi, Photophysics and photochemistry of zinc phthalocyanine/bovine serum albumin adducts, Photochem. Photobiol. Sci. 8 (2009) 255–263.
[51] H. Mojzisova, S. Bonneau, C. Vever-Bizet, D. Brault, Cellular uptake and subcellular distribution of chlorin e6 as functions of pH and interactions with membranes and lipoproteins, Biochim. Biophys. Acta 1768 (2007) 2748–2756.
[52] K.W. Woodburn, N.J. Vardaxis, J.S. Hill, A.H. Kaye, D.R. Phillips, Subcellular localization of porphyrins using confocal laser scanning microscopy, Photochem. Photobiol. 54 (1991) 725–732.
[53] L.B. Chen, Mitochondrial-membrane potential in living cells, Ann. Rev. Cell Biol. 4 (1988) 155–181.
[54] C.W. Lin, J.R. Shulok, S.D. Kirley, L. Cincotta, J.W. Foley, Lysosomal localization and mechanism of uptake of Nile Blue photosensitizers in tumor cells, Cancer Res. 51 (1991) 2710–2719.
[55] J.M. Wessels, W. Strauss, H.K. Seidlitz, A. Ruck, H. Schneckenburger, Intracellular localization of *meso*-tetraphenylporphine tetrasulfonate probed by time-resolved and microscopic fluorescence spectroscopy, J. Photochem. Photobiol. B 12 (1992) 275–284.
[56] J. Moan, K. Berg, S. H.B., W. T., M. K., Fluorescence and photodynamic effects of phthalocyanines and porphyrins in cells, in: B.W. Henderson, T.J. Dougherty (Eds.), Photodynamic Therapy. Basic Principles and Clinical Applications, Marcel-Dekker, New York, 1992, pp. 19–36.
[57] B.C. Wilson, M. Olivo, G. Singh, Subcellular localization of Photofrin(R) and aminolevulinic acid and photodynamic cross-resistance in vitro in radiation-induced fibrosarcoma cells sensitive or resistant to Photofrin-mediated photodynamic therapy, Photochem. Photobiol. 65 (1997) 166–176.
[58] J.R. Shulok, M.H. Wade, C.W. Lin, Subcellular localization of hematoporphyrin derivative in bladder tumor cells in culture, Photochem. Photobiol. 51 (1990) 451–457.
[59] Y.J. Hsieh, C.C. Wu, C.J. Chang, J.S. Yu, Subcellular localization of Photofrin(R) determines the death phenotype of human epidermoid carcinoma A431 cells triggered by photodynamic therapy: when plasma membranes are the main targets, J. Cell. Physiol. 194 (2003) 363–375.
[60] M.H. Teiten, L. Bezdetnaya, P. Morliere, R. Santus, F. Guillemin, Endoplasmic reticulum and Golgi apparatus are the preferential sites of Foscan((R)) localisation in cultured tumour cells, Br. J. Cancer 88 (2003) 146–152.
[61] C. Fabris, G. Valduga, G. Miotto, L. Borsetto, G. Jori, S. Garbisa, E. Reddi, Photosensitization with zinc(II) phthalocyanine as a switch in the decision between apoptosis and necrosis, Cancer Res. 61 (2001) 7495–7500.
[62] H.B. Ris, H.J. Altermatt, B. Nachbur, J.C.M. Stewart, Q. Wang, C.K. Lim, R. Bonnett, U. Althaus, Effect of drug-light interval on photodynamic therapy with meta-tetrahydroxyphenylchlorin in malignant mesothelioma, Int. J. Cancer 53 (1993) 141–146.
[63] W.M. Sharman, C.M. Allen, J.E. van Lier, Role of activated oxygen species in photodynamic therapy, Methods Enzymol. 319 (2000) 376–400.
[64] K.R. Weishaupt, C.J. Gomer, T.J. Dougherty, Identification of singlet oxygen as cytotoxic agent in photo-inactivation of a murine tumor, Cancer Res. 36 (1976) 2326–2329.
[65] R.W. Redmond, I.E. Kochevar, Spatially resolved cellular responses to singlet oxygen, Photochem. Photobiol. 82 (2006) 1178–1186.
[66] M. Broekgaarden, R. Weijer, A.C. van Wijk, R.C. Cox, M.R. Egmond, R. Hoebe, T. M. van Gulik, M. Heger, Photodynamic therapy with liposomal zinc phtalocyanine and tirapazamine increases tumor cell death via DNA damage. Manuscript submitted, 2015.
[67] S. Tada-Oikawa, S. Oikawa, J. Hirayama, K. Hirakawa, S. Kawanishi, DNA damage and apoptosis induced by photosensitization of 5,10,15,20-tetrakis (*N*-methyl-4-pyridyl)-21H,23H-porphyrin via singlet oxygen generation, Photochem. Photobiol. 85 (2009) 1391–1399.
[68] M. Broekgaarden, R. Weijer, T.M. van Gulik, M.R. Hamblin, M. Heger, Tumor cell survival pathways activated by photodynamic therapy: a molecular framework for inhibition strategies, Cancer Metastasis Rev. (2015) (in press).
[69] Z. Huang, H.P. Xu, A.D. Meyers, A.I. Musani, L.W. Wang, R. Tagg, A.B. Barqawi, Y.K. Chen, Photodynamic therapy for treatment of solid tumors—potential and technical challenges, Technol. Cancer Res. Treat. 7 (2008) 309–320.
[70] A.P. Castano, T.N. Demidova, M.R. Hamblin, Mechanisms in photodynamic therapy: part one—photosensitizers, photochemistry and cellular localization, Photodiagn. Photodyn. Ther. 1 (2004) 279–293.
[71] A.W. Girotti, Photodynamic lipid peroxidation in biological systems, Photochem. Photobiol. 51 (1990) 497–509.
[72] E. Niki, Lipid peroxidation: physiological levels and dual biological effects, Free Rad. Biol. Med. 47 (2009) 469–484.
[73] E. Tyrode, P. Niga, M. Johnson, M.W. Rutland, Molecular structure upon compression and stability toward oxidation of Langmuir films of unsaturated fatty acids: a vibrational sum frequency spectroscopy study, Langmuir 26 (2010) 14024–14031.
[74] M. Broekgaarden, A.I. de Kroon, T.M. van Gulik, M. Heger, Development and in vitro proof-of-concept of interstitially targeted zinc-phthalocyanine liposomes for photodynamic therapy, Curr. Med. Chem. 21 (2013) 377–391.
[75] K. Berg, K. Madslien, J.C. Bommer, R. Oftebro, J.W. Winkelman, J. Moan, Light-induced relocalization of sulfonated *meso*-tetraphenylporphines in Nhik 3025 cells and effects of dose fractionation, Photochem. Photobiol. 53 (1991) 203–210.
[76] J. Moan, K. Berg, H. Anholt, K. Madslien, Sulfonated aluminum phthalocyanines as sensitizers for photochemotherapy—effects of small light doses on localization, dye fluorescence and photosensitivity in V79 cells, Int. J. Cancer 58 (1994) 865–870.
[77] P.D. Wilson, R.A. Firestone, J. Lenard, The role of lysosomal enzymes in killing of mammalian cells by the lysosomotropic detergent *N*-dodecylimidazole, J. Cell Biol. 104 (1987) 1223–1229.
[78] D. Kessel, M. Conley, M.G.H. Vicente, J.J. Reiners, Studies on the subcellular localization of the porphycene CPO, Photochem. Photobiol. 81 (2005) 569–572.
[79] E. Buytaert, G. Callewaert, N. Hendrickx, L. Scorrano, D. Hartmann, L. Missiaen, J.R. Vandenheede, I. Heirman, J. Grooten, P. Agostinis, Role of endoplasmic reticulum depletion and multidomain proapoptotic BAX and BAK proteins in shaping cell death after hypericin-mediated photodynamic therapy, FASEB J. 20 (2006) 756–758.
[80] I. Moserova, J. Kralova, Role of ER stress response in photodynamic therapy: ROS generated in different subcellular compartments trigger diverse cell death pathways, Plos One 7 (2012) e32972.
[81] J.M. Timmins, L. Ozcan, T.A. Seimon, G. Li, C. Malagelada, J. Backs, T. Backs, R. Bassel-Duby, E.N. Olson, M.E. Anderson, I. Tabas, Calcium/calmodulin-dependent protein kinase II links ER stress with Fas and mitochondrial apoptosis pathways, J. Clin. Invest. 119 (2009) 2925–2941.
[82] J.J. Lemasters, A.L. Nieminen, T. Qian, L.C. Trost, S.P. Elmore, Y. Nishimura, R.A. Crowe, W.E. Cascio, C.A. Bradham, D.A. Brenner, B. Herman, The mitochondrial permeability transition in cell death: a common mechanism in necrosis, apoptosis and autophagy, Biochim. Biophys. Acta 1366 (1998) 177–196.
[83] D. Kessel, Y. Luo, Y.Q. Deng, C.K. Chang, The role of subcellular localization in initiation of apoptosis by photodynamic therapy, Photochem. Photobiol. 65 (1997) 422–426.
[84] D. Kessel, Y. Luo, Mitochondrial photodamage and PDT-induced apoptosis, J. Photochem. Photobiol. B 42 (1998) 89–95.
[85] S.R. Chatterjee, H. Possel, T.S. Srivastava, J.P. Kamat, G. Wolf, T.P.A. Devasagayam, Photodynamic effects induced by meso-tetrakis[4-(carboxymethyleneoxy)phenyl]porphyrin on isolated Sarcoma 180 ascites mitochondria, J. Photochem. Photobiol. B 50 (1999) 79–87.
[86] S.R. Chatterjee, T.S. Srivastava, J.P. Kamat, T.P.A. Devasagayam, Lipid peroxidation induced by a novel porphyrin plus light in isolated mitochondria: possible implications in photodynamic therapy, Mol. Cell. Biochem. 166 (1997) 25–33.
[87] K. Plaetzer, T. Kiesslich, B. Krammer, P. Hammerl, Characterization of the cell death modes and the associated changes in cellular energy supply in response to AlPcS4-PDT, Photochem. Photobiol. Sci. 1 (2002) 172–177.
[88] C. Soldani, M.G. Bottone, A.C. Croce, A. Fraschini, G. Bottiroli, C. Pellicciari, The Golgi apparatus is a primary site of intracellular damage after photosensitization with Rose Bengal acetate, Eur. J. Histochem. 48 (2004) 443–448.
[89] S. Mukherjee, R. Chiu, S.M. Leung, D. Shields, Fragmentation of the Golgi apparatus: an early apoptotic event independent of the cytoskeleton, Traffic 8 (2007) 369–378.
[90] R. Chin, L. Novikov, S. Mukherjee, D. Shields, A caspase cleavage fragment of p115 induces fragmentation of the Golgi apparatus and apoptosis, J. Cell Biol. 159 (2002) 637–648.
[91] M. Ogata, O. Inanami, M. Nakajima, T. Nakajima, W. Hiraoka, M. Kuwabara, Ca (2+)-dependent and caspase-3-independent apoptosis caused by damage in

golgi apparatus due to 2,4,5,7-tetrabromorhodamine 123 bromide-induced photodynamic effects, Photochem. Photobiol. 78 (2003) 241–247.
[92] P. Agostinis, K. Berg, K.A. Cengel, T.H. Foster, A.W. Girotti, S.O. Gollnick, S.M. Hahn, M.R. Hamblin, A. Juzeniene, D. Kessel, M. Korbelik, J. Moan, P. Mroz, D. Nowis, J. Piette, B.C. Wilson, J. Golab, Photodynamic therapy of cancer: an update, CA Cancer J. Clin. 61 (2011) 250–281.
[93] T.J. Dougherty, C.J. Gomer, B.W. Henderson, G. Jori, D. Kessel, M. Korbelik, J. Moan, Q. Peng, Photodynamic therapy, J. Natl. Cancer Inst. 90 (1998) 889–905.
[94] M. Korbelik, Induction of tumor immunity by photodynamic therapy, J. Clin. Laser Med. Surg. 14 (1996) 329–334.
[95] M. Korbelik, G. Krosl, J. Krosl, G.J. Dougherty, The role of host lymphoid populations in the response of mouse EMT6 tumor to photodynamic therapy, Cancer Res. 56 (1996) 5647–5652.
[96] A.P. Castano, P. Mroz, M.R. Hamblin, Photodynamic therapy and anti-tumour immunity, Nat. Rev. Cancer 6 (2006) 535–545.
[97] G.Y. Chen, G. Nunez, Sterile inflammation: sensing and reacting to damage, Nature Rev. Immunol. 10 (2010) 826–837.
[98] P.M. Gallo, S. Gallucci, The dendritic cell response to classic, emerging, and homeostatic danger signals. Implications for autoimmunity, Front. Immunol. 4 (2013) 138.
[99] A.D. Garg, D. Nowis, J. Golab, P. Agostinis, Photodynamic therapy: illuminating the road from cell death towards anti-tumour immunity, Apoptosis 15 (2010) 1050–1071.
[100] A.D. Garg, D. Nowis, J. Golab, P. Vandenabeele, D.V. Krysko, P. Agostinis, Immunogenic cell death, DAMPs and anticancer therapeutics: an emerging amalgamation, Biochim. Biophys. Acta 1805 (2010) 53–71.
[101] A.D. Garg, D.V. Krysko, P. Vandenabeele, P. Agostinis, DAMPs and PDT-mediated photo-oxidative stress: exploring the unknown, Photochem. Photobiol. Sci. 10 (2011) 670–680.
[102] P. Srivastava, Roles of heat-shock proteins in innate and adaptive immunity, Nat. Rev. Immunol. 2 (2002) 185–194.
[103] S. Basu, R.J. Binder, T. Ramalingam, P.K. Srivastava, CD91 is a common receptor for heat shock proteins gp96, hsp90, hsp70, and calreticulin, Immunity 14 (2001) 303–313.
[104] M. Korbelik, Complement upregulation in photodynamic therapy-treated tumors: role of toll-like receptor pathway and NF kappa B, Cancer Lett. 281 (2009) 232–238.
[105] B. Stott, M. Korbelik, Activation of complement C3, C5, and C9 genes in tumors treated by photodynamic therapy, Cancer Immunol. Immunother. 56 (2007) 649–658.
[106] J.R. Theriault, H. Adachi, S.K. Calderwood, Role of scavenger receptors in the binding and internalization of heat shock protein 70, J. Immunol. 177 (2006) 8604–8611.
[107] A.A. Beg, Endogenous ligands of Toll-like receptors: implications for regulating inflammatory and immune responses, Trends Immunol. 23 (2002) 509–512.
[108] N. Fischer, M. Haug, W.W. Kwok, H. Kalbacher, D. Wernet, G.E. Dannecker, U. Holzer, Involvement of CD91 and scavenger receptors in Hsp70-facilitated activation of human antigen-specific CD4(+) memory T cells, Eur. J. Immunol. 40 (2010) 986–997.
[109] A.D. Garg, D.V. Krysko, T. Verfaillie, A. Kaczmarek, G.B. Ferreira, T. Marysael, N. Rubio, M. Firczuk, C. Mathieu, A.J.M. Roebroek, W. Annaert, J. Golab, P. de Witte, P. Vandenabeele, P. Agostinis, A novel pathway combining calreticulin exposure and ATP secretion in immunogenic cancer cell death, EMBO J. 31 (2012) 1062–1079.
[110] S. Pawaria, R.J. Binder, CD91-dependent programming of T-helper cell responses following heat shock protein immunization, Nat. Commun. 2 (2011) 521.
[111] M. Korbelik, J.H. Sun, I. Cecic, Photodynamic therapy-induced cell surface expression and release of heat shock proteins: relevance for tumor response, Cancer Res. 65 (2005) 1018–1026.
[112] F.F. Zhou, D. Xing, W.R. Chen, Regulation of HSP70 on activating macrophages using PDT-induced apoptotic cells, Int. J. Cancer 125 (2009) 1380–1389.
[113] N. Etminan, C. Peters, D. Lakbir, E. Bunemann, V. Borger, M.C. Sabel, D. Hanggi, H.J. Steiger, W. Stummer, R.V. Sorg, Heat-shock protein 70-dependent dendritic cell activation by 5-aminolevulinic acid-mediated photodynamic treatment of human glioblastoma spheroids in vitro, Br. J. Cancer 105 (2011) 961–969.
[114] S. Mitra, B.R. Giesselman, F.J. De Jesus-Andino, T.H. Foster, Tumor response to mTHPC-mediated photodynamic therapy exhibits strong correlation with extracellular release of HSP70, Lasers Surg. Med. 43 (2011) 632–643.
[115] E. Panzarini, V. Inguscio, L. Dini, Immunogenic cell death: can it be exploited in photodynamic therapy for cancer? Biomed. Res. Int. (2013) 482160.
[116] E.C. Tracy, M.J. Bowman, B.W. Henderson, H. Baumann, Interleukin-1 alpha is the major alarmin of lung epithelial cells released during photodynamic therapy to induce inflammatory mediators in fibroblasts, Br. J. Cancer 107 (2012) 1534–1546.
[117] K.H. Krause, M. Michalak, Calreticulin, Cell 88 (1997) 439–443.
[118] T.J. Ostwald, D.H. MacLennan, Isolation of a high affinity calcium-binding protein from sarcoplasmic reticulum, J. Biol. Chem. 249 (1974) 974–979.
[119] S.J. Gardai, K.A. McPhillips, S.C. Frasch, W.J. Janssen, A. Starefeldt, J.E. Murphy-Ullrich, D.L. Bratton, P.A. Oldenborg, M. Michalak, P.M. Henson, Cell-surface calreticulin initiates clearance of viable or apoptotic cells through trans-activation of LRP on the phagocyte, Cell 123 (2005) 321–334.
[120] D.V. Krysko, A.D. Garg, A. Kaczmarek, O. Krysko, P. Agostinis, P. Vandenabeele, Immunogenic cell death and DAMPs in cancer therapy, Nat. Rev. Cancer 12 (2012) 860–875.
[121] M. Obeid, A. Tesniere, F. Ghiringhelli, G.M. Fimia, L. Apetoh, J.L. Perfettini, M. Castedo, G. Mignot, T. Panaretakis, N. Casares, D. Metivier, N. Larochette, P. van Endert, F. Ciccosanti, M. Piacentini, L. Zitvogel, G. Kroemer, Calreticulin exposure dictates the immunogenicity of cancer cell death, Nat. Med. 13 (2007) 54–61.
[122] A.M. Dudek, A.D. Garg, D.V. Krysko, D. De Ruysscher, P. Agostinis, Inducers of immunogenic cancer cell death, Cytokine Growth Factor Rev. 24 (2013) 319–333.
[123] A.D. Garg, D.V. Krysko, P. Vandenabeele, P. Agostinis, Hypericin-based photodynamic therapy induces surface exposure of damage-associated molecular patterns like HSP70 and calreticulin, Cancer Immunol. Immunother. 61 (2012) 215–221.
[124] A.D. Garg, A.M. Dudek, G.B. Ferreira, T. Verfaillie, P. Vandenabeele, D.V. Krysko, C. Mathieu, P. Agostinis, ROS-induced autophagy in cancer cells assists in evasion from determinants of immunogenic cell death, Autophagy 9 (2013) 1292–1307.
[125] J.O. Thomas, A.A. Travers, HMG1 and 2, and related 'architectural' DNA-binding proteins, Trends Biochem. Sci. 26 (2001) 167–174.
[126] T. Bonaldi, F. Talamo, P. Scaffidi, D. Ferrera, A. Porto, A. Bachi, A. Rubartelli, A. Agresti, M.E. Bianchi, Monocytic cells hyperacetylate chromatin protein HMGB1 to redirect it towards secretion, EMBO J. 22 (2003) 5551–5560.
[127] S. Gardella, C. Andrei, D. Ferrera, L.V. Lotti, M.R. Torrisi, M.E. Bianchi, A. Rubartelli, The nuclear protein HMGB1 is secreted by monocytes via a non-classical, vesicle-mediated secretory pathway, EMBO Rep. 3 (2002) 995–1001.
[128] R. Palumbo, M. Sampaolesi, F. De Marchis, R. Tonlorenzi, S. Colombetti, A. Mondino, G. Cossu, M.E. Bianchi, Extracellular HMGB1 a signal of tissue damage, induces mesoangioblast migration and proliferation, J. Cell Biol. 164 (2004) 441–449.
[129] P. Scaffidi, T. Misteli, M.E. Bianchi, Release of chromatin protein HMGB1 by necrotic cells triggers inflammation, Nature 418 (2002) 191–195.
[130] U. Andersson, H.C. Wang, K. Palmblad, A.C. Aveberger, O. Bloom, H. Erlandsson-Harris, A. Janson, R. Kokkola, M.H. Zhang, H. Yang, K.J. Tracey, High mobility group 1 protein (HMG-1) stimulates proinflammatory cytokine synthesis in human monocytes, J. Exp. Med. 192 (2000) 565–570.
[131] G.Q. Chen, M.F. Ward, A.E. Sama, H.C. Wang, Extracellular HMGB1 as a proinflammatory cytokine, J. Interferon Cytokine Res. 24 (2004) 329–333.
[132] V.V. Orlova, E.Y. Choi, C.P. Xie, E. Chavakis, A. Bierhaus, E. Ihanus, C.M. Ballantyne, C.G. Gahmberg, M.E. Bianchi, P.P. Nawroth, T. Chavakis, A novel pathway of HMGB1-mediated inflammatory cell recruitment that requires Mac-1-integrin, EMBO J. 26 (2007) 1129–1139.
[133] D. Yang, Q. Chen, H. Yang, K.J. Tracey, M. Bustin, J.J. Oppenheim, High mobility group box-1 protein induces the migration and activation of human dendritic cells and acts as an alarmin, J. Leukocyte Biol. 81 (2007) 59–66.
[134] C.W. Bell, W.W. Jiang, C.F. Reich, D.S. Pisetsky, The extracellular release of HMGB1 during apoptotic cell death, Am. J. Physiol. Cell Physiol. 291 (2006) C1318–C1325.
[135] J. Thorburn, H. Horita, J. Redzic, K. Hansen, A.E. Frankel, A. Thorburn, Autophagy regulates selective HMGB1 release in tumor cells that are destined to die, Cell Death Differ. 16 (2009) 175–183.
[136] M.E. Bianchi, HMGB1 loves company, J. Leukocyte Biol. 86 (2009) 573–576.
[137] H. Yang, D.J. Antoine, U. Andersson, K.J. Tracey, The many faces of HMGB1: molecular structure-functional activity in inflammation, apoptosis, and chemotaxis, J. Leukocyte Biol. 93 (2013) 865–873.
[138] M. Korbelik, W. Zhang, S. Merchant, Involvement of damage-associated molecular patterns in tumor response to photodynamic therapy: surface expression of calreticulin and high-mobility group box-1 release, Cancer Immunol. Immunother. 60 (2011) 1431–1437.
[139] M.R. Elliott, F.B. Chekeni, P.C. Trampont, E.R. Lazarowski, A. Kadl, S.F. Walk, D. Park, R.I. Woodson, M. Ostankovich, P. Sharma, J.J. Lysiak, T.K. Harden, N. Leitinger, K.S. Ravichandran, Nucleotides released by apoptotic cells act as a find-me signal to promote phagocytic clearance, Nature 461 (2009) 282-U165.
[140] F. Ghiringhelli, L. Apetoh, A. Tesniere, L. Aymeric, Y.T. Ma, C. Ortiz, K. Vermaelen, T. Panaretakis, G. Mignot, E. Ullrich, J.L. Perfettini, F. Schlemmer, E. Tasdemir, M. Uhl, P. Genin, A. Civas, B. Ryffel, J. Kanellopoulos, J. Tschopp, F. Andre, R. Lidereau, N.M. McLaughlin, N.M. Haynes, M.J. Smyth, G. Kroemer, L. Zitvogel, Activation of the NLRP3 inflammasome in dendritic cells induces IL-1 beta-dependent adaptive immunity against tumors, Nat. Med. 15 (2009) 1170–1171U1199.
[141] L. Zitvogel, O. Kepp, L. Galluzzi, G. Kroemer, Inflammasomes in carcinogenesis and anticancer immune responses, Nat. Immunol. 13 (2012) 343–351.
[142] P.A. Lang, D. Merkler, P. Funkner, N. Shaabani, A. Meryk, C. Krings, C. Barthuber, M. Recher, W. Bruck, D. Haussinger, P.S. Ohashi, K.S. Lang, Oxidized ATP inhibits T-cell-mediated autoimmunity, Eur. J. Immunol. 40 (2010) 2401–2408.
[143] C.M. Brackett, S.O. Gollnick, Photodynamic therapy enhancement of anti-tumor immunity, Photochem. Photobiol. Sci. 10 (2011) 649–652.
[144] M. Firczuk, D. Nowis, J. Golab, PDT-induced inflammatory and host responses, Photochem. Photobiol. Sci. 10 (2011) 653–663.

[145] P. Mroz, J.T. Hashmi, Y.Y. Huang, N. Lang, M.R. Hamblin, Stimulation of anti-tumor immunity by photodynamic therapy, Expert Rev. Clin. Immunol. 7 (2011) 75–91.
[146] M. Korbelik, PDT-associated host response and its role in the therapy outcome, Lasers Surg. Med. 38 (2006) 500–508.
[147] E.S. Trombetta, I. Mellman, Cell biology of antigen processing in vitro and in vivo, Annu. Rev. Immunol. 23 (2005) 975–1028.
[148] G. Canti, D. Lattuada, A. Nicolin, P. Taroni, G. Valentini, R. Cubeddu, Antitumor immunity induced by photodynamic therapy with aluminum disulfonated phthalocyanines and laser-light, Anticancer Drugs 5 (1994) 443–447.
[149] E. Kabingu, L. Vaughan, B. Owczarczak, K.D. Ramsey, S.O. Gollnick, CD8(+) T cell-mediated control of distant tumours following local photodynamic therapy is independent of CD4(+) T cells and dependent on natural killer cells, Br. J. Cancer 96 (2007) 1839–1848.
[150] P.S.P. Thong, K.W. Ong, N.S.G. Goh, K.W. Kho, V. Manivasager, R. Bhuvaneswari, M. Oliva, K.C. Soo, Photodynamic-therapy-activated immune response against distant untreated tumours in recurrent angiosarcoma, Lancet Oncol. 8 (2007) 950–952.
[151] E.S. Abdel-Hady, P. Martin-Hirsch, M. Duggan-Keen, P.L. Stern, J.V. Moore, G. Corbitt, H.C. Kitchener, I.N. Hampson, Immunological and viral factors associated with the response of vulval intraepithelial neoplasia to photodynamic therapy, Cancer Res. 61 (2001) 192–196.
[152] E. Kabingu, A.R. Oseroff, G.E. Wilding, S.O. Gollnick, Enhanced systemic immune reactivity to a basal cell carcinoma associated antigen following photodynamic therapy, Clin. Cancer Res. 15 (2009) 4460–4466.
[153] G. Dragieva, J. Hafner, R. Dummer, P. Schmid-Grendelmeier, M. Roos, B.M. Prinz, G. Burg, U. Binswanger, W. Kempf, Topical photodynamic therapy in the treatment of actinic keratoses and Bowen's disease in transplant recipients, Transplantation 77 (2004) 115–121.
[154] A. Szokalska, M. Makowski, D. Nowis, G.M. Wilczynski, M. Kujawa, C. Wojcik, I. Mlynarczuk-Bialy, P. Salwa, J. Bil, S. Janowska, P. Agostinis, T. Verfaillie, M. Bugajski, J. Gietka, T. Issat, E. Glodkowska, P. Mrowka, T. Stoklosa, M.R. Hamblin, P. Mroz, M. Jakobisiak, J. Golab, Proteasome inhibition potentiates antitumor effects of photodynamic therapy in mice through induction of endoplasmic reticulum stress and unfolded protein response, Cancer Res. 69 (2009) 4235–4243.
[155] J. Debnath, E.H. Baehrecke, G. Kroemer, Does autophagy contribute to cell death? Autophagy 1 (2005) 66–74.
[156] D. Kessel, J.J. Reiners, Apoptosis and autophagy after mitochondrial or endoplasmic reticulum photodamage, Photochem. Photobiol. 83 (2007) 1024–1028.
[157] H.R.C. Kim, Y. Luo, G.Y. Li, D. Kessel, Enhanced apoptotic response to photodynamic therapy after bcl-2 transfection, Cancer Res. 59 (1999) 3429–3432.
[158] L.Y. Xue, S.M. Chiu, N.L. Oleinick, Photochemical destruction of the Bcl-2 oncoprotein during photodynamic therapy with the phthalocyanine photosensitizer Pc 4, Oncogene 20 (2001) 3420–3427.
[159] D. Kessel, M. Castelli, Evidence that bcl-2 is the target of three photosensitizers that induce a rapid apoptotic response, Photochem. Photobiol. 74 (2001) 318–322.
[160] X.H. Liang, L.K. Kleeman, H.H. Jiang, G. Gordon, J.E. Goldman, G. Berry, B. Herman, B. Levine, Protection against fatal Sindbis virus encephalitis by Beclin, a novel Bcl-2-interacting protein, J. Virol. 72 (1998) 8586–8596.
[161] S. Pattingre, A. Tassa, X.P. Qu, R. Garuti, X.H. Liang, N. Mizushima, M. Packer, M.D. Schneider, B. Levine, Bcl-2 antiapoptotic proteins inhibit Beclin 1-dependent autophagy, Cell 122 (2005) 927–939.
[162] D. Kessel, A.S. Arroyo, Apoptotic and autophagic responses to Bcl-2 inhibition and photodamage, Photochem. Photobiol. Sci. 6 (2007) 1290–1295.
[163] M. Andrzejak, M. Price, D.H. Kessel, Apoptotic and autophagic responses to photodynamic therapy in 1c1c7 murine hepatoma cells, Autophagy 7 (2011) 979–984.
[164] P. Boya, R.A. Gonzalez-Polo, N. Casares, J.L. Perfettini, P. Dessen, N. Larochette, D. Metivier, D. Meley, S. Souquere, T. Yoshimori, G. Pierron, P. Codogno, G. Kroemer, Inhibition of macroautophagy triggers apoptosis, Mol. Cell. Biol. 25 (2005) 1025–1040.
[165] C.H. Yan, Z.Q. Liang, Z.L. Gu, Y.P. Yang, P. Reid, Z.H. Qin, Contributions of autophagic and apoptotic mechanisms to CrTX-induced death of K562 cells, Toxicon 47 (2006) 521–530.
[166] C.M. Allen, W.M. Sharman, J.E. Van Lier, Current status of phthalocyanines in the photodynamic therapy of cancer, J. Porphyrins Phthalocyanines 5 (2001) 161–169.
[167] N. Brasseur, Sensitizers for PDT: phthalocyanines, in: T. Patrice (Ed.), Photodynamic Therapy, Royal Society of Chemistry, Cambridge, 2004, pp. 107–114.
[168] J.E. van Lier, J.D. Spikes, The chemistry, photophysics and photosensitizing properties of phthalocyanines, Ciba Found. Symp. 146 (1989) 17–26.
[169] J.R. Wagner, H. Ali, R. Langlois, N. Brasseur, J.E. Vanlier, Biological activities of phthalocyanines VI. Photooxidation of L-tryptophan by selectively sulfonated gallium phthalocyanines—singlet oxygen yields and effect of aggregation, Photochem. Photobiol. 45 (1987) 587–594.
[170] J.R. Darwent, P. Douglas, A. Harriman, G. Porter, M.C. Richoux, Metal phthalocyanines and porphyrins as photosensitizers for reduction of water to hydrogen, Coord. Chem. Rev. 44 (1982) 83–126.
[171] E. Ben-Hur, Basic photobiology and mechanisms of action of phthalocyanines, in: T.J. Dougherty, B.W. Henderson (Eds.), Photodynamic Therapy, Basic Principles and Clinical Applications, Marcel Dekker, New York, 1992, pp. 63–77.
[172] M. Ochsner, Light scattering of human skin: a comparison between zinc(II)-phthalocyanine and Photofrin II, J. Photochem. Photobiol. B 32 (1996) 3–9.
[173] E.D. Baron, C.L. Malbasa, D. Santo-Domingo, P.F. Fu, J.D. Miller, K.K. Hanneman, A.H. Hsia, N.L. Oleinick, V.C. Colussi, K.D. Cooper, Silicon phthalocyanine (Pc 4) photodynamic therapy is a safe modality for cutaneous neoplasms: results of a phase 1 clinical trial, Lasers Surg. Med. 42 (2010) 728–735.
[174] M. Ochsner, Photophysical and photobiological processes in the photodynamic therapy of tumours, J. Photochem. Photobiol. B 39 (1997) 1–18.
[175] D.A. Bellnier, W.R. Greco, G.M. Loewen, H. Nava, A.R. Oseroff, T.J. Dougherty, Clinical pharmacokinetics of the PDT photosensitizers porfimer sodium (Photofrin), 2-[1-hexyloxyethyl]-2-devinyl pyropheophorbide-a (Photochlor) and 5-ALA-induced protoporphyrin IX, Lasers Surg. Med. 38 (2006) 439–444.
[176] J. Berlanda, T. Kiesslich, V. Engelhardt, B. Krammer, K. Plaetzer, Comparative in vitro study on the characteristics of different photosensitizers employed in PDT, J. Photochem. Photobiol. B 100 (2010) 173–180.
[177] R.M. Amin, C. Hauser, I. Kinzler, A. Rueck, C. Scalfi-Happ, Evaluation of photodynamic treatment using aluminum phthalocyanine tetrasulfonate chloride as a photosensitizer: new approach, Photochem. Photobiol. Sci. 11 (2012) 1156–1163.
[178] E.C.C. Tapajos, J.P. Longo, A.R. Simioni, Z.G.M. Lacava, M.F.M.A. Santos, P.C. Morais, A.C. Tedesco, R.B. Azevedo, In vitro photodynamic therapy on human oral keratinocytes using chloroaluminum-phthalocyanine, Oral Oncol. 44 (2008) 1073–1079.
[179] E. Ben-Hur, T. Fujihara, F. Suzuki, M.M. Elkind, Genetic toxicology of the photosensitization of Chinese hamster cells by phthalocyanines, Photochem. Photobiol. 45 (1987) 227–230.
[180] K. Halkiotis, D. Yova, G. Pantelias, In vitro evaluation of the genotoxic and clastogenic potential of photodynamic therapy, Mutagenesis 14 (1999) 193–198.
[181] F.I. Mcnair, B. Marples, C.M.L. West, J.V. Moore, A comet assay of DNA damage and repair in K562 cells after photodynamic therapy using haematoporphyrin derivative, methylene blue and meso-tetrahydroxyphenylchlorin, Br. J. Cancer 75 (1997) 1721–1729.
[182] C.M.N. Yow, N.K. Mak, S. Szeto, J.Y. Chen, Y.L. Lee, N.H. Cheung, D.P. Huang, A. W.N. Leung, Photocytotoxic and DNA damaging effect of Temoporfin (mTHPC) and merocyanine 540 (MC540) on nasopharyngeal carcinoma cell, Toxicol. Lett. 115 (2000) 53–61.
[183] P. Duez, M. Hanocq, J. Dubois, Photodynamic DNA damage mediated by delta-aminolevulinic acid-induced porphyrins, Carcinogenesis 22 (2001) 771–778.
[184] D.M. Fiedler, P.M. Eckl, B. Krammer, Does delta-aminolaevulinic acid induce genotoxic effects? J. Photochem. Photobiol. B 33 (1996) 39–44.
[185] V.A. Bohr, T. Stevnsner, N.C. de Souza-Pinto, Mitochondrial DNA repair of oxidative damage in mammalian cells, Gene 286 (2002) 127–134.
[186] T. Kiesslich, J. Berlanda, K. Plaetzer, B. Krammer, F. Berr, Comparative characterization of the efficiency and cellular pharmacokinetics of Foscan-(R) and Foslip (R)-based photodynamic treatment in human biliary tract cancer cell lines, Photochem. Photobiol. Sci. 6 (2007) 619–627.
[187] M. Leunig, C. Richert, F. Gamarra, W. Lumper, E. Vogel, D. Jocham, A.E. Goetz, Tumor-localization kinetics of Photofrin and three synthetic prophyrinoids in an amelanotic melanoma of the hamster, Br. J. Cancer 68 (1993) 225–234.
[188] S. Iinuma, R. Bachor, T. Flotte, T. Hasan, Biodistribution and phototoxicity of 5-aminolevulinic acid-induced PpIX in an orthotopic rat bladder tumor model, J. Urol. 153 (1995) 802–806.
[189] A.M. Ronn, M. Nouri, L.A. Lofgren, B.M. Steinberg, A. Westerborn, T. Windahl, M.J. Shikowitz, A.L. Abramson, Human tissue levels and plasma pharmacokinetics of temoporfin (Foscan(R), mTHPC), Lasers Med. Sci. 11 (1996) 267–272.
[190] E. Reddi, G. Locastro, R. Biolo, G. Jori, Pharmacokinetic studies with zinc(II)-phthalocyanine in tumor-bearing mice, Br. J. Cancer 56 (1987) 597–600.
[191] L. Polo, A. Segalla, G. Jori, G. Bocchiotti, G. Verna, R. Franceschini, R. Mosca, P. G. DeFilippi, Liposome-delivered I-131-labelled Zn(II)-phthalocyanine as a radiodiagnostic agent for tumours, Cancer Lett. 109 (1996) 57–61.
[192] Q. Peng, J. Moan, M. Kongshaug, J.F. Evensen, H. Anholt, C. Rimington, Sensitizer for photodynamic therapy of cancer—a comparison of the tissue distribution of Photofrin II and aluminum phthalocyanine tetrasulfonate in nude mice bearing a human malignant tumor, Int. J. Cancer 48 (1991) 258–264.
[193] K.W. Woodburn, Q. Fan, D.R. Miles, D. Kessel, Y. Luo, S.W. Young, Localization and efficacy analysis of the phototherapeutic lutetium texaphyrin (PCI-0123) in the murine EMT6 sarcoma model, Photochem. Photobiol. 65 (1997) 410–415.
[194] J.F. Chiou, Y.H. Wang, M.J. Jou, T.Z. Liu, C.Y. Shiau, Verteporfin-photoinduced apoptosis in HepG2 cells mediated by reactive oxygen and nitrogen species intermediates, Free Rad. Res. 44 (2010) 155–170.
[195] P.P. Deshpande, S. Biswas, V.P. Torchilin, Current trends in the use of liposomes for tumor targeting, Nanomedicine 8 (2013) 1509–1528.
[196] A. Lukyanov, Z. Gao, L. Mazzola, V. Torchilin, Polyethylene glycol-diacyllipid micelles demonstrate increased accumulation in subcutaneous tumors in mice, Pharm. Res. 19 (2002) 1424–1429.
[197] A. Fundarò, R. Cavalli, A. Bargoni, D. Vighetto, G.P. Zara, M.R. Gasco, Non-stealth and stealth solid lipid nanoparticles (SLN) carrying doxorubicin:

pharmacokinetics and tissue distribution after i.v. administration to rats, Pharmacol. Res. 42 (2000) 337–343.
[198] P. Guo, S. Song, Z. Li, Y. Tian, J. Zheng, X. Yang, W. Pan, In vitro and in vivo evaluation of APRPG-modified angiogenic vessel targeting micelles for anticancer therapy, Int. J. Pharm. 486 (2015) 356–366.
[199] Y.-C. Kuo, C.-Y. Shih-Huang, Solid lipid nanoparticles with surface antibody for targeting the brain and inhibiting lymphatic phagocytosis, J. Taiwan Inst. Chem. Eng. 45 (2014) 1154–1163.
[200] M.R. Hamblin, E.L. Newman, Photosensitizer targeting in photodynamic therapy. II. Conjugates of haematoporphyrin with serum lipoproteins, J. Photochem. Photobiol. B 26 (1994) 147–157.
[201] E. Reddi, C. Zhou, R. Biolo, E. Menegaldo, G. Jori, Liposome- or LDL-administered Zn(II)-phthalocyanine as a photodynamic agent for tumors I. Pharmacokinetic properties and phototherapeutic efficiency, Br. J. Cancer 61 (1990) 407–411.
[202] G.I. Harisa, F.K. Alanazi, Low density lipoprotein bionanoparticles: from cholesterol transport to delivery of anti-cancer drugs, Saudi Pharm. J. 22 (2014) 504–515.
[203] S. Svenson, D.A. Tomalia, Dendrimers in biomedical applications—reflections on the field, Adv. Drug Deliv. Rev. 64 (Suppl) (2012) 102–115.
[204] K. Madaan, S. Kumar, N. Poonia, V. Lather, D. Pandita, Dendrimers in drug delivery and targeting: drug-dendrimer interactions and toxicity issues, J. Pharm. Bioallied Sci. 6 (2014) 139–150.
[205] V.P. Torchilin, Micellar nanocarriers: pharmaceutical perspectives, Pharm. Res. 24 (2007) 1–16.
[206] M. Yokoyama, Clinical applications of polymeric micelle carrier systems in chemotherapy and image diagnosis of solid tumors, J. Exp. Clin. Med. 3 (2011) 151–158.
[207] S.A. Sibani, P.A. McCarron, A.D. Woolfson, R.F. Donnelly, Photosensitiser delivery for photodynamic therapy. Part 2: systemic carrier platforms, Expert Opin. Drug Deliv. 5 (2008) 1241–1254.
[208] M.A. Manoukian, S.V. Ott, J. Rajadas, M. Inayathullah, Polymeric nanoparticles to combat squamous cell carcinomas in patients with dystrophic epidermolysis bullosa, Recent Pat. Nanomed. 4 (2014) 15–24.
[209] A. Kumari, S.K. Yadav, S.C. Yadav, Biodegradable polymeric nanoparticles based drug delivery systems, Colloids Surf. B 75 (2010) 1–18.
[210] E. Ricci-Júnior, J.M. Marchetti, Zinc(II) phthalocyanine loaded PLGA nanoparticles for photodynamic therapy use, Int. J. Pharm. 310 (2006) 187–195.
[211] E.S. Shibu, M. Hamada, N. Murase, V. Biju, Nanomaterials formulations for photothermal and photodynamic therapy of cancer, J. Photochem. Photobiol. C. 15 (2013) 53–72.
[212] N.F. Gamaleia, I.O. Shton, Gold mining for PDT: Great expectations from tiny nanoparticles, Photodiagn. Photodyn. Ther. (2015), doi:http://dx.doi.org/10.1016/j.pdpdt.2015.03.002.
[213] B.N. Khlebtsov, V.A. Khanadeev, I.L. Maksimova, G.S. Terentyuk, N.G. Khlebtsov, Silver nanocubes and gold nanocages: Fabrication and optical and photothermal properties, Nanotechnol. Russ. 5 (2010) 454–468.
[214] L. Li, J.F. Zhao, N. Won, H. Jin, S. Kim, J.Y. Chen, Quantum dot-aluminum phthalocyanine conjugates perform photodynamic reactions to kill cancer cells via fluorescence resonance energy transfer, Nanoscale Res. Lett. 7 (2012) 386.
[215] H.I. Chang, M.K. Yeh, Clinical development of liposome-based drugs: formulation, characterization, and therapeutic efficacy, Int. J. Nanomed. 7 (2012) 49–60.
[216] M.L. Immordino, F. Dosio, L. Cattel, Stealth liposomes: review of the basic science, rationale, and clinical applications existing and potential, Int. J. Nanomed. 1 (2006) 297–315.
[217] G. Aguilar, B. Choi, M. Broekgaarden, O.W. Yang, B. Yang, P. Ghasri, J.K. Chen, R. Bezemer, J.S. Nelson, A.M. van Drooge, A. Wolkerstorfer, K.M. Kelly, M. Heger, An overview of three promising mechanical, optical, and biochemical engineering approaches to improve selective photothermolysis of refractory port wine stains, Ann. Biomed. Eng. 40 (2012) 486–506.
[218] X. Damoiseau, H.J. Schuitmaker, J.W.M. Lagerberg, M. Hoebeke, Increase of the photosensitizing efficiency of the bacteriochlorin a by liposome-incorporation, J. Photochem. Photobiol. B 60 (2001) 50–60.
[219] S. Dhami, D. Phillips, Comparison of the photophysics of an aggregating and non-aggregating aluminium phthalocyanine system incorporated into unilamellar vesicles, J. Photochem. Photobiol. A 100 (1996) 77–84.
[220] A.M. Garcia, E. Alarcon, M. Munoz, J.C. Scaiano, A.M. Edwards, E. Lissi, Photophysical behaviour and photodynamic activity of zinc phthalocyanines associated to liposomes, Photochem. Photobiol. Sci. 10 (2011) 507–514.
[221] A.S.L. Derycke, P.A.M. de Witte, Liposomes for photodynamic therapy, Adv. Drug Deliv. Rev. 56 (2004) 17–30.
[222] G. Jori, Factors controlling the selectivity and efficiency of tumour damage in photodynamic therapy, Lasers Med. Sci. 5 (1990) 115–120.
[223] P.I. Campbell, Toxicity of some charged lipids used in liposome preparations, Cytobios 37 (1983) 21–26.
[224] E. Mayhew, M. Ito, R. Lazo, Toxicity of non-drug containing liposomes for cultured human cells, Exp. Cell Res. 171 (1987) 195–202.
[225] R. Banerjee, Liposomes: applications in medicine, J. Biomater. Appl. 16 (2001) 3–21.
[226] V.D. Awasthi, D. Garcia, B.A. Goins, W.T. Phillips, Circulation and biodistribution profiles of long-circulating PEG-liposomes of various sizes in rabbits, Int. J. Pharm. 253 (2003) 121–132.
[227] T.M. Allen, C. Hansen, F. Martin, C. Redemann, A. Yauyoung, Liposomes containing synthetic lipid derivatives of poly(ethylene glycol) show prolonged circulation half-lives in vivo, Biochim. Biophys. Acta 1066 (1991) 29–36.
[228] A.L. Klibanov, K. Maruyama, V.P. Torchilin, L. Huang, Amphipathic polyethyleneglycols effectively prolong the circulation time of liposomes, FEBS Lett. 268 (1990) 235–237.
[229] D. Papahadjopoulos, T.M. Allen, A. Gabizon, E. Mayhew, K. Matthay, S.K. Huang, K.D. Lee, M.C. Woodle, D.D. Lasic, C. Redemann, F.J. Martin, Sterically stabilized liposomes—improvements in pharmacokinetics and antitumor therapeutic efficacy, Proc. Natl. Acad. Sci. U. S. A. 88 (1991) 11460–11464.
[230] J. Senior, C. Delgado, D. Fisher, C. Tilcock, G. Gregoriadis, Influence of surface hydrophilicity of liposomes on their interaction withp plasma protein and clearance from the circulation—studies with poly(ethylene glycol)-coated vesicles, Biochim. Biophys. Acta 1062 (1991) 77–82.
[231] V.P. Torchilin, V.G. Omelyanenko, M.I. Papisov, A.A. Bogdanov, V.S. Trubetskoy, J.N. Herron, C.A. Gentry, Poly(ethylene glycol) on the liposome surface—on the mechanism of polymer-coated liposome longevity, Biochim. Biophys. Acta 1195 (1994) 11–20.
[232] D. Needham, T.J. Mcintosh, D.D. Lasic, Repulsive interactions and mechanical stability of polymer-grafted lipid membranes, Biochim. Biophys. Acta 1108 (1992) 40–48.
[233] A. Gabizon, D. Papahadjopoulos, The role of surface charge and hydrophilic groups on liposome clearance in vivo, Biochim. Biophys. Acta 1103 (1992) 94–100.
[234] D.D. Lasic, F.J. Martin, A. Gabizon, S.K. Huang, D. Papahadjopoulos, Sterically stabilized liposomes—a hypothesis on the molecular origin of the extended circulation times, Biochim. Biophys. Acta 1070 (1991) 187–192.
[235] J.A. Harding, C.M. Engbers, M.S. Newman, N.I. Goldstein, S. Zalipsky, Immunogenicity and pharmacokinetic attributes of poly(ethylene glycol)-grafted immunoliposomes, Biochim. Biophys. Acta 1327 (1997) 181–192.
[236] M.J. Bovis, J.H. Woodhams, M. Loizidou, D. Scheglmann, S.G. Bown, A.J. MacRobert, Improved in vivo delivery of m-THPC via pegylated liposomes for use in photodynamic therapy, J. Control. Release 157 (2012) 196–205.
[237] J. Buchholz, B. Kaser-Hotz, T. Khan, C.R. Bleyl, K. Melzer, R.A. Schwendener, M. Roos, H. Walt, Optimizing photodynamic therapy: in vivo pharmacokinetics of liposomal meta-(tetrahydroxyphenyl) chlorin in feline squamous cell carcinoma, Clin. Cancer Res. 11 (2005) 7538–7544.
[238] C.B. Hansen, G.Y. Kao, E.H. Moase, S. Zalipsky, T.M. Allen, Attachment of antibodies to sterically stabilized liposomes—evaluation, comparison and optimization of coupling procedures, Biochim. Biophys. Acta 1239 (1995) 133–144.
[239] S. Shahinian, J.R. Silvius, A novel strategy affords high-yield coupling of antibody Fab' fragments to liposomes, Biochim. Biophys. Acta 1239 (1995) 157–167.
[240] V.P. Torchilin, A.L. Klibanov, L. Huang, S. Odonnell, N.D. Nossiff, B.A. Khaw, Targeted accumulation of polyethylene glycol-coated immunoliposomes in infarcted rabbit myocardium, FASEB J. 6 (1992) 2716–2719.
[241] V.P. Torchilin, J. Narula, E. Halpern, B.A. Khaw, Poly(ethylene glycol)-coated anti-cardiac myosin immunoliposomes: factors influencing targeted accumulation in the infarcted myocardium, Biochim. Biophys. Acta 1279 (1996) 75–83.
[242] J. Montanari, C. Maidana, M.I. Esteva, C. Salomon, M.J. Morilla, E.L. Romero, Sunlight triggered photodynamic ultradeformable liposomes against *Leishmania braziliensis* are also leishmanicidal in the dark, J. Control. Release 147 (2010) 368–376.
[243] W.G. Love, S. Duk, R. Biolo, G. Jori, P.W. Taylor, Liposome-mediated delivery of photosensitizers: localization of zinc(II)-phthalocyanine within implanted tumors after intravenous administration, Photochem. Photobiol. 63 (1996) 656–661.
[244] U. Isele, K. Schieweck, R. Kessler, P. Van Hoogevest, H.G. Capraro, Pharmacokinetics and body distribution of liposomal zinc phthalocyanine in tumor-bearing mice—influence of aggregation state, particle-size, and composition, J. Pharm. Sci. 84 (1995) 166–173.
[245] A. Visona, G. Jori, Targeting of experimentally-induced atherosclerotic lesions by liposome-delivered Zn(II)-phthalocyanine, Atherosclerosis 100 (1993) 213–222.
[246] C. Larroque, A. Pelegrin, J.E. Vanlier, Serum albumin as a vehicle for zinc phthalocyanine: photodynamic activities in solid tumour models, Br. J. Cancer 74 (1996) 1886–1890.
[247] M. Fadel, K. Kassab, D.A. Fadeel, Zinc phthalocyanine-loaded PLGA biodegradable nanoparticles for photodynamic therapy in tumor-bearing mice, Lasers Med. Sci. 25 (2010) 283–292.
[248] M.D. Soares, M.R. Oliveira, E.P. dos Santos, L.D. Gitirana, G.M. Barbosa, C.H. Quaresma, E. Ricci, Nanostructured delivery system for zinc phthalocyanine: preparation, characterization, and phototoxicity study against human lung adenocarcinoma A549 cells, Int. J. Nanomed. 6 (2011) 227–238.
[249] H.L.L.M. Van Leengoed, V. Cuomo, A.A.C. Versteeg, N. Vanderveen, G. Jori, W. M. Star, In vivo fluorescence and photodynamic activity of zinc phthalocyanine administered in liposomes, Br. J. Cancer 69 (1994) 840–845.
[250] E.R. da Silva, Z.M.F. de Freitas, L.D. Gitirana, E. Ricci, Improving the topical delivery of zinc phthalocyanine using oleic acid as a penetration enhancer: in vitro permeation and retention, Drug Dev. Ind. Pharm. 37 (2011) 569–575.
[251] J.R. Lakowicz, Solvent and environmental effects, Principles of Fluorescence Spectroscopy, third ed., Springer, Baltimore, 2006, pp. 205–235.

[252] K. Suwa, T. Kimura, A.P. Schaap, Reaction of singlet oxygen with cholesterol in liposomal membranes—effect of membrane fluidity on photooxidation of cholesterol, Photochem. Photobiol. 28 (1978) 469–473.
[253] S.P. Stratton, D.C. Liebler, Determination of singlet oxygen-specific versus radical-mediated lipid peroxidation in photosensitized oxidation of lipid bilayers: effect of beta-carotene and alpha-tocopherol, Biochemistry 36 (1997) 12911–12920.
[254] A.W. Girotti, Mechanisms of lipid peroxidation, Free Radic. Biol. Med. 1 (1985) 87–95.
[255] S.M.T. Nunes, F.S. Sguilla, A.C. Tedesco, Photophysical studies of zinc phthalocyanine and chloroaluminum phthalocyanine incorporated into liposomes in the presence of additives, Braz. J. Med. Biol. Res. 37 (2004) 273–284.
[256] A. Molinari, M. Colone, A. Calcabrini, A. Stringaro, L. Toccacieli, G. Arancia, S. Mannino, A. Mangiola, G. Maira, C. Bombelli, G. Mancini, Cationic liposomes loaded with m-THPC, in photodynamic therapy for malignant glioma, Toxicol. In Vitro 21 (2007) 230–234.
[257] A. Gijsens, L. Derycke, D. Missiaen, J. De Vos, E.A.P. Huwyler, Targeting of the photocytotoxic compound AlPcS4 to Hela cells by transferrin conjugated PEG-liposomes, Int. J. Cancer 101 (2002) 78–85.
[258] A. Villanueva, J.C. Stockert, M. Canete, P. Acedo, A new protocol in photodynamic therapy: enhanced tumour cell death by combining two different photosensitizers, Photochem. Photobiol. Sci. 9 (2010) 295–297.
[259] D. Hanahan, R.A. Weinberg, The hallmarks of cancer, Cell 100 (2000) 57–70.
[260] D. Hanahan, R.A. Weinberg, Hallmarks of cancer: the next generation, Cell 144 (2011) 646–674.
[261] A. Koshkaryev, R. Sawant, M. Deshpande, V. Torchilin, Immunoconjugates and long circulating systems: origins, current state of the art and future directions, Adv. Drug Deliv. Rev. 65 (2013) 24–35.
[262] S.X. Song, D. Liu, J.L. Peng, Y. Sun, Z.H. Li, J.R. Gu, Y.H. Xu, Peptide ligand-mediated liposome distribution and targeting to EGFR expressing tumor in vivo, Int. J. Pharm. 363 (2008) 155–161.
[263] M. Broekgaarden, R. van Vught, T.M. van Gulik, E. Breukink, M. Heger, Development of anti-epidermal growth factor receptor functionalized liposomes with zinc-phthalocyanine for photodynamic therapy. Manuscript in preparation, 2015.
[264] C. Mamot, D.C. Drummond, C.O. Noble, V. Kallab, Z.X. Guo, K.L. Hong, D.B. Kirpotin, J.W. Park, Epidermal growth factor receptor-targeted immunoliposomes significantly enhance the efficacy of multiple anticancer drugs in vivo, Cancer Res. 65 (2005) 11631–11638.
[265] J.W. Park, K.L. Hong, D.B. Kirpotin, G. Colbern, R. Shalaby, J. Baselga, Y. Shao, U. B. Nielsen, J.D. Marks, D. Moore, D. Papahadjopoulos, C.C. Benz, Anti-HER2 immunoliposomes: enhanced efficacy attributable to targeted delivery, Clin. Cancer Res. 8 (2002) 1172–1181.
[266] K. Nishikawa, T. Asai, H. Shigematsu, K. Shimizu, H. Kato, Y. Asano, S. Takashima, E. Mekada, N. Oku, T. Minamino, Development of anti-HB-EGF immunoliposomes for the treatment of breast cancer, J. Control. Release 160 (2012) 274–280.
[267] M. Garcia-Diaz, S. Nonell, A. Villanueva, J.C. Stockert, M. Canete, A. Casado, M. Mora, M.L. Sagrista, Do folate-receptor targeted liposomal photosensitizers enhance photodynamic therapy selectivity? Biochim. Biophys. Acta 1808 (2011) 1063–1071.
[268] Y. Mir, S.A. Elrington, T. Hasan, A new nanoconstruct for epidermal growth factor receptor-targeted photo-immunotherapy of ovarian cancer, Nanomed. Nanotechnol. Biol. Med. 9 (2013) 1114–1122.
[269] M. Triesscheijn, M. Ruevekamp, M. Aalders, P. Baas, F.A. Stewart, Outcome of mTHPC mediated photodynamic therapy is primarily determined by the vascular response, Photochem. Photobiol. 81 (2005) 1161–1167.
[270] V.H. Fingar, K.A. Siegel, T.J. Wieman, K.W. Doak, The effects of thromboxane inhibitors on the microvascular and tumor response to photodynamic therapy, Photochem. Photobiol. 58 (1993) 393–399.
[271] P. Cramers, M. Ruevekamp, H. Oppelaar, O. Dalesio, P. Baas, F.A. Stewart, Foscan(R) uptake and tissue distribution in relation to photodynamic efficacy, Br. J. Cancer 88 (2003) 283–290.
[272] B. Chen, P.A. de Witte, Photodynamic therapy efficacy and tissue distribution of hypericin in a mouse P388 lymphoma tumor model, Cancer Lett. 150 (2000) 111–117.
[273] D.E.J.G. Dolmans, A. Kadambi, J.S. Hill, C.A. Waters, B.C. Robinson, J.P. Walker, D. Fukumura, R.K. Jain, Vascular accumulation of a novel photosensitizer MV6401, causes selective thrombosis in tumor vessels after photodynamic therapy, Cancer Res. 62 (2002) 2151–2156.
[274] V.H. Fingar, P.K. Kik, P.S. Haydon, P.B. Cerrito, M. Tseng, E. Abang, T.J. Wieman, Analysis of acute vascular damage after photodynamic therapy using benzoporphyrin derivative (BPD), Br. J. Cancer 79 (1999) 1702–1708.
[275] M. Heger, J.F. Beek, N.I. Moldovan, C.M.A.M. van der Horst, M.J.C. van Gemert, Towards optimization of selective photothermolysis: prothrombotic pharmaceutical agents as potential adjuvants in laser treatment of port wine stains—a theoretical study, Thromb. Haemost. 93 (2005) 242–256.
[276] M. Heger, R.F. van Golen, M. Broekgaarden, R.R. van den Bos, H.A.M. Neumann, T.M. van Gulik, M.J.C. van Gemert, Endovascular laser-tissue interactions and biological responses in relation to endovenous laser therapy, Lasers Med. Sci. 29 (2014) 405–422.
[277] J. Zilberstein, S. Schreiber, M.C.W.M. Bloemers, P. Bendel, M. Neeman, E. Schechtman, F. Kohen, A. Scherz, Y. Salomon, Antivascular treatment of solid melanoma tumors with bacteriochlorophyll-serine-based photodynamic therapy, Photochem. Photobiol. 73 (2001) 257–266.
[278] N. Madar-Balakirski, C. Tempel-Brami, V. Kalchenko, O. Brenner, D. Varon, A. Scherz, Y. Salomon, Permanent occlusion of feeding arteries and draining veins in solid mouse tumors by vascular targeted photodynamic therapy (VTP) with Tookad, Plos One 5 (2010) .
[279] G. Zhao, B.L. Rodriguez, Molecular targeting of liposomal nanoparticles to tumor microenvironment, Int. J. Nanomed. 8 (2013) 61–71.
[280] C. Lonez, M. Vandenbranden, J.M. Ruysschaert, Cationic lipids activate intracellular signaling pathways, Adv. Drug Deliv. Rev. 64 (2012) 1749–1758.
[281] W.J. Choi, J.K. Kim, S.H. Choi, J.S. Park, W.S. Ahn, C.K. Kim, Low toxicity of cationic lipid-based emulsion for gene transfer, Biomaterials 25 (2004) 5893–5903.
[282] G. Thurston, J.W. Mclean, M. Rizen, P. Baluk, A. Haskell, T.J. Murphy, D. Hanahan, D.M. McDonald, Cationic liposomes target angiogenic endothelial cells in tumors and chronic inflammation in mice, J. Clin. Invest. 101 (1998) 1401–1413.
[283] R.B. Campbell, D. Fukumura, E.B. Brown, L.M. Mazzola, Y. Izumi, R.K. Jain, V.P. Torchilin, L.L. Munn, Cationic charge determines the distribution of liposomes between the vascular and extravascular compartments of tumors, Cancer Res. 62 (2002) 6831–6836.
[284] S.L. Diaz, V. Padler-Karavani, D. Ghaderi, N. Hurtado-Ziola, H. Yu, X. Chen, E.C. M. Brinkman-Van der Linden, A. Varki, N.M. Varki, Sensitive and specific detection of the non-human sialic acid *N*-glycolylneuraminic acid in human tissues and biotherapeutic products, PloS One 4 (2009) .
[285] M. Broekgaarden, R. Weijer, A.I. de Kroon, T.M. van Gulik, M. Heger, Liposomal delivery of Zn(II)-phthalocyanine towards tumor vascular endothelial cells increases efficacy of photodynamic therapy. Manuscript in preparation, 2015.
[286] N. Gross, M. Ranjbar, C. Evers, J. Hua, G. Martin, B. Schulze, U. Michaelis, L.L. Hansen, H.T. Agostini, Choroidal neovascularization reduced by targeted drug delivery with cationic liposome-encapsulated paclitaxel or targeted photodynamic therapy with verteporfin encapsulated in cationic liposomes, Mol. Vision 19 (2013) 54–61.
[287] L.M. Coussens, Z. Werb, Inflammation and cancer, Nature 420 (2002) 860–867.
[288] M.M. Mueller, N.E. Fusenig, Friends or foes—bipolar effects of the tumour stroma in cancer, Nat. Rev. Cancer 4 (2004) 839–849.
[289] J.W. Pollard, Tumour-educated macrophages promote tumour progression and metastasis, Nat. Rev. Cancer 4 (2004) 71–78.
[290] C.J. Gomer, A. Ferrario, M. Luna, N. Rucker, S. Wong, Photodynamic therapy: combined modality approaches targeting the tumor microenvironment, Lasers Surg. Med. 38 (2006) 516–521.
[291] M.D.C. Pazos, H.B. Nader, Effect of photodynamic therapy on the extracellular matrix and associated components, Braz. J. Med. Biol. Res. 40 (2007) 1025–1035.
[292] R.F. van Golen, T.M. van Gulik, M. Heger, The sterile immune response during hepatic ischemia/reperfusion, Cytokine Growth Factor Rev. 23 (2012) 69–84.
[293] Z. Amoozgar, Y. Yeo, Recent advances in stealth coating of nanoparticle drug delivery systems, Wiley Interdiscip. Rev. Nanomed. Nanobiotechnol. 4 (2012) 219–233.
[294] V.P. Torchilin, V.S. Trubetskoy, Which polymers can make nanoparticulate drug carriers long-circulating? Adv. Drug Deliv. Rev. 16 (1995) 141–155.
[295] S.K. Hobbs, W.L. Monsky, F. Yuan, W.G. Roberts, L. Griffith, V.P. Torchilin, R.K. Jain, Regulation of transport pathways in tumor vessels: role of tumor type and microenvironment, Proc. Natl. Acad. Sci. U. S. A. 95 (1998) 4607–4612.
[296] N.Z. Wu, D. Da, T.L. Rudoll, D. Needham, A.R. Whorton, M.W. Dewhirst, Increased microvascular permeability contributes to preferential accumulation of stealth liposomes in tumor tissue, Cancer Res. 53 (1993) 3765–3770.
[297] N. Oku, N. Saito, Y. Namba, H. Tsukada, D. Dolphin, S. Okada, Application of long-circulating liposomes to cancer photodynamic therapy, Biol. Pharm. Bull. 20 (1997) 670–673.
[298] L. Polo, G. Bianco, E. Reddi, G. Jori, The effect of different liposomal formulations on the interaction of Zn(II)-phthalocyanine with isolated low and high-density lipoproteins, Int. J. Biochem. Cell Biol. 27 (1995) 1249–1255.
[299] C. Decker, F. Steiniger, A. Fahr, Transfer of a lipophilic drug (temoporfin) between small unilamellar liposomes and human plasma proteins: influence of membrane composition on vesicle integrity and release characteristics, J. Liposome Res. 23 (2013) 154–165.
[300] V. Reshetov, V. Zorin, A. Siupa, M.A. D'Hallewin, F. Guillemin, L. Bezdetnaya, Interaction of liposomal formulations of meta-tetra(hydroxyphenyl) chlorin (temoporfin) with serum proteins: protein binding and liposome destruction, Photochem. Photobiol. 88 (2012) 1256–1264.
[301] E. Reddi, S. Cernuschi, R. Biolo, G. Jori, Liposome- or LDL-administered Zn(II)-phthalocyanine as a photodynamic agent for tumours III. Effect of cholesterol on pharmacokinetic and phototherapeutic properties, Lasers Med. Sci. 5 (1990) 339–343.
[302] L. Polo, G. Valduga, G. Jori, E. Reddi, Low-density lipoprotein receptors in the uptake of tumour photosensitizers by human and rat transformed fibroblasts, Int. J. Biochem. Cell Biol. 34 (2002) 10–23.
[303] J.L. Goldstein, M.S. Brown, Low-density lipoprotein pathway and its relation to atherosclerosis, Ann. Rev. Biochem. 46 (1977) 897–930.
[304] P. Shum, J.-M. Kim, D.H. Thompson, Phototriggering of liposomal drug delivery systems, Adv. Drug Deliv. Rev. 53 (2001) 273–284.
[305] N. Fomina, J. Sankaranarayanan, A. Almutairi, Photochemical mechanisms of light-triggered release from nanocarriers, Adv. Drug Deliv. Rev. 64 (2012) 1005–1020.

[306] S.J. Leung, M. Romanowski, Light-activated content release from liposomes, Theranostics 2 (2012) 1020–1036.
[307] A. Andreoni, R. Cubeddu, S. Desilvestri, P. Laporta, G. Jori, E. Reddi, Hematoporphyrin derivative—experimental evidence for aggregated species, Chem. Phys. Lett. 88 (1982) 33–36.
[308] A. Maier, F. Tomaselli, V. Matzi, P. Rehak, H. Pinter, F.M. Smolle-Juttner, Photosensitization with hematoporphyrin derivative compared to 5-aminolaevulinic acid for photodynamic therapy of esophageal carcinoma, Ann. Thorac. Surg. 72 (2001) 1136–1140.
[309] P. Zimcik, M. Miletin, Photodynamic therapy, in: A.R. Lang (Ed.), Dyes and Pigments: New Reserach, Nova Science Publishers Inc., New York, 2009, pp. 1–62.
[310] M. Oertel, S.I. Schastak, A. Tannapfel, R. Hermann, U. Sack, J. Mossner, F. Berr, Novel bacteriochlorine for high tissue-penetration: photodynamic properties in human biliary tract cancer cells in vitro and in a mouse tumour model, J. Photochem. Photobiol. B 71 (2003) 1–10.
[311] S.P. Pereira, L. Ayaru, R. Ackroyd, D. Mitton, G. Fullarton, M. Zammit, Z. Grzebieniak, H. Messmann, M.A. Ortner, L. Gao, M.M. Trinh, J. Spenard, The pharmacokinetics and safety of porfimer after repeated administration 30–45 days apart to patients undergoing photodynamic therapy, Aliment. Pharmacol. Ther. 32 (2010) 821–827.
[312] T.J. Dougherty, M.T. Cooper, T.S. Mang, Cutaneous phototoxic occurrences in patients receiving Photofrin, Lasers Surg. Med. 10 (1990) 485–488.
[313] J.A. Woods, N.J. Traynor, L. Brancaleon, H. Moseley, The effect of Photofrin on DNA strand breaks and base oxidation in HaCaT keratinocytes: a comet assay study, Photochem. Photobiol. 79 (2004) 105–113.
[314] J.T. Dalton, C.R. Yates, D.H. Yin, A. Straughn, S.L. Marcus, A.L. Golub, M.C. Meyer, Clinical pharmacokinetics of 5-aminolevulinic acid in healthy volunteers and patients at high risk for recurrent bladder cancer, J. Pharmacol. Exp. Ther. 301 (2002) 507–512.
[315] J. Webber, D. Kessel, D. Fromm, Plasma levels of protoporphyrin IX in humans after oral administration of 5-aminolevulinic acid, J. Photochem. Photobiol. B 37 (1997) 151–153.
[316] G. Ackermann, C. Abels, W. Baumler, S. Langer, M. Landthaler, E.W. Lang, R.M. Szeimies, Simulations on the selectivity of 5-aminolaevulinic acid-induced fluorescence in vivo, J. Photochem. Photobiol. B 47 (1998) 121–128.
[317] H.B. Ris, H.J. Altermatt, R. Inderbitzi, R. Hess, B. Nachbur, J.C.M. Stewart, Q. Wang, C.K. Lim, R. Bonnett, M.C. Berenbaum, U. Althaus, Photodynamic therapy with chlorins for diffuse malignant mesothelioma—initial clinical results, Br. J. Cancer 64 (1991) 1116–1120.
[318] E. Ricci-Junior, J.M. Marchetti, Zinc(II) phthalocyanine loaded PLGA nanoparticles for photodynamic therapy use, Int. J. Pharm. 310 (2006) 187–195.
[319] Z. Chen, S.Y. Zhou, J.C. Chen, Y.C. Deng, Z.P. Luo, H.W. Chen, M.R. Hamblin, M.D. Huang, Pentalysine beta-carbonylphthalocyanine zinc: an effective tumor-targeting photosensitizer for photodynamic therapy, Chem. Med. Chem. 5 (2010) 890–898.
[320] J. Taillefer, M.C. Jones, N. Brasseur, J.E. van Lier, J.C. Leroux, Preparation and characterization of pH-responsive polymeric micelles for the delivery of photosensitizing anticancer drugs, J. Pharm. Sci. 89 (2000) 52–62.
[321] Y.P. Fang, P.C. Wu, Y.H. Tsai, Y.B. Huang, Physicochemical and safety evaluation of 5-aminolevulinic acid in novel liposomes as carrier for skin delivery, J. Liposome Res. 18 (2008) 31–45.
[322] Y. Sadzuka, K. Tokutomi, F. Iwasaki, I. Sugiyama, T. Hirano, H. Konno, N. Oku, T. Sonobe, The phototoxicity of Photofrin was enhanced by PEGylated liposome in vitro, Cancer Lett. 241 (2006) 42–48.
[323] J. Soriano, M. Garcia-Diaz, M. Mora, M.L. Sagrista, S. Nonell, A. Villanueva, J.C. Stockert, M. Canete, Liposomal temocene (*m*-THPPo) photodynamic treatment induces cell death by mitochondria-independent apoptosis, Biochim. Biophys. Acta 1830 (2013) 4611–4620.
[324] G. Sharma, S. Anabousi, C. Ehrhardt, M.N.V. Ravi Kumar, Liposomes as targeted drug delivery systems in the treatment of breast cancer, J. Drug Target. 14 (2006) 301–310.
[325] D.E. Marotta, W. Cao, E.P. Wileyto, H. Li, I. Corbin, E. Rickter, J.D. Glickson, B. Chance, G. Zheng, T.M. Busch, Evaluation of bacteriochlorophyll-reconstituted low-density lipoprotein nanoparticles for photodynamic therapy efficacy in vivo, Nanomedicine (London England) 6 (2011) 475–487.
[326] H. Li, D.E. Marotta, S. Kim, T.M. Busch, E.P. Wileyto, G. Zheng, High payload delivery of optical imaging and photodynamic therapy agents to tumors using phthalocyanine-reconstituted low-density lipoprotein nanoparticles, J. Biomed. Opt. 10 (2005) 41203.
[327] R. Decreau, M.J. Richard, P. Verrando, M. Chanon, M. Julliard, Photodynamic activities of silicon phthalocyanines against achromic M6 melanoma cells and healthy human melanocytes and keratinocytes, J. Photochem. Photobiol. B 48 (1999) 48–56.
[328] M. Garcia-Diaz, M. Kawakubo, P. Mroz, M.L. Sagrista, M. Mora, S. Nonell, M.R. Hamblin, Cellular and vascular effects of the photodynamic agent temocene are modulated by the delivery vehicle, J. Control. Release 162 (2012) 355–363.
[329] J. Shao, Y. Dai, W. Zhao, J. Xie, J. Xue, J. Ye, L. Jia, Intracellular distribution and mechanisms of actions of photosensitizer Zinc(II)-phthalocyanine solubilized in Cremophor EL against human hepatocellular carcinoma HepG2 cells, Cancer Lett. 330 (2013) 49–56.
[330] R.P. Bagwe, J.R. Kanicky, B.J. Palla, P.K. Patanjali, D.O. Shah, Improved drug delivery using microemulsions: rationale, recent progress, and new horizons, Crit. Rev. Ther. Drug Carrier Syst. 18 (2001) 77–140.
[331] A.M. Lima, C.D. Pizzol, F.B. Monteiro, T.B. Creczynski-Pasa, G.P. Andrade, A.O. Ribeiro, J.R. Perussi, Hypericin encapsulated in solid lipid nanoparticles: phototoxicity and photodynamic efficiency, J. Photochem. Photobiol. B 125 (2013) 146–154.
[332] F.P. Navarro, G. Creusat, C. Frochot, A. Moussaron, M. Verhille, R. Vanderesse, J. S. Thomann, P. Boisseau, I. Texier, A.C. Couffin, M. Barberi-Heyob, Preparation and characterization of *m*THPC-loaded solid lipid nanoparticles for photodynamic therapy, J. Photochem. Photobiol. B 130 (2014) 161–169.
[333] C. Pardeshi, P. Rajput, V. Belgamwar, A. Tekade, G. Patil, K. Chaudhary, A. Sonje, Solid lipid based nanocarriers: an overview, Acta Pharm. (Zagreb, Croatia) 62 (2012) 433–472.
[334] S.H. Battah, C.E. Chee, H. Nakanishi, S. Gerscher, A.J. MacRobert, C. Edwards, Synthesis and biological studies of 5-aminolevulinic acid-containing dendrimers for photodynamic therapy, Bioconjugate Chem. 12 (2001) 980–988.
[335] O. Taratula, C. Schumann, M.A. Naleway, A.J. Pang, K.J. Chon, O. Taratula, A multifunctional theranostic platform based on phthalocyanine-loaded dendrimer for image-guided drug delivery and photodynamic therapy, Mol. Pharm. 10 (2013) 3946–3958.
[336] Z. Mohammadi, A. Sazgarnia, O. Rajabi, S. Soudmand, H. Esmaily, H.R. Sadeghi, An in vitro study on the photosensitivity of 5-aminolevulinic acid conjugated gold nanoparticles, Photodiagn. Photodyn. Ther. 10 (2013) 382–388.
[337] H. Eshghi, A. Sazgarnia, M. Rahimizadeh, N. Attaran, M. Bakavoli, S. Soudmand, Protoporphyrin IX-gold nanoparticle conjugates as an efficient photosensitizer in cervical cancer therapy, Photodiagn. Photodyn. Ther. 10 (2013) 304–312.
[338] T. Stuchinskaya, M. Moreno, M.J. Cook, D.R. Edwards, D.A. Russell, Targeted photodynamic therapy of breast cancer cells using antibody-phthalocyanine-gold nanoparticle conjugates, Photochem. Photobiol. Sci. 10 (2011) 822–831.
[339] R. Arvizo, R. Bhattacharya, P. Mukherjee, Gold nanoparticles: opportunities and challenges in nanomedicine, Expert Opin. Drug Deliv. 7 (2010) 753–763.
[340] J.W. Hofman, M.G. Carstens, F. van Zeeland, C. Helwig, F.M. Flesch, W.E. Hennink, C.F. van Nostrum, Photocytotoxicity of mTHPC (temoporfin) loaded polymeric micelles mediated by lipase catalyzed degradation, Pharm. Res. 25 (2008) 2065–2073.
[341] A.M. Master, M.E. Rodriguez, M.E. Kenney, N.L. Oleinick, A.S. Gupta, Delivery of the photosensitizer Pc 4 in PEG-PCL micelles for in vitro PDT studies, J Pharm Sci. 99 (2010) 2386–2398.
[342] L. Lamch, U. Bazylinska, J. Kulbacka, J. Pietkiewicz, K. Biezunska-Kusiak, K.A. Wilk, Polymeric micelles for enhanced Photofrin II (R) delivery, cytotoxicity and pro-apoptotic activity in human breast and ovarian cancer cells, Photodiagn. Photodyn. Ther. 11 (2014) 570–585.
[343] M.N. Sibata, A.C. Tedesco, J.M. Marchetti, Photophysicals and photochemicals studies of zinc(II) phthalocyanine in long time circulation micelles for photodynamic therapy use, Eur. J. Pharm. Sci. 23 (2004) 131–138.
[344] M. Yokoyama, Polymeric micelles as a new drug carrier system and their required considerations for clinical trials, Expert Opin. Drug Deliv. 7 (2010) 145–158.
[345] L. Shi, X. Wang, F. Zhao, H. Luan, Q. Tu, Z. Huang, H. Wang, H. Wang, In vitro evaluation of 5-aminolevulinic acid (ALA) loaded PLGA nanoparticles, Int. J. Nanomed. 8 (2013) 2669–2676.
[346] A. Vaidya, Y. Sun, Y. Feng, L. Emerson, E.K. Jeong, Z.R. Lu, Contrast-enhanced MRI-guided photodynamic cancer therapy with a pegylated bifunctional polymer conjugate, Pharm. Res. 25 (2008) 2002–2011.
[347] I.V. Martynenko, V.A. Kuznetsova, A.O. Orlova, P.A. Kanaev, V.G. Maslov, A. Loudon, V. Zaharov, P. Parfenov, Y.K. Gun'ko, A.V. Baranov, A.V. Fedorov, Chlorin e6-ZnSe/ZnS quantum dots based system as reagent for photodynamic therapy, Nanotechnology 26 (2015) 55102.
[348] C. Fowley, N. Nomikou, A.P. McHale, B. McCaughan, J.F. Callan, Extending the tissue penetration capability of conventional photosensitisers: a carbon quantum dot-protoporphyrin IX conjugate for use in two-photon excited photodynamic therapy, Chem. Commun. (Cambridge, England) 49 (2013) 8934–8936.
[349] J.M. Tsay, M. Trzoss, L. Shi, X. Kong, M. Selke, M.E. Jung, S. Weiss, Singlet oxygen production by peptide-coated quantum dot-photosensitizer conjugates, J. Am. Chem. Soc. 129 (2007) 6865–6871.
[350] J. Drbohlavova, V. Adam, R. Kizek, J. Hubalek, Quantum dots—characterization, preparation and usage in biological systems, Int. J. Mol. Sci. 10 (2009) 656–673.
[351] P. Sapra, T.M. Allen, Internalizing antibodies are necessary for improved therapeutic efficacy of antibody-targeted liposomal drugs, Cancer Res. 62 (2002) 7190–7194.
[352] P. Sapra, E.H. Moase, J. Ma, T.M. Allen, Improved therapeutic responses in a xenograft model of human B lymphoma (Namalwa) for liposomal vincristine versus liposomal doxorubicin targeted via anti-CD19 IgG2a or Fab' fragments, Clin. Cancer Res. 10 (2004) 1100–1111.
[353] C. Mamot, R. Ritschard, W. Kung, J.W. Park, R. Herrmann, C.F. Rochlitz, EGFR-targeted immunoliposomes derived from the monoclonal antibody EMD72000 mediate specific and efficient drug delivery to a variety of colorectal cancer cells, J. Drug Target. 14 (2006) 215–223.
[354] I.Y. Kim, Y.S. Kang, D.S. Lee, H.J. Park, E.K. Choi, Y.K. Oh, H.J. Son, J.S. Kim, Antitumor activity of EGFR targeted pH-sensitive immunoliposomes encapsulating gemcitabine in A549 xenograft nude mice, J. Control. Release 140 (2009) 55–60.

[355] J.H. Mortensen, M. Jeppesen, L. Pilgaard, R. Agger, M. Duroux, V. Zachar, T. Moos, Targeted antiepidermal growth factor receptor (cetuximab) immunoliposomes enhance cellular uptake in vitro and exhibit increased accumulation in an intracranial model of glioblastoma multiforme, J. Drug Deliv. 2013 (2013) 209205.
[356] J. Lehtinen, M. Raki, K.A. Bergstrom, P. Uutela, K. Lehtinen, A. Hiltunen, J. Pikkarainen, H.M. Liang, S. Pitkanen, A.M. Maatta, R.A. Ketola, M. Yliperttula, T. Wirth, A. Urtti, Pre-targeting and direct immunotargeting of liposomal drug carriers to ovarian carcinoma, Plos One 7 (2012) e41410.
[357] F. Pastorino, C. Brignole, D. Marimpietri, P. Sapra, E.H. Moase, T.M. Allen, M. Ponzoni, Doxorubicin-loaded Fab' fragments of anti-disialoganglioside immunoliposomes selectively inhibit the growth and dissemination of human neuroblastoma in nude mice, Cancer Res. 63 (2003) 86–92.
[358] U.B. Nielsen, D.B. Kirpotin, E.M. Pickering, K.L. Hong, J.W. Park, M.R. Shalaby, Y. Shao, C.C. Benz, J.D. Marks, Therapeutic efficacy of anti-ErbB2 immunoliposomes targeted by a phage antibody selected for cellular endocytosis, Biochim. Biophys. Acta. 1591 (2002) 109–118.
[359] J. Gao, W. Zhong, J.Q. He, H.M. Li, H. Zhang, G.C. Zhou, B.H. Li, Y. Lu, H. Zou, G. Kou, D.P. Zhang, H. Wang, Y.J. Guo, Y.Q. Zhong, Tumor-targeted PE38KDEL delivery via PEGylated anti-HER2 immunoliposomes, Int. J. Pharm. 374 (2009) 145–152.
[360] D. Kirpotin, J.W. Park, K. Hong, S. Zalipsky, W.L. Li, P. Carter, C.C. Benz, D. Papahadjopoulos, Sterically stabilized anti-HER2 immunoliposomes: design and targeting to human breast cancer cells in vitro, Biochemistry 36 (1997) 66–75.
[361] C. Hantel, F. Lewrick, S. Schneider, O. Zwermann, A. Perren, M. Reincke, R. Suss, F. Beuschlein, Anti insulin-like growth factor I receptor immunoliposomes: a single formulation combining two anticancer treatments with enhanced therapeutic efficiency, J. Clin. Endocrinol. Metab. 95 (2010) 943–952.
[362] H. Hatakeyama, H. Akita, E. Ishida, K. Hashimoto, H. Kobayashi, T. Aoki, J. Yasuda, K. Obata, H. Kikuchi, T. Ishida, H. Kiwada, H. Harashima, Tumor targeting of doxorubicin by anti-MT1-MMP antibody-modified PEG liposomes, Int. J. Pharm. 342 (2007) 194–200.
[363] S. Gosk, T. Moos, C. Gottstein, G. Bendas, VCAM-1 directed immunoliposomes selectively target tumor vasculature in vivo, Biochim. Biophys. Acta 1778 (2008) 854–863.
[364] P. Roth, C. Hammer, A.C. Piguet, M. Ledermann, J.F. Dufour, E. Waelti, Effects on hepatocellular carcinoma of doxorubicin-loaded immunoliposomes designed to target the VEGFR-2, J. Drug Target. 15 (2007) 623–631.
[365] A. Wicki, C. Rochlitz, A. Orleth, R. Ritschard, I. Albrecht, R. Herrmann, G. Christofori, C. Mamot, Targeting tumor-associated endothelial cells: anti-VEGFR2 immunoliposomes mediate tumor vessel disruption and inhibit tumor growth, Clin. Cancer Res. 18 (2012) 454–464.
[366] P. Lipponen, M. Eskelinen, Expression of epidermal growth factor receptor in bladder cancer as related to established prognostic factors, oncoprotein (c-erbB-2, p53) expression and long-term prognosis, Br. J. Cancer 69 (1994) 1120–1125.
[367] L.N. Turkeri, M.L. Erton, I. Cevik, A. Akdas, Impact of the expression of epidermal growth factor, transforming growth factor alpha, and epidermal growth factor receptor on the prognosis of superficial bladder cancer, Urology 51 (1998) 645–649.
[368] H. Olsson, I.M. Fyhr, P. Hultman, S. Jahnson, HER2 status in primary stage T1 urothelial cell carcinoma of the urinary bladder, Scand. J. Urol. Nephrol. 46 (2012) 102–107.
[369] T.A. Abd Elazeez, A. El-Balshy, M.M. Khalil, M.M. El-Tabye, H. Abdul-Halim, Prognostic significance of P27 (Kip 1) and MUC1 in papillary transitional cell carcinoma of the urinary bladder, Urol. Ann. 1 (2011) 8–13.
[370] X.J. Cao, J.F. Hao, X.H. Yang, P. Xie, L.P. Liu, C.P. Yao, J. Xu, Prognostic value of expression of EGFR and nm23 for locoregionally advanced nasopharyngeal carcinoma, Med. Oncol. 29 (2012) 263–271.
[371] T.J. Kim, Y.S. Lee, J.H. Kang, Y.S. Kim, C.S. Kang, Prognostic significance of expression of VEGF and Cox-2 in nasopharyngeal carcinoma and its association with expression of C-erbB2 and EGFR, J. Surg. Oncol. 103 (2011) 46–52.
[372] J.J. Pan, L. Kong, S.N. Lin, G. Chen, Q. Chen, J.J. Lu, The clinical significance of coexpression of cyclooxygenases-2, vascular endothelial growth factors, and epidermal growth factor receptor in nasopharyngeal carcinoma, Laryngoscope 118 (2008) 1970–1975.
[373] R. Soo, T. Putti, Q. Tao, B.C. Goh, K.H. Lee, L. Kwok-Seng, L. Tan, W.S. Hsieh, Overexpression of cyclooxygenase-2 in nasopharyngeal carcinoma and association with epidermal growth factor receptor expression, Arch. Otolaryngol. Head Neck Surg. 131 (2005) 147–152.
[374] Y.L. Yuan, X.H. Zhou, J. Song, X.P. Qiu, J. Li, L.F. Ye, X.P. Meng, D. Xia, Expression and clinical significance of epidermal growth factor receptor and type 1 insulin-like growth factor receptor in nasopharyngeal carcinoma, Ann. Otol. Rhinol. Laryngol. 117 (2008) 192–200.
[375] J. Harder, O. Waiz, F. Otto, M. Geissler, M. Olschewski, B. Weinhold, H.E. Blum, A. Schmitt-Graeff, O.G. Opitz, EGFR and HER2 expression in advanced biliary tract cancer, World J. Gastroenterol. 15 (2009) 4511–4517.
[376] Y. Pignochino, I. Sarotto, C. Peraldo-Neia, J.Y. Penachioni, G. Cavalloni, G. Migliardi, L. Casorzo, G. Chiorino, M. Risio, A. Bardelli, M. Aglietta, F. Leone, Targeting EGFR/HER2 pathways enhances the antiproliferative effect of gemcitabine in biliary tract and gallbladder carcinomas, BMC Cancer 10 (2010) 631.
[377] M. Wiedmann, J. Feisthammel, T. Bluthner, A. Tannapfel, T. Kamenz, A. Kluge, J. Mossner, K. Caca, Novel targeted approaches to treating biliary tract cancer: the dual epidermal growth factor receptor and ErbB-2 tyrosine kinase inhibitor NVP-AEE788 is more efficient than the epidermal growth factor receptor inhibitors gefitinib and erlotinib, Anticancer Drugs 17 (2006) 783–795.
[378] D. Yoshikawa, H. Ojima, M. Iwasaki, N. Hiraoka, T. Kosuge, S. Kasai, S. Hirohashi, T. Shibata, Clinicopathological and prognostic significance of EGFR, VEGF, and HER2 expression in cholangiocarcinoma, Br. J. Cancer 98 (2008) 418–425.
[379] T. Kawamoto, S. Krishnamurthy, E. Tarco, S. Trivedi, I.I. Wistuba, D. Li, I. Roa, J. C. Roa, M.B. Thomas, HER receptor family: novel candidate for targeted therapy for gallbladder and extrahepatic bile duct cancer, Gastrointest. Cancer Res. 6 (2007) 221–227.
[380] H.J. Kim, T.W. Yoo, D.I. Park, J.H. Park, Y.K. Cho, C.I. Sohn, W.K. Jeon, B.I. Kim, M. K. Kim, S.W. Chae, J.H. Sohn, Gene amplification and protein overexpression of HER-2/neu in human extrahepatic cholangiocarcinoma as detected by chromogenic in situ hybridization and immunohistochemistry: its prognostic implication in node-positive patients, Ann. Oncol. 18 (2007) 892–897.
[381] J. Zheng, Y.M. Zhu, Expression of c-erbB-2 proto-oncogene in extrahepatic cholangiocarcinoma and its clinical significance, Hepatobiliary Pancreat. Dis. Int. 6 (2007) 412–415.
[382] VCCLAB, Virtual Computational Chemistry Laboratory, http://www.vcclab.org, 2005.
[383] S. Jacques, Optical absorption of melanin, Oregon Medical Laser Center, http://omlc.ogi.edu/spectra/melanin/, 2012.
[384] S. Prahl, Optical absorption of hemoglobin, Oregon Medical Laser Center, http://omlc.ogi.edu/spectra/hemoglobin/, 2012.
[385] R. Kang, K.M. Livesey, H.J. Zeh, M.T. Lotze, D.L. Tang, HMGB1 A novel Beclin 1-binding protein active in autophagy, Autophagy 6 (2010) 1209–1211.
[386] J.J. Kloek, X. Marechal, J. Roelofsen, R.H. Houtkooper, A.B.P. van Kuilenburg, W. Kulik, R. Bezemer, R. Neviere, T.M. van Gulik, M. Heger, Cholestasis is associated with hepatic microvascular dysfunction and aberrant energy metabolism before and during ischemia-reperfusion, Antioxid. Redox Signaling 17 (2012) 1109–1123.
[387] I.C.J.H. Post, W.M.I. de Boon, M. Heger, A.C.W.A. van Wijk, J. Kroon, J.D. van Buul, T.M. van Gulik, Endothelial cell preservation at hypothermic to normothermic conditions using clinical and experimental organ preservation solutions, Exp. Cell Res. 319 (2013) 2501–2513.